AFRRI REPORTS

January • February • March 1988

Defense Nuclear Agency
Armed Forces Radiobiology Research Institute
Bethesda, Maryland 20814-5415

UNCLASSIFIED

SECURITY CLASSIFICATION OF THIS PAGE

REPORT DOCUMENTATION PAGE

1a. REPORT SECURITY CLASSIFICATION UNCLASSIFIED	1b. RESTRICTIVE MARKINGS
2a. SECURITY CLASSIFICATION AUTHORITY	3. DISTRIBUTION/AVAILABILITY OF REPORT Approved for public release; distribution unlimited.
2b. DECLASSIFICATION/DOWNGRADING SCHEDULE	
4. PERFORMING ORGANIZATION REPORT NUMBER(S) SR88-1 - SR88-9, TR88-1	5. MONITORING ORGANIZATION REPORT NUMBER(S)
6a. NAME OF PERFORMING ORGANIZATION Armed Forces Radiobiology Research Institute 6b. OFFICE SYMBOL (If applicable) AFRRI	7a. NAME OF MONITORING ORGANIZATION
6c. ADDRESS (City, State and ZIP Code) Defense Nuclear Agency Bethesda, Maryland 20814-5145	7b. ADDRESS (City, State and ZIP Code)
8a. NAME OF FUNDING/SPONSORING ORGANIZATION Defense Nuclear Agency 8b. OFFICE SYMBOL (If applicable) DNA	9. PROCUREMENT INSTRUMENT IDENTIFICATION NUMBER
8c. ADDRESS (City, State and ZIP Code) Washington, DC 20305	10. SOURCE OF FUNDING NOS. PROGRAM ELEMENT NO.: NWED PROJECT NO.: TASK NO.: WORK UNIT NO.: QAXM
11. TITLE (Include Security Classification) AFRRI Reports Jan-Mar 1988	
12. PERSONAL AUTHOR(S)	
13a. TYPE OF REPORT Reprint/Technical 13b. TIME COVERED FROM _____ TO _____	14. DATE OF REPORT (Yr., Mo., Day) May 1988 15. PAGE COUNT
16. SUPPLEMENTARY NOTATION	

17. COSATI CODES			18. SUBJECT TERMS (Continue on reverse if necessary and identify by block number)
FIELD	GROUP	SUB. GR.	

19. ABSTRACT (Continue on reverse if necessary and identify by block number)

This volume contains AFRRI Scientific Reports SR88-1 through SR88-9 and Technical Report TR88-1 for Jan-Mar 1988.

20. DISTRIBUTION/AVAILABILITY OF ABSTRACT UNCLASSIFIED/UNLIMITED ☐ SAME AS RPT ☐ DTIC USERS ☐	21. ABSTRACT SECURITY CLASSIFICATION UNCLASSIFIED
22a. NAME OF RESPONSIBLE INDIVIDUAL Junith A. Van Deusen	22b. TELEPHONE NUMBER (Include Area Code) (202)295-3536 22c. OFFICE SYMBOL ISDP

DD FORM 1473, 83 APR EDITION OF 1 JAN 73 IS OBSOLETE

UNCLASSIFIED

SECURITY CLASSIFICATION OF THIS PAGE

CONTENTS

Scientific Reports

Technical Reports

Free Radical Biology & Medicine, Vol. 4, pp. 215–218, 1988
Printed in the USA.

0891-5849/88 $3.00 + .00

Original Contribution

REACTION OF DISODIUM CROMOGLYCATE WITH HYDRATED ELECTRONS

ALASDAIR J. CARMICHAEL, CARMEN M. ARROYO*, and LORRIS G. COCKERHAM**
Radiation Sciences and Physiology Departments, Armed Forces Radiobiology Research Institute Bethesda, MD 20814-5145

(*Received* 6 *July* 1987; *Accepted* 21 *July* 1987)

Abstract—A possible mechanism by which disodium cromoglycate (DSCG) prevents a decrease in regional cerebral blood flow but not hypotension in primates following whole body gamma-irradiation was studied. Several studies have implicated superoxide radicals ($O_2\cdot^-$) in intestinal and cerebral vascular disorders following ischemia and ionizing radiation, respectively. $O_2\cdot^-$ is formed during radiolysis in the reaction between hydrated electrons (e_{aq}^-) and dissolved oxygen. For this reason, the efficiency of DSCG to scavenge e_{aq}^- and possibly prevent the formation of $O_2\cdot^-$ was studied. Hydrated electrons were produced by photolysis of potassium ferrocyanide solutions. The rate constant, $k = 2.92 \times 10^{10}\ M^{-1}s^{-1}$ for the reaction between e_{aq}^- and DSCG was determined in competition experiments using the spin trap 5,5-dimethyl-1-pyrroline-*N*-oxide (DMPO). This spin trap reacts rapidly with e_{aq}^- followed by protonation to yield the ESR observable DMPO-H spin adduct. The results show that DSCG is an efficient e_{aq}^- scavenger and may effectively compete with oxygen for e_{aq}^- preventing the radiolytic formation of $O_2\cdot^-$.

Keywords—Disodium cromoglycate, Cromolyn, Hydrated electrons, Spin trapping, Electron spin resonance.

INTRODUCTION

A marked decrease in regional cerebral blood flow and hypotension have been observed in primates following their supralethal exposure to whole body gamma-irradiation.[1] These effects may in some manner be associated with the phenomena known as performance decrement (PD) and early transient incapacitation (ETI).[2] Disodium cromoglycate (DSCG), a mast cell stabilizer (Fig. 1), has been shown to inhibit the decrease in cerebral blood flow but not the hypotension.[3] Since superoxide radicals ($O_2\cdot^-$) have been involved in several vascular disorders following ischemia and ionizing radiation,[4–6] it is of interest to this work to study the possibility that DSCG may inhibit the radiolytic formation of $O_2\cdot^-$. During gamma-radiolysis, $O_2\cdot^-$ are formed by the direct interaction of hydrated electrons (e_{aq}^-) with dissolved oxygen.[7] For this reason, the reaction of e_{aq}^- with DSCG was studied in order to determine whether DSCG is an effective scanvenger, possibly preventing the formation of $O_2\cdot^-$. The reactions were studied using the method of spin trapping and electron spin resonance (ESR). Spin trapping consists of reacting a short lived free radical with a spin trap, usually a nitrone or nitroso compound, to form a longer lived nitroxide spin adduct which can be identified by ESR.[8,9] Hydrated electrons react rapidly with the spin trap 5,5-dimethyl-1-pyrroline-*N*-oxide (DMPO) which is subsequently protonated forming the DMPO—H spin adduct. The rate of this reaction ($k = 2 \times 10^{10}\ M^{-1}s^{-1}$) is approximately equal to the rate of the reaction between e_{aq}^- and oxygen ($k = 2.2 \times 10^{10}\ M^{-1}s^{-1}$).[7,10] These properties make spin trapping a reliable system to study the competition kinetics of e_{aq}^- with DMPO and DSCG.

Address correspondence to Alasdair J. Carmichael, Ph.D., Radiation Science Department, Armed Forces Radiobiology Research Institute, Bethesda, MD 20814-5145
*Current address: Department of Medicine, Ross Hall, George Washington University, Washington, DC 20032
**Current address: Air Force Office of Scientific Research, Bolling AFB, DC 20332-6448

EXPERIMENTAL PROCEDURES

Disodium cromoglycate was obtained in pure form from Fisons (Bedford, MA). Glycylglycine was obtained from Sigma (St. Louis, MO). The spin traps 2-methyl-2-nitrosopropane (MNP) and DMPO were pur-

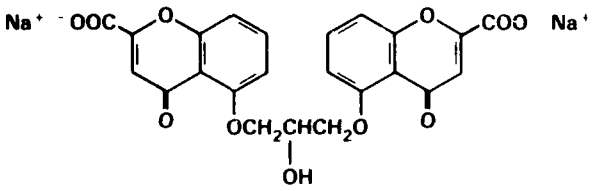

Fig. 1. Disodium cromoglycate (DSCG)

chased from Aldrich (Milwaukee, WI). MNP was used without further purification and was dissolved by stirring overnight at a concentration of 1 mg/ml. DMPO was purified using the method described by Buettner and Oberley.[11] This method consists of successively treating the DMPO with activated charcoal until all free radical impurities disappear as verified by ESR. The concentration of DMPO was measured spectrophotometrically (λ = 227 nm, ϵ = 8 × 10^3 M^{-1} cm^{-1}).[12]

Hydrated electrons were generated by photolysis (313 nm) of potassium ferrocyanide. Samples, with and without DSCG, containing the spin trap and potassium ferrocyanide were placed in a standard ESR quartz flat cell (60 × 10 × 0.25 mm) and photolyzed *in situ* in the ESR cavity. A 1000 W Hg-Xe arc lamp with a Schoeffle grating monochromator was used to photoirradiate the samples. The reactions were carried out in air-saturated and nitrogen-saturated solutions; however, the low concentration of oxygen in the air-saturated solutions, in comparison with other reactants, made no difference in the results. The ESR spectra were recorded on a Varian E-109 X-band spectrometer at 100 mHz magnetic field modulation. The magnetic field was set at: 3398 G; modulation amplitude: 0.5 G; microwave power: 10 mW; microwave frequency: 9.510 GHz. For the kinetic experiments the accuracy of the ESR measurements was ± 10%.

RESULTS AND DISCUSSION

Two experiments were done to verify that e_{aq}^- were produced during the photolysis (313 nm) of potassium ferrocyanide. In the first experiment, a solution of potassium ferrocyanide (0.1 M) containing DMPO (0.01 M) was photolyzed generating the ESR spectrum shown in Figure 2b. This spectrum consists of a primary nitrogen triplet with each of the lines split into triplets in a 1:2:1 pattern due to the interaction of the unpaired nitroxide electron with two β hydrogens. The hyperfine coupling constants, a_N^N = 16.6 G and a_H^β = 22.5 G, are consistent with the hydrogen spin adduct of DMPO (DMPO—H). It is known that e_{aq}^- react rapidly with DMPO (k = 2 × 10^{10} $M^{-1}s^{-1}$) followed by protonation to form the DMPO—H spin adduct.[13] In the second experiment a potassium ferrocyanide solution (0.1 M) containing MNP (0.01 M) and glycylglycine (0.1 M) were photolyzed generating the ESR spectrum observed in Figure 2d. This spectrum also consists of a triplet of triplets with the secondary triplet split into a 1:2:1 pattern due to an equal interaction of the unpaired nitroxide electron with two β hydrogens. Hydrated electrons react rapidly with dipeptides (k = 10^9 $M^{-1}s^{-1}$) deaminating them and forming a carbon centered radical which is readily spin trapped by MNP.[14] The hyperfine coupling constants, a_N^N = 15.5 G and a_H^β = 8.85 G, in Figure 2d are identical to those previously reported for the deaminated glycylglycine spin adduct of MNP.[15] The results shown in Figure 2 indicate that e_{aq}^- are produced during the photolysis of potassium ferrocyanide solutions.

To determine whether DSCG is an efficient hydrated electron scavenger, several solutions containing potassium ferrocyanide (0.1 M), DMPO (0.01 M) and varying concentrations of DSCG were photoirradiated (313 nm). The results are shown in Figure 3 and clearly indicate that there is an inverse relationship between the DSCG concentration and the DMPO—H ESR signal intensity. These results indicate the DSCG effec-

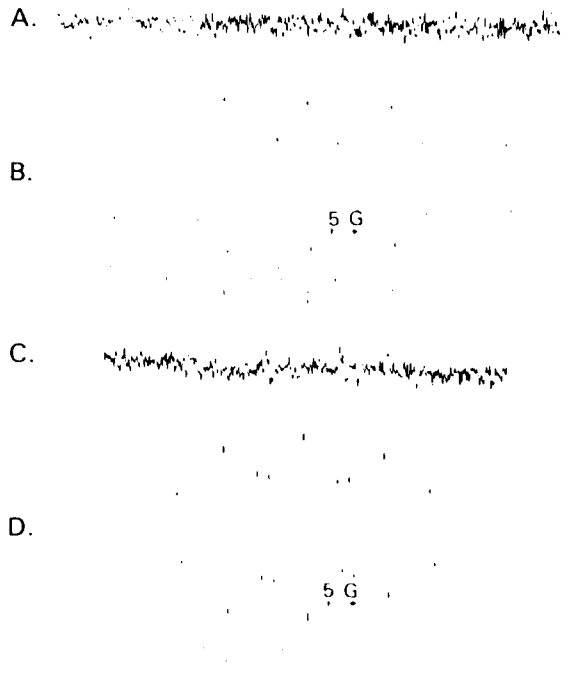

Fig. 2. ESR spectra of non illuminated controls [(a) and (c)] and of 313 nm photoirradiated [(b) and (d)] potassium ferrocyanide (0.1 M) solutions containing: (a) and (b), 0.01 M DMPO; (c) and (d), 0.1 M glycylglycine and 0.01 M MNP. Receiver gain for control experiments was 1.25×10^5 and for photoirradiated experiments 5×10^5.

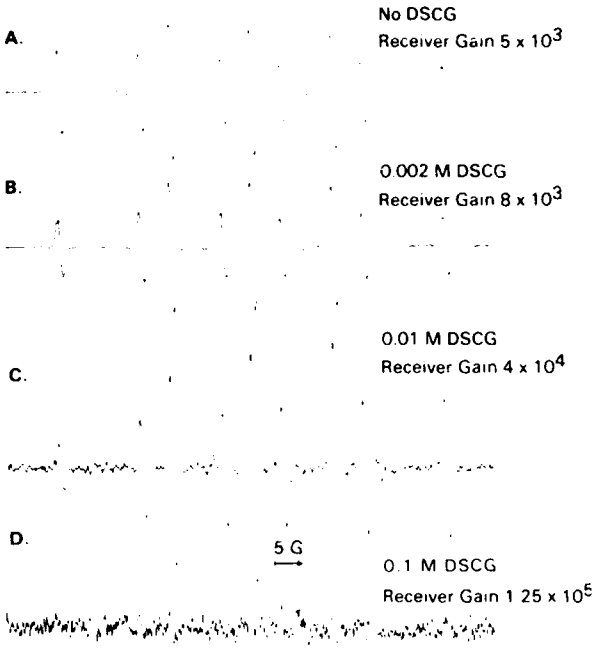

Fig. 3. ESR spectra following photolysis (313 nm) of solutions containing potassium ferrocyanide (0.1 M), DMPO (0.01 M) and varying concentrations of DSCG.

tively competes with DMPO for the e_{aq}^- produced in the photoirradiated solutions.

It is of interest to determine the rate of the reaction between e_{aq}^- and DSCG. However, prior to calculating this reaction rate the instability of DMPO—H ($t_{1/2} \sim$ 1 min) must be considered.[12] For this reason, an experiment measuring the formation of DMPO—H in time was necessary. Several solutions, each containing equal concentrations of potassium ferrocyanide (0.1 M) and an equal concentration of DMPO (0.01 M) were photoirradiated for various lengths of time and their ESR spectra recorded. Figure 4a shows the intensity of the DMPO—H low field ESR line plotted against the time of photoirradiation. This result shows that the formation of DMPO—H rapidly reaches a maximum, at which point its rate of decomposition predominates over its rate of formation leading to a decrease in the DMPO—H ESR signal intensity. It is clear from Figure 4a that for any kinetic measurement involving DSCG and DMPO, the DMPO—H ESR signal should be measured within the first few seconds of photoirradiation. Figure 4b shows the decrease in DMPO—H ESR signal intensity when several potassium ferrocyanide (0.1 M) solutions containing DMPO (0.01 M) and different concentrations of DSCG were photoirradiated (313 nm). In this case the low field DMPO—H ESR line was measured immediately beginning light irradiation of the sample.

The rate constant for the reaction between hydrated electrons and DSCG can be determined, from the data in Figure 4b, using the equation for determining rate constants in pulse radiolysis experiments.[14] This is possible because similar to pulse radiolysis measurements, in the ESR experiments in this work there are two competing reactions (Eqs. 1 and 2) from which only

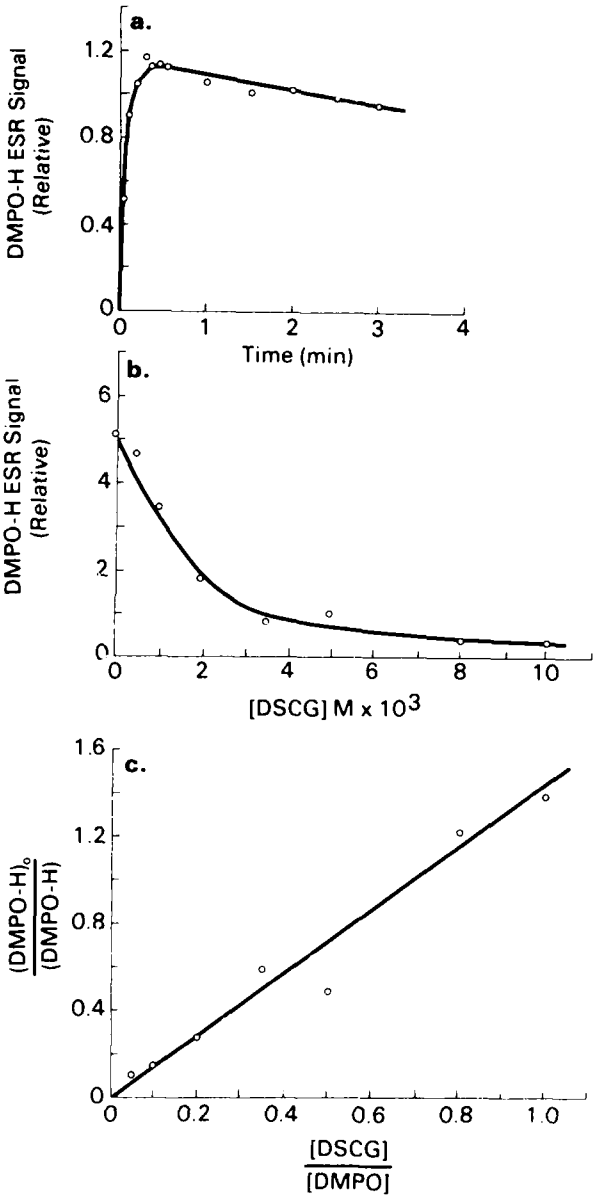

Fig. 4. (a) Low field DMPO—H ESR signal intensity versus time of photo-irradiation (313 nm). (b) Low field DMPO—H ESR signal intensity immediately starting photoirradiation (313 nm) versus varying concentrations of DSCG. (c) Kinetic plot of parameters in Eq. 3 in which the slope, 2.92×10^9 $M^{-1}s^{-1}$, is equal to the rate constant for the reaction between hydrated electrons and DSCG. All solutions contained 0.1 M potassium ferrocyanide and 0.01 M DMPO.

one generates an ESR observable product (Eq. 1) and has a known rate constant ($k_1 = 2 \times 10^{10}\ M^{-1}s^{-1}$).

$$DMPO + e^-_{aq} \xrightarrow{k_1} DMPO—H \quad \text{(ESR observable product)} \quad (1)$$

$$DSCG + e^-_{aq} \xrightarrow{k_2} P \quad \text{(nonobservable product)} \quad (2)$$

Since DMPO and DSCG will react with hydrated electrons proportionally to the product of their concentrations and the rate constants of their respective reactions (Eqs. 1 and 2), the competition kinetics is given by the following equation (Eq. 3):

$$\frac{(DMPO—H)_0}{(DMPO—H)} = 1 + \frac{k_2}{k_1}\frac{[DSCG]}{[DMPO]} \quad (3)$$

where, $(DMPO—H)_0$ = ESR signal intensity of DMPO—H in the absence of DSCG
$(DMPO—H)$ = ESR signal intensity of DMPO—H in the presence of DSCG
[DMPO] = concentration of DMPO
[DSCG] = concentration of DSCG

Plotting $(DMPO—H)_0/(DMPO—H)$ against [DSCG]/[DMPO] (Fig. 4c), a linear relationship is obtained in which the slope of the straight line is equal to the ratio of the constants, k_2/k_1, for Eqs. 1 and 2. Therefore, knowing the rate constant for Eq. 1, the rate constant for Eq. 2, $k_2 = 2.92 \times 10^{10}\ M^{-1}s^{-1}$, is easily determined.

Since DMPO and oxygen react with e_{aq} at approximately the same rate, the results obtained for DSCG indicate that DSCG is an efficient hydrated electron scavenger. Furthermore, the results also suggest that DSCG may effectively compete with oxygen for e_{aq} produced radiolytically and thus prevent the formation of $O_2^{\cdot -}$.

REFERENCES

1. Cockerham, L.G.; Cerveny, T. J.; Hampton, J. D. Postradiation regional cerebral blood flow in primates. *Aviat. Space Environ. Med.* **57**:578–582; 1986.
2. Kimeldorf, D. J.; Hunt, E. L. Neurophysiological effects of ionizing radiation. In: Kimeldorf, D. J.; Hunt, E. L., eds. *Ionizing radiation: Neural function and behavior* New York: Academic Press; 1965:59–108.
3. Cockerham, L. G.; Doyle, T. F.; Pautler, E. L.; Hampton, J. D. Disodium cromoglycate, a mast cell stabilizer, alters postradiation regional cerebral blood flow in primates. *J. Toxicol. Environ. Health* **18**:91–101; 1986.
4. Parks, D. A.; Bulkley, G. B.; Granger, D. N.; Hamilton, S. R.; McCord, J. M. Ischemic injury in the cat small intestine: Role of superoxide radicals. *Gastroenterology* **82**:9–15; 1982.
5. Schoenberg, M. H.; Fredholm, B. B.; Haglund, U.; Jung, H.; Sellin, D.; Younes, M.; Schildberg, F. W. Studies on the oxygen radical mechanism in the small intestinal reperfusion damage. *Acta Physiol. Scand.* **124**:581–589; 1985.
6. Cockerham, L. G.; Arroyo, C. M.; Hampton, J. D. Effects of 4-hydroxypyrazolo (3,4-d) pyrimidine (Allopurinol) on postirradiation blood flow. submitted for publication.
7. Anbar, M.; Bambenek, M.; Ross, A. B. Selected specific rates of reactions of transients from water in aqueous solutions. I. Hydrated electron. NSRDS-NBS 43. Washington, DC: U.S. Government Printing Office; 1973.
8. Perkins, M. J. Spin trapping. In: Gold, V.; Bethall, D.; eds. *Advances in physical organic chemistry*, Vol. 17. New York: Academic Press; 1980:1–64.
9. Janzen, E. G. A critical review of spin trapping in biological systems. In: Pryor, W. A., ed. *Free radicals in biology*, Vol. IV New York: Academic Press; 1980:115–154.
10. Farragi, M.; Carmichael, A.; Riesz, P. OH radical formation by photolysis of aqueous porphyrin solutions. A spin trapping and ESR study. *Int. J. Radiat. Biol.* **46**:703–713; 1984.
11. Buettner, G. R.; Oberley, L. W. Considerations in spin trapping of superoxide and hydroxyl radicals in aqueous solutions using 5,5-dimethyl-1-pyrroline-1-oxide. *Biochem. Biophy. Res. Commun.* **83**:69–74; 1978.
12. Kalyanaraman, B.; Felix, C. C.; Sealy, R. C. Photoionization of melanin precursors: an electron spin resonance investigation using the spin trap 5,5-dimethyl-1-pyrroline-1-oxide (DMPO). *Photochem. Photobiol.* **36**:5–12; 1982.
13. Rustgi, S.; Riesz, P. Spin trapping of the reactions of hydrated electrons with dipeptides. *Int. J. Radiat. Biol.* **34**:127–148; 1978.
14. Dorfman, L. M.; Adams, G. E. Reactivity of the hydroxyl radical in aqueous solutions. NSRDS-NBS 46. Washington, DC: U.S. Government Printing Office, 1973.

Free Radical Biology & Medicine, Vol. 4, pp. 279–284, 1988
Printed in the USA. All rights reserved

0891-5849/88 $3.00 + .00
©1988 Pergamon Press plc

Original Contribution

EFFECT OF 4-HYDROXYPYRAZOLO (3,4-d) PYRIMIDINE (ALLOPURINOL) ON POSTIRRADIATION CEREBRAL BLOOD FLOW: IMPLICATIONS OF FREE RADICAL INVOLVEMENT

LORRIS G. COCKERHAM, CARMEN M. ARROYO, and JOHN D. HAMPTON
Physiology and Radiation Science Departments
Armed Forces Radiobiology Research Institute
Bethesda, Maryland 20814-5145

(*Received* 30 *April* 1987, *Revised* 17 *July* 1987; *Accepted* 29 *July* 1987)

Abstract—In an attempt to elucidate mechanisms underlying the irradiation-induced decrease in regional cerebral blood flow (rCBF) in primates, hippocampal and hypothalamic blood flows of rhesus monkeys were measured by hydrogen clearance, before and after exposure to 100 Gy, whole body, gamma irradiation. Systemic blood pressures were monitored simultaneously. Compared to control animals, the irradiated monkeys exhibited an abrupt decline in systemic blood pressure to 35% of the preirradiation level within 10 min postirradiation, falling to 12% by 60 min. A decrease in hippocampal blood flow to 32% of the preirradiation level was noted at 10 min postirradiation, followed by a slight recovery to 43% at 30 min and a decline to 23% by 60 min. The hypothalamic blood flow of the same animals showed a steady decrease to 43% of the preirradiation levels by 60 min postirradiation. The postradiation systemic blood pressure of the allopurinol treated monkeys was not statistically different from the untreated, irradiated monkeys and was statistically different from the control monkeys. However, the treated, irradiated monkeys displayed rCBF values that were not significantly different from the nonirradiated controls. These findings suggest the involvement of free radicals in the postirradiation decrease in regional cerebral blood flow but not necessarily in the postirradiation hypotension seen in the primate.

Keywords—Allopurinol, Cerebral blood flow, Free radicals, Hippocampus, Hypothalamus, Radiation

INTRODUCTION

Early transient incapacitation (ETI) is the complete cessation of motor performance, occurring transiently and within the first 30 min following exposure to supralethal doses of ionizing irradiation.[1] Studies have reported severe decreases in regional cerebral blood flow (rCBF) in primates at the same postirradiation time after receiving supralethal doses of gamma irradiation.[2,3] One study[4] demonstrated a dramatic fall of total cerebral blood flow following a single, 25 Gy, ^{60}Co exposure.

The irradiation-induced reduction in cerebral blood flow may employ intermediate mediators such as free radicals[5] produced with exposure to ionizing irradiation.[6–8] Free radical interactions have been implicated in a large number of pathological conditions including irradiation injury, ischemia, microvascular injury, and cell membrane damage.[6,7,9–12] The triphasic cerebral ischemic response seen after irradiation[2,3] may be even more damaging than complete ischemia[13] since reperfusion may lead to the formation of additional free radicals.[14,15] A possible mode of pharmacologic intervention may be the introduction of superoxide dismutase[16,17] or allopurinol[15,17] since both have been used to attenuate the biochemical and functional damage usually associated with free radical production.

This study was designed to determine whether the inhibition of free radical formation via the preirradiation administration of allopurinol would be successful in altering the postirradiation hypotension and reduced rCBF. Two regions of the brain previously studied,[2–4] the hippocampus and the hypothalamus, were selected for the determination of blood flow in this study since a dramatic, postirradiation decrease in blood flow has been reported in these areas.

Correspondence should be addressed to: Lorris G. Cockerham, Ph.D., Air Force Office of Scientific Research, AFOSR/NL, Bldg. 410, Bolling AFB, DC 20332-6448.

MATERIALS AND METHODS

Seventeen rhesus monkeys (*Macaca mulatta*), weighing between 2.6 and 3.8 kg (3.1 ± 0.26 SEM) were used in this study. The animals were divided randomly into three groups as follows: Group I—six sham-irradiated monkeys; Group II—six irradiated monkeys; and Group III—five monkeys given allopurinol orally (50 mg/kg) for 2 days prior to irradiation.[17] Food was withheld from all animals for 18 h before the experiment, but water was available *ad libitum*. Research was conducted according to the principles enunciated in the "Guide for the Care and Use of Laboratory Animals" prepared by the Institute of Laboratory Animal Resources, National Research Council. The monkeys were initially anesthetized in their cages with an i.m. injection of Ketamine hydrochloride (20 mg/kg) with 0.015 mg/kg Atropine sulfate and were then moved to the laboratory where the remainder of the experiment was conducted.

A systemic venous catheter was used to administer physiological saline and the primary anesthetic, α-Chloralose (100 mg), with supplemental infusions provided as needed, based on heart rate, blood pressure, respiration rate, blood pH, and peripheral reflexes. A femoral arterial catheter was used to withdraw blood for blood chemistry and blood gas determinations and to measure systemic arterial blood pressure via a Stathem P23 Db pressure transducer.

Approximately 2 h before irradiation or sham-irradiation, the animals were intubated with a cuffed endotracheal tube and ventilated using a forced volume respirator to maintain a stable blood pH and oxygen tension. After insertion of the endotracheal tube, each animal was placed on a circulating water blanket to maintain body temperature between 36° and 38°C. A rectal probe was inserted to monitor body temperature.

The animal's head was positioned on the headholder of a stereotaxic instrument (David Kopf Instruments, Tujunga, CA) and the scalp shaved and incised, allowing access to the skull. Using the stereotaxic micromanipulator, the skull was marked for insertion of four electrodes and small burr holes were drilled through the skull at these marks. Again, using the micromanipulator, one electrode was placed in the left and one in the right hippocampus.[19] In the same manner, one electrode was placed in the left and one in the right supraoptic nucleus of the hypothalamus. The electrodes were Teflon-coated, platinum-iridium wire of 0.178 mm diameter, encased in, but insulated from, rigid stainless steel tubing (22 gauge spinal needle) with exposed tips of approximately 2 mm. The exposed dura was covered with moistened pledgetts and the electrodes were sealed and secured to the skull with dental acrylic. A stainless steel reference electrode was placed in neck tissue.

Regional cerebral blood flow was measured by the hydrogen clearance technique for 30 min before irradiation or sham-irradiation and for 60 min after.[20,21] This technique is essentially an amperometric method, which measures the current induced in a platinum electrode by the reduction of hydrogen. The current produced has a linear relationship with the concentration of hydrogen in the tissue.[22] Hydrogen was introduced into the blood via inhalation through the endotracheal tube at a rate of approximately 5% of the normal respiratory intake for each flow measurement. Blood flow was measured by each of the four electrodes every 10 min. The electrodes were maintained electrically at +600 mV in respect to the reference electrode, to reduce possible oxygen and ascorbate interference. This method has been successfully employed in several similar studies.[2,3,18]

After 30 min of recording, the animals were disconnected from the respirator and recording apparatus to facilitate irradiation in a separate room. The animals were reconnected to the respirator and recording apparatus at 4 min postirradiation or sham-irradiation and measurements were continued for a minimum of 60 min. At 30 and 10 min preirradiation or sham-irradiation, and at 6, 15, 30, 45, and 60 min postirradiation or sham-irradiation, blood samples were taken via the arterial catheter to monitor stability of blood pH and oxygen tension, and respiration was adjusted to maintain preirradiation levels. Mean systemic arterial blood pressure was determined via the arterial catheter for the duration of the experiment. After termination of the measurements, while still under anesthesia, the animals were humanely euthanized with an i.v. injection of saturated $MgSO_4$, and the electrodes examined visually via disection for verification of placement.

Irradiation was accomplished with a bilateral, whole-body, exposure to gamma ray photons from a cobalt-60 source located at the Armed Forces Radiobiology Research Institute. Exposure was limited to a mean of 1.38 min at 74 Gy/min steady state, free-in-air. Dose rate measurements at depth were made with an ionization chamber placed in a tissue equivalent model. The measured midline tissue dose rate was 69 Gy/min, producing a calculated total dose of 100 Gy, taking into account the rise and fall of the radiation source.

Blood pressure and blood flow data were grouped into 10 min intervals, measured in relation to midtime of radiation, and plotted at the middle of the interval. The Wilcoxon Rank Sum Test was used for the statistical analysis of the data. A 95% level of confidence was employed to determine significance. Since all the animals were treated identically before irradiation or sham-irradiation, and since the preradiation data for

the control and test animals showed no significant difference. the preradiation data for the irradiated and sham-irradiated animals were combined.

RESULTS

As seen in Figure 1, the mean systemic arterial blood pressure (MABP) of untreated, irradiated animals decreased to 35% of the preradiation mean of 106.0 ± 2.3 mm Hg within 10 min postradiation. This was followed by a steady decline to a 60-min postirradiation level that was 20% of the preirradiation values. After sham-irradiation there was no significant change in MABP for the six control monkeys but the values for the group differed significantly ($p \leq 0.05$) from the other two groups. The MABP for the allopurinol treated, irradiated group did not display a statistically significant difference from the untreated, irradiated group. The respiration of each subject was maintained at preradiation levels and, although not presented, the blood gas data revealed a general stability of blood pH and oxygen tension throughout the experimental period.

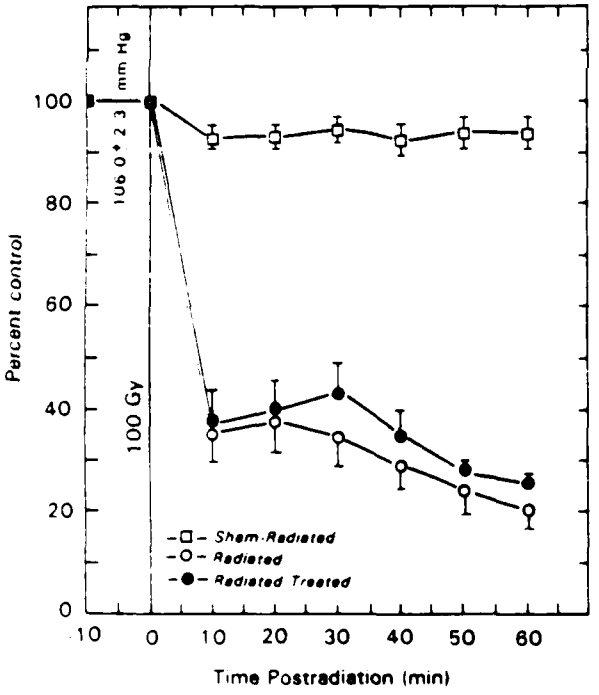

Fig. 1. Percent change in mean arterial blood pressure after exposure to 100 Gy, whole-body, gamma irradiation (±SEM), compared to a preirradiation mean of 106.0 ± 2.3 mm Hg. Animals in the sham-irradiated group ($n = 6$) were given physiological saline for 60 min before and after sham-irradiation. The untreated, irradiated group ($n = 6$) also received saline but were exposed to 100 Gy gamma irradiation. The treated, irradiated group ($n = 5$) also received saline and irradiation but were given allopurinol (50 mg/kg, orally) for 2 days prior to irradiation.

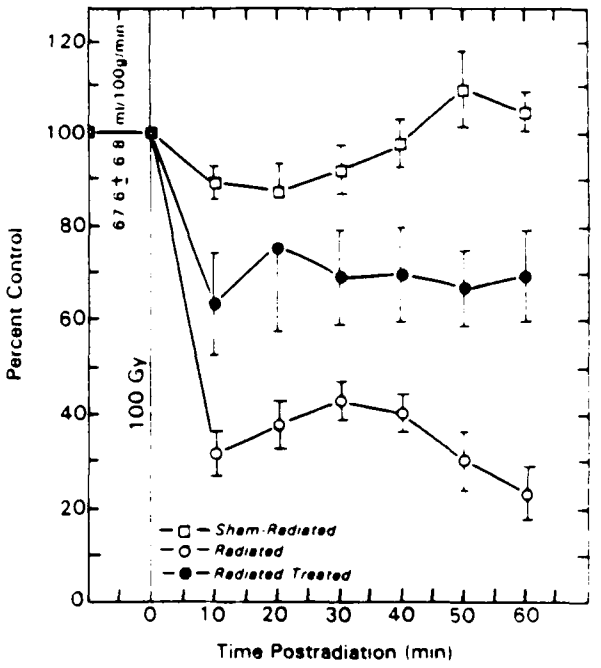

Fig. 2. Percent change in hippocampal blood flow after exposure to 100 Gy, whole-body, gamma irradiation (±SEM), compared to a preirradiation mean of 67.6 ± 6.8 ml/g of tissue/min. Animals in the sham-irradiated group ($n = 6$) were given physiological saline for 60 min before and after sham-irradiation. The untreated, irradiated group ($n = 6$) also received saline but were exposed to 100 Gy gamma irradiation. The treated, irradiated group ($n = 5$) also received saline and irradiation but were given allopurinol (50 mg/kg, orally) for 2 days prior to irradiation.

The preirradiation hippocampal blood flow, as shown in Figure 2, was 67.6 ± 6.8 ml per 100 g of tissue per min. The postirradiation blood flow for the sham-irradiated group of monkeys showed no significant changes for the 60-min observation period while the values for the untreated, irradiated monkeys showed a rapid, significant decline to 32% of the preirradiation levels by 10 min postirradiation. Following a slight increase to 43% below preirradiation levels at 30 min postirradiation, the blood flow values decreased to 23% of the preirradiation levels by 60 min postirradiation. The control and untreated, irradiated groups of monkeys were significantly different ($p \leq 0.05$) from each other at all postirradiation measurement points. The allopurinol treated, irradiated monkeys displayed a postirradiation hippocampal blood flow that decreased to only 63% of the preirradiation level at 10 min. Even though they did not drop any lower, these levels were not significantly different from the untreated, irradiated group's blood flow levels until 40 min postirradiation. Likewise, the blood flow levels of the treated, irradiated monkeys were not significantly different from those of the control monkeys until 50 min postirradiation.

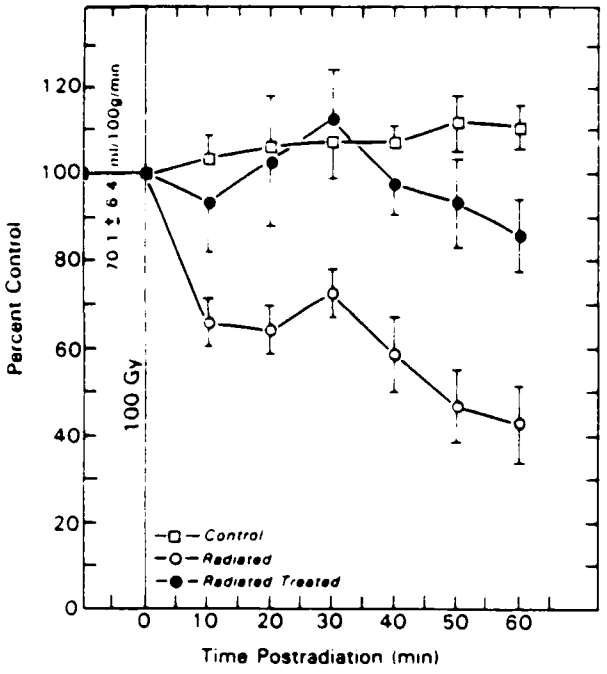

Fig. 3. Percent change in hypothalamic blood flow after exposure to 100 Gy, whole-body, gamma irradiation (±SEM), compared to a preirradiation mean of 70.1 ± 6.4 ml/g of tissue/min. Animals in the sham-irradiated group (n = 6) were given physiological saline for 60 min before and after sham-irradiation. The untreated, irradiated group (n = 6) also received saline but were exposed to 100 Gy gamma irradiation. The treated, irradiated group (n = 5) also received saline and irradiation but were given allopurinol (50 mg/kg, orally) for 2 days prior to irradiation.

Figure 3 displays a preirradiation mean blood flow of 70.1 ± 6.4 ml per 100 g of tissue per minute in the hypothalamus. The postirradiation blood flow for the sham-irradiated group of monkeys showed no significant changes for the 60 min observation period while the values for the untreated, irradiated monkeys showed a decline to 43% of the preirradiation levels by 60 min postirradiation. These levels became significantly different ($p \leq 0.05$) from those of the sham-irradiated group at 10 min postirradiation and remained that way for the remainder of the observations. The blood flow measurements of monkeys pretreated with allopurinol were not significantly different from those of the control monkeys at any time postirradiation. However, a significant difference was seen between the blood flow measurement of the pretreated, irradiated group and the untreated, irradiated group beginning at 40 min postirradiation.

DISCUSSION

Postirradiation hypotension has been well documented in the rhesus monkey and a critical postirradiation mean arterial blood pressure (MABP) of 50%–60% of the preirradiation MABP must be maintained for adequate autoregulation of cerebral circulation.[4,23,24] The initial precipitous decline in MABP to 35% of the preirradiation levels may then be associated with the similar immediate decrease in blood flow seen in both the hippocampus and hypothalamus of the untreated, irradiated animals. In fact the decline in MABP and cerebral blood flow (CBF) reported here corresponds closely in time with the observed occurrence of ETI[23,25,26] and suggests a causal relationship between the depressed MABP, CBF and the appearance of ETI.

Autoregulation of cerebral blood flow appeared to be intact in animals pretreated with allopurinol, even though the postirradiation MABP fell to approximately 35% of the preirradiation level. The difference noted in the effect of allopurinol in the hippocampus and the hypothalamus may be attributed to the presence of fenestrations of the blood–brain barrier near the hypothalamus.[27,28] These fenestrations, or windows, would allow the preirradiation administered allopurinol to enter the hypothalamus before irradiation. Their absence in the area of the hippocampus would inhibit the entrance of allopurinol into that area until after the irradiation-induced alteration of the blood–brain barrier.[29] Therefore, the radioprotective effect of allopurinol would be present in the hypothalamus at the time of irradiation, but not in the hippocampus until after irradiation.

Allopurinol interferes with the xanthine oxidase catalyzed production of free radicals and has been used to attenuate cellular damage associated with the reperfusion induced production of free radicals.[30,31] This action would have been expected during the partial cerebral reperfusion that occurred between 10 and 30 min postirradiation. However, the administration of allopurinol altered the immediate postirradiation decrease in cerebral blood flow, thereby eliminating the reperfusion-xanthine oxidase production of free radicals. It is therefore highly likely that the immediate action of allopurinol may have been by some means other than xanthine oxidase inhibition.

A possible explanation of the mechanistic effect of allopurinol in diminishing the postirradiation decrease in rCBF is an interference in the formation of superoxide radicals. Superoxide radicals can be generated in the reaction of hydrated electrons or hydrogen atoms with dissolved oxygen following gamma irradiation of aqueous solutions. This radiolytically-formed free radical is involved in oxidative chain reactions[32] with the possibility of interconversion and postirradiation generation of other forms of activated oxygen, leading indirectly to further irradiation-induced cellular damage.[33] A possible mode of pharmacologic intervention may well be the introduction of allopurinol to intervene

in the production of free radicals, thereby explaining why treatment with allopurinol would maintain rCBF during the entire observation period even with the presence of profound hypotension in treated animals at 60 min. Thus, the allopurinol prevention of irradiation-induced free radical formation would allow the maintainance of rCBF in the initial 20–30 min. Thus, the allopurinol prevention of irradiation-induced free radical formation would allow the maintainance of rCBF in the initial 20–30 min. Therefore, there would be no reperfusion-induced formation of additional free radicals, allowing the rCBF to be maintained during the second portion of the observation period.

Examination of the chemical/physical structure of allopurinol suggests that its effectiveness may be due to an ability to scavage hydrated electrons and hydrogen atoms that would react with oxygen to form superoxide. Certainly, this may be elucidated further with spin trapping experiments in gamma irradiated aqueous solutions of allopurinol in the presence of a spin trap such as DMPO (5,5-dimethyl-1-pyroline-1-oxide). This spin trapping [34] consists of reacting a short-lived free radical, such as superoxide, with a spin trap, usually a nitrone or nitroso compound, producing a longer-lived nitrooxide radical which can be detected and identified by electron spin resonance (ESR).

In conclusion, we have shown that the administration of allopurinol will alter significantly the postirradiation-reduced regional cerebral blood flow without affecting the irradiation induced hypotension. We have also introduced a theoretical mechanism through which the administration of allopurinol may prevent an irradiation-induced reduction in rCBF. The next logical step will be to show that allopurinol actually does prevent the irradiation-induced production of free radicals. Further study with spin trapping experiments may be able to elucidate the mechanism.

Acknowledgments—The authors thank Mr. E. J. Golightly for technical assistance and Mrs. M. H. Owens for preparation of the manuscript. This research was supported by the Armed Forces Radiobiology Research Institute, Defense Nuclear Agency, under work unit MJ00053. Views presented in this paper are those of the authors; no endorsement by the Defense Nuclear Agency has been given or should be inferred.

REFERENCES

1. Kimeldorf, D. J., Hunt, E. L. Neurophysiological effects of ionizing radiation. In: Kimeldorf, D. J., Hunt, E. L., editors. *Ionizing Radiation: Neutral Function and Behavior*. New York: Academic Press; 1965:59–108.
2. Cockerham, L. G., Cerveny, T. J., Hampton, J. D. Postradiation regional cerebral blood flow in primates. *Aviat. Space Environ. Med.* **57**:578–582; 1986.
3. Cockerham, L. G., Doyle, T. F., Pautler, E. L., Hampton, J. D. Disodium cromoglycate, a mast cell stabilizer, alters postradiation regional cerebral blood flow in primates. *J. Toxicol. Environ. Health* **18**:91–101; 1986.
4. Chapman, P. H., Young, R. J. Effect of cobalt-60 gamma irradiation on blood pressure and cerebral blood flow in the *Macaca mulatta*. *Radiat. Res.* **35**:78–85; 1968.
5. Ohmori, H., Komoriya, K., Azuma, A., Kurosumi, S., Hashimoto, Y. Xanthine oxidase-induced histamine release from isolated rat peritoneal mast cells: involvement of hydrogen peroxide. *Biochem. Pharmacol.* **28**:333–334; 1979.
6. Del Maestro, R. F., Thaw, H. H., Bjork, J., Planker, M., Arfors, K.-E. Free radicals as mediators of tissue injury. *Acta Physiol. Scand. Suppl.* **492**:43–57; 1980.
7. Del Maestro, R. F. An approach to free radicals in medicine and biology. *Acta Physiol. Scand. Suppl.* **492**:153–168; 1980.
8. Kennedy, A. R., Troll, W., Little, J. B. Role of free radicals in the initiation and promotion of radiation transformation *in vitro*. *Carcinogenesis* **5**(10):1213–1218; 1984.
9. Hammond, B., Kontos, H. A., Hess, H. L. Oxygen radicals in the adult respiratory distress syndrome, in myocardial ischemia and reperfusion injury, and in cerebral vascular damage. *Can. J. Physiol. Pharmacol.* **63**:173–187; 1985.
10. Konat, G. W., Wiggins, R. C. Effect of reactive oxygen species on myelin membrane proteins. *J. Neurochem.* **45**:1113–1118; 1985.
11. Kontos, H. A. Oxygen radicals in cerebral vascular injury. *Circ. Res.* **57**(4):508–516; 1985.
12. McCord, J. M. Oxygen-derived free radicals in postischemic tissue injury. *New England J. Med.* **312**(3):159–163; 1985.
13. Rehncrona, S., Siesjo, B. K., Smith, D. S. Reversible ischemia of the brain: Biochemical factors influencing restitution. *Acta Physiol. Scand. Suppl.* **492**:135–140; 1980.
14. Julicher, R. H. M., Tijburg, L. B. M., Sterrenberg, L., Bast, A., Koomen, J. M., Noordhoek, J. Decreased defence against free radicals in rat heart during normal reperfusion after hypoxic, ischemic and calcium-free perfusion. *Life Sci.* **35**(12):1281–1288; 1984.
15. Peterson, D. A., Asinger, R. W., Elsperger, K. J., Homans, D. C., Eaton, J. W. Reactive oxygen species may cause myocardial reperfusion injury. *Biochem. Biophys. Res. Communications* **127**(1):87–93; 1985.
16. Burton, K. P. Superoxide dismutase enhances recover following myocardial ischemia. *A. J. Physiol.* **248**:H637–H643; 1985.
17. Parks, D. A., Bulkley, G. B., Granger, D. N., Hamilton, S. R., McCord, J. M. Ischemic injury in the cat small intestine: role of superoxide radicals. *Gastroenterology* **82**:9–15; 1982.
18. Cockerham, L. G., Pautler, E. L., Carraway, R. E., Cochrane, D. E., Hampton, J. D. Effect of disodium cromoglycate (DSCG) and antihistamines on postirradiation cerebral blood flow and plasma levels of histamine and neurotensin. *Fundam. Appl. Toxicol.*; in press, 1988.
19. Snider, R. S., Lee, J. C. *A Stereotaxic Atlas of the Monkey Brain (Macaca mulatta)*. Chicago; The University of Chicago Press; 1961.
20. Aukland, K., Bower, B. B., Berliner, R. W. Measurement of local blood flow with hydrogen gas. *Circ. Res.* **14**:164–287; 1964.
21. Young, W. H_2 clearance measurement of blood flow. A review of technique and polarographic principles. *Stroke* **11**(5):552–564; 1980.
22. Hyman, E. S. Linear system for quantitating hydrogen at a platinum electrode. *Circ. Res.* **9**:1093–1097; 1961.
23. Doyle, T. F., Curran, C. R., Turns, J. E. The prevention of radiation-induced, early transient incapacitation of monkeys by an antihistamine. *Proc. Soc. Exper. Biol. Med.* **145**:1018–1024; 1974.
24. Farrar, J. K., Gamache, F. W. Jr., Ferguson, G. G., Barker, J., Varkey, G. P., Drake, C. G. Effects of profound hypotension on cerebral blood flow during surgery for intracranial aneurysms. *J. Neurosurg.* **55**:857–864; 1981.
25. Curran, C. R., Young, R. W., Davis, W. F. The performance of primates following exposure to pulsed whole-body gamma-neu-

tron radiation. AFRRI SR73-1. MD: Armed Forces Radiobiology Research Institute, Bethesda, 1973

26. Bruner, A. Immediate dose-rate effects of ^{60}Co on performance and blood pressure in monkeys. *Radiat. Res.* **70**:378–390; 1977
27. Landas, S., Fischer, J., Wilkin, L.D., Mitchell, L.D., Johnson, A.K., Turner, J.W., Theriac, M., Moore, K.C. Demonstration of regional blood-brain barrier permeability in human brain. *Neurosci. Letters* **57**:251–256; 1985.
28. Pardridge, W.M. Strategies for delivery of drugs through the blood-brain barrier. *Ann. Reports in Medicinal Chem.* **20**:305–313, 1985.
29. Storm, A.J., Van Der Kogel, A.J., Nooter, K. Effect of X-irradiation on the pharmacokinetics of methotrexate in rats: alteration of the blood-brain barrier. *Eur. J. Cancer Clin. Oncol.* **21**(6):759–764, 1985
30. Granger, D.N., Hollwarth, M.E., Parks, D.A. Ischemia-reperfusion injury: role of oxygen-derived free radicals. *Acta Physiol. Scand. Suppl.* **548**:47–63; 1986
31. Parks, D.A., Granger, D.N. Xanthine oxidase: biochemistry, distribution and physiology. *Acta Physiol. Scand. Suppl.* **548**:87–99; 1986.
32. Fridovich, I. Oxygen radicals, hydrogen peroxide, and oxygen toxicity. In: Pryor, W.A., editor. *Free Radicals in Biology*. Vol. 1. New York: Academic Press; 1976: 239–277
33. Greenstock, C.L. Oxy-radicals and radiobiological oxygen effect. *Israel J. Chem.* **24**:1–10; 1984
34. Janzen, E.G. A critical review of spin trapping in biological systems. In: Pryor, W.A., editor. *Free Radicals in Biology*. Vol. 4. New York: Academic Press, 1980: 115–154

FUNDAMENTAL AND APPLIED TOXICOLOGY **10**, 233–242 (1988)

Effect of Disodium Cromoglycate (DSCG) and Antihistamines on Postirradiation Cerebral Blood Flow and Plasma Levels of Histamine and Neurotensin[1]

L. G. COCKERHAM, E. L. PAUTLER, R. E. CARRAWAY, D. E. COCHRANE, AND J. D. HAMPTON

Physiology Department, Armed Forces Radiobiology Research Institute, Bethesda, Maryland 20814-5145; Department of Physiology and Biophysics, College of Veterinary Medicine and Biomedical Science, Colorado State University, Fort Collins, Colorado 80523; Department of Physiology, University of Massachusetts Medical School, Worcester, Massachusetts 01605; and Department of Biology, Tufts University, Medford, Massachusetts 02155

Received March 24, 1987; accepted August 18, 1987

Effect of Disodium Cromoglycate (DSCG) and Antihistamines on Postirradiation Cerebral Blood Flow and Plasma Levels of Histamine and Neurotensin. COCKERHAM, L. G., PAUTLER, E. L., CARRAWAY, R. E., COCHRANE, D. E., AND HAMPTON, J. D. (1988). *Fundam. Appl. Toxicol.* **10**, 233–242. In an attempt to elucidate mechanisms underlying the irradiation-induced decrease in regional cerebral blood flow (rCBF) in primates, hippocampal and visual cortical blood flows of rhesus monkeys were measured by hydrogen clearance, before and after exposure to 100 Gy, whole-body, γ irradiation. Systemic blood pressures were monitored simultaneously. Systemic arterial plasma histamine and neurotensin levels were determined preirradiation and postirradiation. Compared to control animals, the irradiated monkeys exhibited an abrupt decline in systemic blood pressure to 23% of the preirradiation level within 10 min postirradiation, falling to 12% by 60 min. A decrease in hippocampal blood flow to 32% of the preirradiation level was noted at 10 min postirradiation, followed by a slight recovery to 43% at 30 min and a decline to 23% by 60 min. The cortical blood flow for the same animals showed a steady decrease to 29% of the preirradiation levels by 60 min postirradiation. Animals given the mast cell stabilizer disodium cromoglycate and the antihistamines mepyramine and cimetidine before irradiation did not exhibit an abrupt decline in blood pressure but displayed a gradual decrease to a level 33% below preirradiation levels by 60 min postirradiation. Also, the treated, irradiated monkeys displayed rCBF values that were not significantly different from the nonirradiated controls. The plasma neurotensin levels in the irradiated animals, treated and untreated, indicated a nonsignificant postirradiation increase above control levels. However, the postirradiation plasma histamine levels in both irradiated groups showed an increase of approximately 1600% above the preirradiation levels and the postirradiation control levels. These findings implicate histamine in the postirradiation hypotension, but not necessarily in the direct responsibility for the decrease in regional cerebral blood flow seen immediately postirradiation in the primate.

Some of the many consequences which result from exposure to high levels of ionizing radiation are dramatic changes in the ability of an animal to perform a trained task. Early transient incapacitation (ETI), characterized as a complete but temporary cessation of trained behavior occurring within the first 30 min postirradiation, is one event which follows exposure to supralethal doses of ionizing radiation (Kimeldorf and Hunt, 1965). This dramatic alteration in motor function is characterized by a transient reduction in performance, with recovery, followed by a recurring, gradual performance decrement (PD),

[1] Supported by Armed Forces Radiobiology Research Institute, Defense Nuclear Agency, under Research Work Unit MJ 00053. The views presented in this paper are those of the authors. No endorsement by the Defense Nuclear Agency has been given or should be inferred.

0272-0590/88 $3.00

which may or may not be associated with ETI (Curran *et al.*, 1973). Irradiation-induced hypotension has been implicated as the cause of ETI found with supralethal irradiation exposure (Miletich and Strike, 1970). However, postirradiation hypotension does not occur with equal frequency in all species, having been reported in monkeys and rats but not in cats and dogs (Miletich and Strike, 1970; Chaput *et al.*, 1972; Pitchford, 1968). Likewise, ETI was not seen in dogs following irradiation exposure of up to 400 Gy (1 Gy = 100 rad) (Chaput *et al.*, 1972; Pitchford, 1968); however, a dose-related, progressive PD was reported with those animals exposed to doses of 100–300 Gy (Pitchford, 1968). A recent study reported a performance decrement in rats exposed to a 100 Gy, whole-body, bilateral dose of γ radiation received from a ^{60}Co source (Cockerham *et al.*, 1984). ETI has been reported in monkeys (Bruner *et al.*, 1975; Franz, 1985) and in miniature swine (Chaput and Wise, 1969), although the ETI seen in swine differed from that seen in monkeys by the frequent accompaniment of convulsions and spasms of the extremities. Monkeys were selected for this study because they exhibit a transient decrement in performance similar to that described in humans who were accidentally irradiated (Hunt, 1987).

Studies have reported elevations of circulating blood histamines in humans undergoing radiation therapy (Lasser and Stenstrom, 1954), and increases in nonhuman primate plasma histamine levels (Alter *et al.*, 1983; Cockerham *et al.*, 1986a) following irradiation. Histamine may be implicated in radiation-induced hypotension (Alter *et al.*, 1983) and in postirradiation reduced cerebral blood flow (Cockerham *et al.*, 1986a). Also, antihistamines have been used to modify the irradiation-induced release of histamine and early transient incapacitation in the monkey (Doyle *et al.*, 1974; Doyle and Strike, 1977).

The release of histamine from mast cells by ionizing radiation may not be effected directly, but may employ an intermediate chemical mediator such as neurotensin. Reports of *in vivo* neurotensin-mediated release of histamine include rat whole-body infusion (Oishi *et al.*, 1983), rat hindquarter perfusion (Kerouac *et al.*, 1984), and rat head perfusion (Rioux *et al.*, 1985) experiments. Pretreatment with the mast cell stabilizer, disodium cromoglycate (DSCG, cromolyn sodium), inhibited the neurotensin-induced release of histamine (Carraway *et al.*, 1982; Cochrane *et al.*, 1986; Kerouac *et al.*, 1984; Oishi *et al.*, 1983; Rioux *et al.*, 1985), and was successful in diminishing the radiation-induced decrease in cerebral blood flow (Cockerham *et al.*, 1986b).

In the present study we attempt to evaluate further the effect of DSCG on radiation-released histamine, postradiation hypotension, and reduced regional cerebral blood flow (rCBF) in two contrasting regions of the brain. Two regions of the brain not previously studied (Cockerham *et al.*, 1986a,b) were selected for the determination of blood flow in this study. The hippocampus was selected as the first region of interest because this area of the brain is particularly vulnerable to oxygen deprivation (Kirino and Sano, 1984; Suzuki *et al.*, 1983). The second region of interest, the visual cortex, is an area that may be involved with the reduced visual discrimination performance seen in the monkey following 50 Gy γ-neutron radiation (de Haan *et al.*, 1969) and, also, is reported to show changes in neuronal activity following ischemia (Suzuki *et al.*, 1983). We also attempt to determine if the postirradiation systemic plasma levels of histamine and neurotensin are changed with DSCG and antihistamine pretreatment.

The purpose of this investigation, therefore, is threefold: first, to determine if the combined use of DSCG and antihistamines affects the irradiation-induced release of histamine, postirradiation hypotension, and reduced regional cerebral blood flow; second, to determine if the systemic plasma level of neurotensin is changed significantly following irradiation; and finally, if there is an irradiation-induced release of neurotensin, to de-

termine if DSCG will inhibit the neurotensin-induced release of histamine in primates.

Understanding the physiological basis for irradiation-induced incapacitation and shock is essential to providing protection against these irradiation effects, for interpreting the effects of nuclear accidents, and for predicting the effects of nuclear warfare in order to prepare for casualty treatment.

MATERIALS AND METHODS

Sixteen rhesus monkeys (*Macaca mulatta*), weighing between 2.3 and 3.5 kg (2.9 ± 0.08 SE), were used in this study. The animals were divided randomly into two groups of six animals each and one group of four animals, as follows: Group I—six sham-irradiated monkeys; Group II—six irradiated monkeys; and Group III—four monkeys given an iv infusion of physiological saline containing the H_1 blocker mepyramine (pyrilamine) (0.5 mg/min) and the H_2 blocker cimetidine (0.25 mg/min) for 1 hr before and for 1 hr after irradiation, and the mast cell stabilizer DSCG by iv infusion (100 mg/kg) 5 min before irradiation. Food was withheld from all animals for 18 hr before the experiment, but water was available *ad libitum*. Research was conducted according to the principles enunciated in the *Guide for the Care and Use of Laboratory Animals* prepared by the Institute of Laboratory Animal Resources, National Research Council. The monkeys were initially anesthetized in their cages with an im injection of ketamine hydrochloride (20 mg/kg) with 0.015 mg/kg atropine sulfate and were then moved to the laboratory where the remainder of the experiment was conducted.

A systemic venous catheter was used to administer physiological saline and the primary anesthetic, α-chloralose (100 mg), with supplemental infusions provided as needed, based on heart rate, blood pressure, respiration rate, blood pH, and peripheral reflexes. A femoral arterial catheter was used to withdraw blood for blood chemistry and blood gas determinations and to measure systemic arterial blood pressure via a Stathem P23 Db pressure transducer.

Approximately 2 hr before irradiation or sham-irradiation, the animals were intubated with a cuffed endotracheal tube and ventilated using a forced volume respirator to maintain a stable blood pH and oxygen tension. After insertion of the endotracheal tube, each animal was placed on a circulating water blanket to maintain body temperature between 36 and 38°C. A rectal probe was inserted to monitor body temperature.

The animal's head was positioned on the headholder of a stereotaxic instrument (David Kopf Instruments, Tujunga, CA) and the scalp was shaved and incised, allowing access to the skull. Using the stereotaxic micromanipulator, the skull was marked for insertion of four electrodes and small burr holes were drilled through the skull at these marks. Again, using the micromanipulator, one electrode was placed in the left and one in the right hippocampus (Snider and Lee, 1961). In the same manner, one electrode was placed in the left and one in the right visual cortex, 4 mm to each side of the longitudinal fissure. The latter two electrodes were placed so that the tips were 2.5 mm below the surface to ensure that measurements would be taken from the cortical grey matter. The electrodes were Teflon-coated, platinum–iridium wire of 0.178-mm diameter, encased in, but insulated from, rigid stainless-steel tubing (22-ga spinal needle) with exposed tips of approximately 2 mm. The exposed dura was covered with moistened pledgetts and the electrodes were sealed and secured to the skull with dental acrylic. A stainless-steel reference electrode was placed in neck tissue.

Regional cerebral blood flow was measured by the hydrogen clearance technique for 30 min before irradiation or sham-irradiation and for 60 min after. This technique is essentially an amperometric method, which measures the current induced in a platinum electrode by the reduction of hydrogen. The current produced has a linear relationship with the concentration of hydrogen in the tissue (Hyman, 1961). Hydrogen was introduced into the blood via inhalation through the endotracheal tube at a rate of approximately 5% of the normal respiratory intake for each flow measurement. Blood flow was measured by each of the four electrodes every 10 min. The electrodes were maintained electrically at +600 mV in respect to the reference electrode, to reduce possible oxygen and ascorbate interference. This method has been successfully employed in several similar studies (Cockerham *et al.*, 1986a,b).

After 30 min of recording, the animals were disconnected from the respirator and recording apparatus to facilitate irradiation in a separate room. The animals were reconnected to the respirator and recording apparatus at 4 min postirradiation or sham-irradiation and measurements were continued for a minimum of 60 min. At 30 and 10 min preirradiation or sham-irradiation, and at 2, 4, 6, 15, 30, 45, and 60 min postirradiation or sham-irradiation, blood samples were taken via the arterial catheter to determine plasma histamine and neurotensin levels. Blood samples were also taken to monitor stability of blood pH and oxygen tension, and respiration was adjusted to maintain preirradiation levels. Mean systemic arterial blood pressure was determined via the arterial catheter for the duration of the experiment. After termination of the measurements, while still under anesthesia, the animals were humanely euthanized with an iv injection of saturated $MgSO_4$, and the electrodes were examined visually via dissection for verification of placement.

Blood samples for plasma histamine and neurotensin determinations were drawn from the arterial catheter

with plastic syringes and transferred to prelabeled, chilled collection tubes containing EDTA. The tubes were inverted gently and stored on ice until the termination of the experiment. The blood was then centrifuged (5°C) and the plasma was transferred to polypropylene tubes, rapidly frozen, and maintained at −80°C until analyzed. Plasma levels of histamine were determined by the specific, radioenzymatic assay for histamine described by Carraway *et al.* (1982). Plasma levels of neurotensin were measured using a method previously described by Carraway *et al.* (1980). The antiserum, HC-8, used in this method has been characterized earlier (Carraway and Leeman, 1976) and is directed primarily toward the C-terminal, biologically active portion of the neurotensin molecule, cross-reacting 50% with NT^{8-13} and <0.01% with NT^{1-10}.

Irradiation was accomplished with a bilateral, whole-body exposure to γ-ray photons from a cobalt-60 source located at the Armed Forces Radiobiology Research Institute. Exposure was limited to a mean of 1.38 min at 74 Gy/min steady state, free-in-air. Dose rate measurements at depth were made with an ionization chamber placed in a tissue equivalent model. The measured midline tissue dose rate was 69 Gy/min, producing a calculated total dose of 100 Gy, taking into account the rise and fall of the radiation source.

Blood pressure and blood flow data were grouped into 10-min intervals, measured in relation to midtime of radiation, and plotted at the middle of the interval. The Wilcoxon rank sum test was used for the statistical analysis of the data. A 95% level of confidence was employed to determine significance. Since all the animals were treated identically before irradiation or sham-irradiation, and since the preradiation data for the control and test animals showed no significant difference, the preradiation data for the irradiated and sham-irradiated animals were combined.

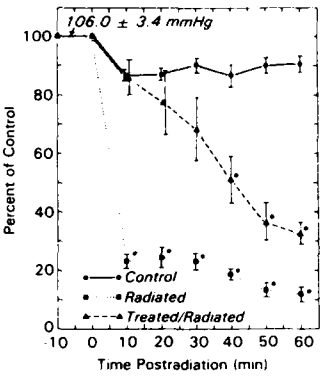

FIG. 1. Percentage change in mean arterial blood pressure after exposure to 100 Gy, whole-body, γ irradiation (± SEM) compared to a preirradiation mean of 106.0 ± 3.41 mm Hg. Animals in the sham-irradiated group (n = 6) were given physiological saline for 60 min before and after sham-irradiation. The untreated, irradiated group (n = 6) also received saline but were exposed to 100 Gy γ irradiation. The treated, irradiated group (n = 4), in addition, received mepyramine (0.5 mg/min) and cimetidine (0.25 mg/min) in the saline infusion and disodium cromoglycate (DSCG) by iv infusion (100 mg/kg) 5 min before irradiation (*, Significantly different from controls; $p = 0.05$).

RESULTS

As seen in Fig. 1, the mean systemic arterial blood pressure (MABP) of untreated, irradiated animals decreased to 23% of the preradiation mean of 106.0 ± 3.41 mm Hg within 10 min postradiation. This was followed by a steady decline to a 60-min postirradiation level that was 12% of the preirradiation values. After sham-irradiation there was no significant change in MABP for the six control monkeys. The four treated, irradiated monkeys (Group III) displayed a MABP that was statistically different from the untreated, irradiated monkeys at all postirradiation times of observation but displayed a significant difference from the controls only after the 30-min postirradiation time. The respiration of each subject was maintained at preradiation levels and, although not presented, the blood gas data revealed a general stability of blood pH and oxygen tension throughout the experimental period.

The preirradiation cortical blood flow, as shown in Fig. 2, was 60.8 ± 5.5 ml per 100 g of tissue per minute. The postirradiation blood flow for the sham-irradiated group of monkeys showed no significant changes for the 60-min observation period while the values for the untreated, irradiated monkeys showed a steady decline to 29% of the preirradiation levels by 60 min postirradiation. These levels became significantly different (p = 0.05) from those of the sham-irradiated group at 10 min postirradiation and remained that way for the remainder of the observations. In contrast, the cortical blood flow

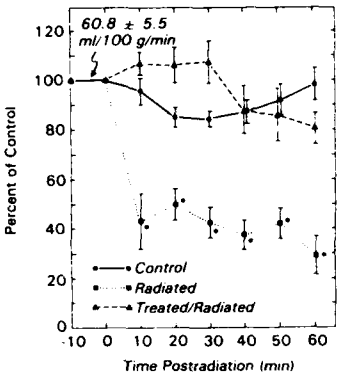

FIG. 2. Percentage change in cortical blood flow after exposure to 100 Gy, whole-body, γ irradiation (± SEM) compared to a preirradiation mean of 60.8 ± 5.5 ml/g of tissue/min. Animals in the sham-irradiated group (n = 6) were given physiological saline for 60 min before and after sham-irradiation. The untreated, irradiated group (n = 6) also received saline but were exposed to 100 Gy γ irradiation. The treated, irradiated group (n = 4), in addition, received mepyramine (0.5 mg/min) and cimetidine (0.25 mg/min) in the saline infusion and disodium cromoglycate (DSCG) by iv infusion (100 mg/kg) 5 min before irradiation (*, Significantly different from controls; $p = 0.05$).

in the treated, irradiated monkeys actually increased for the first 30 min postirradiation and never decreased to less than 80% of the preirradiation levels at any time postirradiation. For any of the postirradiation observations, there was no significant difference between the treated, irradiated group and the control group. However, a statistically significant difference ($p = 0.05$) did exist between the untreated, irradiated group and the other two groups from 10 min postradiation through the remainder of the measurements.

Figure 3 displays a preirradiation mean blood flow of 75.1 ± 5.9 ml per 100 g of tissue per minute in the hippocampus. The postirradiation blood flow values for the untreated, irradiated animals showed a rapid, significant decline to 32% of the preirradiation levels within 10 min postirradiation. Following an increase to 43% below preradiation levels at 30 min postirradiation, the values then decreased to 23% of the preirradiation levels by 60 min postradiation. There was a significant difference ($p = 0.05$) between the untreated, irradiated group of monkeys and the other two groups at all postirradiation times of measurement. At all postirradiation periods of observation the hippocampal blood flow of the treated, irradiated animals was not significantly different from that of the sham-irradiated monkeys.

Figure 4 displays a preirradiation mean plasma neurotensin level of 20.2 ± 2.3 fmol/ml. The postirradiation levels in the untreated, irradiated and the sham-irradiated animals did not differ significantly from this value for 60 min, even though the values for the untreated, irradiated group showed a peak at 6 min, and a gradual rise between 15 and 60 min. Although there was not a significant difference between the neurotensin levels in the treated, irradiated monkeys and that found in the other two groups, the maximum level in the treated group did occur 10

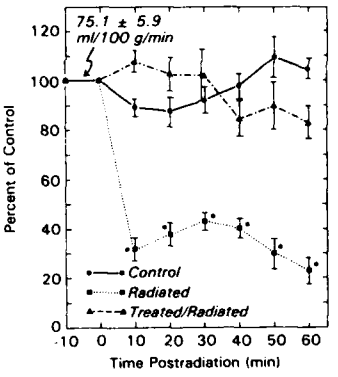

FIG. 3. Percentage change in hippocampal blood flow after exposure to 100 Gy, whole-body, γ irradiation (± SEM) compared to a preirradiation mean of 75.1 ± 5.9 ml/g of tissue/min. Animals in the sham-irradiated group (n = 6) were given physiological saline for 60 min before and after sham-irradiation. The untreated, irradiated group (n = 6) also received saline but were exposed to 100 Gy γ irradiation. The treated, irradiated group (n = 4), in addition, received mepyramine (0.5 mg/min) and cimetidine (0.25 mg/min) in the saline infusion and disodium cromoglycate (DSCG) by iv infusion (100 mg/kg) 5 min before irradiation (*, Significantly different from controls; $p = 0.05$).

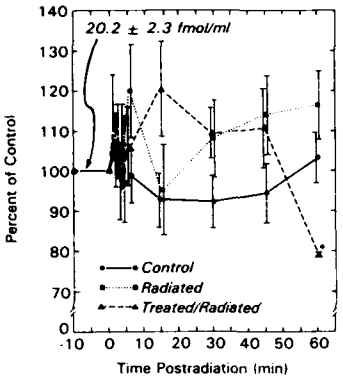

FIG. 4. Percentage change in plasma neurotensin concentration after exposure to 100 Gy, whole-body, γ irradiation (± SEM) compared to a preirradiation mean of 20.2 ± 2.3 fmol/ml. Animals in the sham-irradiated group (n = 6) were given physiological saline for 60 min before and after sham-irradiation. The untreated, irradiated group (n = 6) also received saline but were exposed to 100 Gy γ irradiation. The treated, irradiated group (n = 4), in addition, received mepyramine (0.5 mg/min) and cimetidine (0.25 mg/min) in the saline infusion and disodium cromoglycate (DSCG) by iv infusion (100 mg/kg) 5 min before irradiation (*, Significantly different from controls; p = 0.05).

min later postirradiation than in the untreated animals.

The preirradiation plasma histamine level, as shown in Fig. 5, was 0.58 ± 0.06 ng/100 μl. The postirradiation levels for the sham-irradiated group of monkeys showed no significant changes for 60 min of observation. During this same period the levels for both irradiated groups showed abrupt, significant increases at the 2-min point to levels that were almost 1600% above the preirradiation level. Significant differences were also present between both of the irradiated monkey groups and the sham-irradiated animals at the 4- and 6-min points. The histamine levels of the treated, irradiated group were also significantly higher than those found in the sham-irradiated monkeys at the 15-min time. At no time postirradiation were the plasma histamine levels of the treated, irradiated and the nontreated, irradiated monkeys significantly different. The histamine levels of the irradiated monkeys were significantly lower than for the sham-irradiated monkeys at the 60-min postirradiation point.

DISCUSSION

The initial precipitous decline in postradiation rCBF reported here has been well documented in the rhesus monkey (Chapman and Young, 1968; Cockerham *et al.*, 1986a; Cockerham *et al.*, 1986b). This decline has been associated with the immediate decrease in MABP and a critical MABP of 50 to 60% of normal is said to be necessary for adequate autoregulation of cerebral circulation (Chapman and Young, 1968; Doyle *et al.*, 1974; Farrar *et al.*, 1981). A similar drug-induced decrease in cerebral blood flow accompanied by symptoms and signs of cerebral ischemia has been reported in man (Finnerty *et al.*, 1957), and on the basis of the diminished ce-

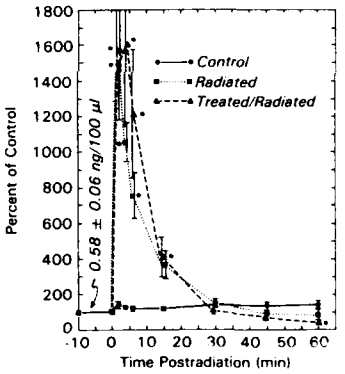

FIG. 5. Percentage change in plasma histamine concentration after exposure to 100 Gy, whole-body, γ irradiation (± SEM) compared to a preirradiation mean of 0.58 ± 0.06 ng/100 μl. Animals in the sham-irradiated group (n = 6) were given physiological saline for 60 min before and after sham-irradiation. The untreated, irradiated group (n = 6) also received saline but were exposed to 100 Gy γ irradiation. The treated, irradiated group (n = 4), in addition, received mepyramine (0.5 mg/min) and cimetidine (0.25 mg/min) in the saline infusion and disodium cromoglycate (DSCG) by iv infusion (100 mg/kg) 5 min before irradiation (*, Significantly different from controls; p = 0.05).

rebral blood flow reported in these animals one might expect a severe functional impairment of the CNS in monkeys following irradiation. In fact, the decline in MABP and rCBF reported here corresponds closely in time with the observed occurrence of irradiation-induced ETI (Curran *et al.*, 1973; Doyle *et al.*, 1974; Bruner, 1977) and suggests a temporal relationship between the depressed MABP, the decreased rCBF, and the appearance of ETI. However, the infusion of monkeys with either saline or norepinephrine after irradiation in an attempt to block hypotension produced no significant difference between the performance of monkeys in which the blood pressure was maintained with norepinephrine and the performance of monkeys that were injected with saline (Turns *et al.*, 1971). Therefore, if there is a causal relationship, as well as a temporal, it seems to exist between the decreased rCBF and the appearance of ETI.

The measurements of blood flow in the hippocampus of 100-Gy, γ-irradiated monkeys, when plotted at postradiation times (Fig. 3), present a graph strikingly similar to the performance graph of monkeys exposed to 89 Gy of mixed γ-neutron radiation (Curran *et al.*, 1973), with the same temporal relationship. Likewise, the abrupt increase in plasma histamine levels 2 min postradiation (Fig. 5) coincides with the initial depression in MABP (Fig. 1) and rCBF (Figs. 2 and 3), and the onset of ETI (Curran *et al.*, 1973). The role of histamine is further supported by investigators who have reported the alteration of ETI by the administration of antihistamines (Doyle *et al.*, 1974).

The plasma histamine levels found in this experiment serve to corroborate the results reported on subhuman primates by other investigators (Doyle and Strike, 1977; Alter *et al.*, 1983; Cockerham *et al.*, 1986a) by showing an immediate rise by 2 min postirradiation followed by a much slower fall to preirradiation levels by 30 min postirradiation. However, the combined administration of DSCG and H_1 and H_2 blocking antihistamines did not alter the irradiation-induced release of histamine, showing plasma histamine levels which appeared to be much like those seen in a previous report (Cockerham *et al.*, 1986a).

The postirradiation hypotension was altered significantly with the combined administration of DSCG and the antihistamines mepyramine and cimetidine. This is in contrast to a previous report using DSCG alone (Cockerham *et al.*, 1986b) in which there was not a significant difference between the DSCG-treated and the untreated postirradiation MABP. Comparison of the results of the two studies, then, suggests the involvement of the irradiation-induced release of histamine with the postirradiation hypotension, since the addition of the H_1 and H_2 receptor blockers resulted in an alteration of the postirradiation MABP not achieved with the administration of DSCG alone. However, the administration of DSCG alone (Cockerham *et al.*, 1986b) or in combination with antihistamines resulted in a postirradiation rCBF that was close to the same level as that found in the control animals. This, then, indicates that the irradiation-induced release of histamine was not directly responsible for the postirradiation decrease in rCBF but may be indirectly responsible through its effect on the MABP. Moreover, since the administration of DSCG did not inhibit the release of histamine or the eventual decrease in MABP, DSCG must act through a different path to prevent the irradiation-induced decrease in rCBF.

Certainly, the action of DSCG does not seem to be by blocking the neurotensin mediated release of histamine since the plasma neurotensin levels in the irradiated monkeys, while exhibiting some indications of a postirradiation increase, were not found to be significantly different from those in the sham-irradiated monkeys. However, these values do not indicate the levels in the tissues, where neurotensin may be degraded very rapidly (Emson *et al.*, 1982; Checlar *et al.*, 1982) as evidenced by a rapid disappearance of neuro-

tensin-like immunoreactivity (Dupont and Merand, 1978).

Even though a temporal relationship does seem to exist between the release of histamine, a reduced MABP, decreased rCBF, and early transient incapacitation, the presence of other factors must be considered. Neurotensin could still conceivably be released by irradiation, cause the release of histamine from mast cells (Carraway *et al.*, 1982; Cochrane *et al.*, 1982; Cochrane *et al.*, 1986; Kerouac *et al.*, 1984; Rioux *et al.*, 1985), and trigger cerebrovascular vasoconstriction and cerebral edema (Rioux *et al.*, 1985).

The irradiation-induced reduction in rCBF may also employ intermediate mediators such as free radicals (Ohmori *et al.*, 1979) produced with exposure to ionizing radiation (Del Maestro, 1980; Kennedy *et al.*, 1984). Free radical interactions have been implicated in a large number of pathological conditions including radiation injury, ischemia, microvascular injury, and cell damage (Del Maestro *et al.*, 1980; Del Maestro, 1980; Hammond *et al.*, 1985; Kontos, 1985). The triphasic cerebral ischemic response seen after irradiation (Cockerham *et al.*, 1986a,b) may be even more damaging than complete ischemia (Rehncrona *et al.*, 1980) since reperfusion may lead to the formation of additional free radicals (Julicher *et al.*, 1984; Peterson *et al.*, 1985). A possible mode of pharmacologic intervention may well be the introduction of DSCG to intervene in the production of free radicals (Carmichael *et al.*, 1987), thereby explaining why treatment with DSCG would maintain rCBF during the entire observation period even with the presence of profound hypotension in treated animals at 60 min. Thus, the DSCG prevention of irradiation-induced free radical formation would allow the maintainance of rCBF in the initial 20–30 min. Therefore, there would be no reperfusion-induced formation of additional free radicals, allowing the rCBF to be maintained during the second portion of the observation period.

In conclusion, we have shown that the combined administration of DSCG and the antihistamines mepyramine and cimetidine did not alter significantly the irradiation-induced release of histamine or the postirradiation plasma levels of neurotensin. We were not able to demonstrate whether DSCG would inhibit the postirradiation, neurotensin-induced release of histamine. However, we were able to demonstrate that DSCG and the antihistamines mepyramine and cimetidine, given in combination, will alter significantly the postirradiation hypotension and the reduced regional cerebral blood flow. We have also introduced a theoretical mechanism through which the administration of DSCG may prevent an irradiation-induced reduction in rCBF. The next logical steps will be to (1) show that DSCG actually does prevent the irradiation-induced production of free radicals, and (2) determine if the administration of DSCG diminishes irradiation-induced ETI.

ACKNOWLEDGMENTS

The authors thank Mr. E. J. Golightly for technical assistance and Mrs. M. H. Owens for preparation of the manuscript.

REFERENCES

ALTER, W. A., III, HAWKINS, R. N., CATRAVAS, G. N., DOYLE, T. F., AND TAKENAGA, J. K. (1983). Possible role of histamine in radiation induced hypotension in the rhesus monkey. *Radiat. Res.* **94**, 654.

BRUNER, A. (1977). Immediate dose-rate effects of ^{60}Co on performance and blood pressure in monkeys. *Radiat. Res.* **70**, 378–390.

BRUNER, A., BOGO, V., AND JONES, R. K. (1975). Delayed match-to-sample early performance decrement in monkeys after ^{60}Co irradiation. *Radiat. Res.* **63**, 83–96.

CARMICHAEL, A. J., ARROYO, C. M., AND COCKERHAM, L. G. (1987). Disodium cromoglycate (DSCG) inhibits the formation of free radicals, potent reactive intermediates. *Toxicologist* **7**(1), 111.

CARRAWAY, R. E., COCHRANE, D. E., LANSMAN, J. B., LEEMAN, S. E., PATERSON, B. M., AND WELCH, H. J. (1982). Neurotensin stimulates exocytotic histamine

secretion from rat mast cells and elevates plasma histamine levels. *J. Physiol.* **323,** 403–414.

CARRAWAY, R. E., HAMMER, R. A., AND LEEMAN, S. E. (1980). Neurotensin in plasma: Immunochemical and chromatographic character of acid/acetone-soluble material. *Endocrinology* **107**(2), 400–406.

CARRAWAY, R. E., AND LEEMAN, S. E. (1976). Radioimmunoassay for neurotensin, a hypothalamic peptide. *J. Biol. Chem.* **251**(22), 7035–7044.

CHAPMAN, P. H., AND YOUNG, R. J. (1968). Effect of cobalt-60 gamma irradiation on blood pressure and cerebral blood flow in the Macaca mulatta. *Radiat. Res.* **35,** 78–85.

CHAPUT, R. L., KOVACIC, R. T., AND BARRON, E. L. (1972). *Performance of Trained Beagles after Supralethal Doses of Radiation.* AFRRI SR72-1, Armed Forces Radiobiology Research Institute, Bethesda, MD.

CHAPUT, R. L., AND WISE, D. (1969). *Miniature Pig Incapacitation and Performance Decrement after Mixed Gamma-Neutron Irradiation.* AFRRI SR69-12, Armed Forces Radiobiology Research Institute, Bethesda, MD.

CHECLER, F., KITABGI, P., AND VINCENT, J.-P. (1982). Degradation of neurotensin by synaptic membranes. *Ann. N. Y. Acad. Sci.* **400,** 413–414.

COCHRANE, D. E., BOUCHER, W., AND BIBB, P. (1986). Neurotensin stimulates histamine release in *in vivo* skin blisters: An effect inhibited by cromolyn or somatostatin. *Int. Arch. Allergy Appl. Immunol.* **80**(3), 225–230.

COCHRANE, D. E., EMIGH, C., LEVINE, G., CARRAWAY, R. E., AND LEEMAN, S. E. (1982). Neurotensin alters cutaneous vascular permeability and stimulates histamine release from isolated skin. *Ann. N. Y. Acad. Sci.* **400,** 396–397.

COCKERHAM, L. G., BOGO, V., AND GOSSET-HAGERMAN, C. J. (1984). Gamma radiation produced performance decrement in rat as assessed with the accelerod. *Neurosci. Lett.* **49,** 297–300.

COCKERHAM, L. G., CERVENY, T. J., AND HAMPTON, J. D. (1986a). Postradiation regional cerebral blood flow in primates. *Aviat. Space Environ. Med.* **57,** 578–582.

COCKERHAM, L. G., DOYLE, T. F., PAUTLER, E. L., AND HAMPTON, J. D. (1986b). Disodium cromoglycate, a mast cell stabilizer, alters postradiation regional cerebral blood flow in primates. *J. Toxicol. Environ. Health* **18,** 91–101.

CURRAN, C. R., YOUNG, R. W., AND DAVIS, W. F. (1973). *The Performance of Primates Following Exposure to Pulsed Whole-Body Gamma-Neutron Radiation.* AFRRI SR73-1, Armed Forces Radiobiology Research Institute, Bethesda, MD.

DE HAAN, H. J., KAPLAN, S. J., AND GERMAS, J. E. (1969). *Visual Discrimination Performance in the Monkey following a 5,000-Rad Pulse of Mixed Gamma-Neutron Radiation.* AFRRI SR69-1, Armed Forces Radiobiology Research Institute, Bethesda, MD.

DEL MAESTRO, R. F. (1980). An approach to free radicals in medicine and biology. *Acta Physiol. Scand. Suppl.* **492,** 153–168.

DEL MAESTRO, R. F., THAW, H. H., BJORK, J., PLANKER, M., AND ARFORS, K.-E. (1980). Free radicals as mediators of tissue injury. *Acta Physiol. Scand. Suppl.* **492,** 43–57.

DOYLE, T. F., CURRAN, C. R., AND TURNS, J. E. (1974). The prevention of radiation-induced, early transient incapacitation of monkeys by an antihistamine. *Proc. Soc. Exper. Biol. Med.* **145,** 1018–1024.

DOYLE, T. F., AND STRIKE, T. A. (1977). Radiation-released histamine in the rhesus monkey as modified by mast-cell depletion and antihistamine. *Experientia* **33,** 1047–1048.

DUPONT, A., AND MERAND, Y. (1978). Enzyme inactivation of neurotensin by hypothalamic and brain extracts of the rat. *Life Sci.* **22,** 1623–1630.

EMSON, P. C., GOEDERT, M., WILLIAMS, B., NINKOVIC, M., AND HUNT, S. P. (1982). Neurotensin: Regional distribution, characterization, and inactivation. *Ann. N. Y. Acad. Sci.* **400,** 198–215.

FARRAR, J. K., GAMACHE, F. W., JR., FERGUSON, G. G., BARKER, J., VARKEY, G. P., AND DRAKE, C. G. (1981). Effects of profound hypotension on cerebral blood flow during surgery for intracranial aneurysms. *J. Neurosurg.* **55,** 857–864.

FINNERTY, F. A., JR., GUILLAUDEU, R. L., AND FAZEKAS, J. F. (1957). Cardiac and cerebral hemodynamics in drug induced postural collapse. *Circ. Res.* **5,** 34–39.

FRANZ, C. G. (1985). Effects of mixed neutron-gamma total-body irradiation on rhesus monkeys physical activity performance. *Radiat. Res.* **101,** 434–441.

HAMMOND, B., KONTOS, H. A., AND HESS, H. L. (1985). Oxygen radicals in the adult respiratory distress syndrome, in myocardial ischemia and reperfusion injury, and in cerebral vascular damage. *Can. J. Physiol. Pharmacol.* **63,** 173–187.

HUNT, W. A. (1987). Effects of ionizing radiation on behavior and the brain. In *Military Radiobiology* (J. J. Conklin and R. I. Walker, Eds.), Academic Press, New York.

HYMAN, E. S. (1961). Linear system for quantitating hydrogen at a platinum electrode. *Circ. Res.* **9,** 1093–1097.

JULICHER, R. H. M., TIJBURG, L. B. M., STERRENBERG, L., BAST, A., KOOMEN, J. M., AND NOORDHOEK, J. (1984). Decreased defence against free radicals in rat heart during normal reperfusion after hypoxic, ischemic and calcium-free perfusion. *Life Sci.* **35**(12), 1281–1288.

KENNEDY, A. R., TROLL, W., AND LITTLE, J. B. (1984). Role of free radicals in the initiation and promotion of

radiation transformation *in vitro*. *Carcinogenesis* **5**(10), 1213–1218.

KEROUAC, R., ST-PIERRE, S., AND RIOUX, F. (1984). Participation of mast cell 5-hydroxytryptamine in the vasoconstrictor effect of neurotensin in the rat perfused hindquarter. *Life Sci.* **34**, 947–959.

KIMELDORF, D. J., AND HUNT, E. L. (1965). Neurophysiological effects of ionizing radiation. In *Ionizing Radiation: Neural Function and Behavior* (D. J. Kimeldorf and E. L. Hunt, Eds.), Academic Press, New York.

KIRINO, T., AND SANO, K. (1984). Selective vulnerability in the gerbil hippocampus following ischemia. *Acta Neuropathol.* **62**, 201–208.

KONTOS, H. A. (1985). Oxygen radicals in cerebral vascular injury. *Circ. Res.* **57**(4), 508–516.

LASSER, E. C., AND STENSTROM, K. W. (1954). Elevation of circulating blood histamine in patients undergoing deep roentgen therapy. *Amer. J. Roentgenology* **72**, 985–988.

MILETICH, D. J., AND STRIKE, T. A. (1970). *Alteration of Postirradiation Hypotension and Incapacitation in the Monkey by Administration of Vasopressor Drugs.* AFRRI SR70-1, Armed Forces Radiobiology Research Institute, Bethesda, MD.

OHMORI, H., KOMORIYA, K., AZUMA, A., KUROSUMI, S., AND HASHIMOTO, Y. (1979). Xanthine oxidase-induced histamine release from isolated rat peritoneal mast cells: involvement of hydrogen peroxide. *Biochem. Pharmacol.* **28**, 333–334.

OISHI, M., ISHIKO, J., INAGAKE, C., AND TAKAORI, S. (1983). Release of histamine and adrenaline *in vivo* following intravenous administration of neurotensin. *Life Sci.* **32**, 2231–2239.

PETERSON, D. A., ASINGER, R. W., ELSPERGER, K. J., HOMANS, D. C., AND EATON, J. W. (1985). Reactive oxygen species may cause myocardial reperfusion injury. *Biochem. Biophys. Res. Commun.* **127**(1), 87–93.

PITCHFORD, T. L. (1968). *Beagle Incapacitation and Survival Time after Pulsed Mixed Gamma-Neutron Irradiation.* AFRRI SR68-24, Armed Forces Radiobiology Research Institute, Bethesda, MD.

REHNCRONA, S., SIESJO, B. K., AND SMITH, D. S. (1980). Reversible ischemia of the brain: Biochemical factors influencing restitution. *Acta Physiol. Scand. Suppl.* **492**, 133–140.

RIOUX, F., KEROUAC, R., AND ST-PIERRE, S. (1985). Release of mast cell mediators, vasoconstriction and edema in the isolated, perfused head of the rat following intracarotid infusion of neurotensin. *Neuropeptides* **6**, 1–12.

SNIDER, R. S., AND LEE, J. C. (1961). *A Stereotaxic Atlas of the Monkey Brain (Macaca mulatta).* Univ. of Chicago Press, Chicago.

SUZUKI, R., YAMAGUCHI, T., LI, C.-L., AND KLATZO, I. (1983). The effects of 5-minute ischemia in mongolian gerbils. II. Changes of spontaneous neuronal activity in cerebral cortex and CA1 sector of hippocampus. *Acta Neuropathol.* **60**, 217–222.

TURNS, J. E., DOYLE, T. F., AND CURRAN, C. R. (1971). *Norepinephrine Effects on Early Postirradiation Performance Decrement in the Monkey.* AFRRI SR71-16, Armed Forces Radiobiology Research Institute, Bethesda, MD.

RADIATION RESEARCH 114, 42–53 (1988)

Implication of Prostaglandins and Histamine H_1 and H_2 Receptors in Radiation-Induced Temperature Responses of Rats

SATHASIVA B. KANDASAMY, WALTER A. HUNT, AND G. ANDREW MICKLEY

Behavioral Sciences Department, Armed Forces Radiobiology Research Institute, Bethesda, Maryland 20814-5145

KANDASAMY, S. B., HUNT, W. A., AND MICKLEY, G. A. Implications of Prostaglandins and Histamine H_1 and H_2 Receptors in Radiation-Induced Temperature Responses of Rats. *Radiat. Res.* **114**, 42–53 (1988).

Exposure of rats to 1–15 Gy γ radiation (^{60}Co) induced hyperthermia, whereas 20–200 Gy induced hypothermia. Exposure either to the head or to the whole body to 10 Gy induced hyperthermia, while body-only exposure produced hypothermia. This observation indicates that radiation-induced fever is a result of a direct effect on the brain. The hyperthermia due to 10 Gy was significantly attenuated by the pre- or post-treatment with a cyclooxygenase inhibitor, indomethacin. Hyperthermia was also altered by the central administration of a μ-receptor antagonist naloxone but only at low doses of radiation. These findings suggest that radiation-induced hyperthermia may be mediated through the synthesis and release of prostaglandins in the brain and to a lesser extent to the release of endogenous opioid peptides. The release of histamine acting on H_1 and H_2 receptors may be involved in radiation-induced hypothermia, since both the H_1 receptor antagonist, mepyramine, and H_2 receptor antagonist, cimetidine, antagonized the hypothermia. The results of these studies suggest that the release of neurohumoral substances induced by exposure to ionizing radiation is dose dependent and has different consequences on physiological processes such as the regulation of body temperature. Furthermore, the antagonism of radiation-induced hyperthermia by indomethacin may have potential therapeutic implications in the treatment of fever resulting from accidental irradiations.

Exposure to ionizing radiation can interfere with the regulation of body temperature. Hyperthermia has been observed after exposure to ionizing radiation in a number of species including rabbits, cats, and humans (*1–3*). This effect is thought to result from actions on the neuroregulatory centers in the hypothalamus, since the response can be prevented by pretreatment with the centrally acting antipyretic, aminopyrine (*1*). In addition, preliminary evidence from our laboratory suggests that radiation can also induce hypothermia in rats and guinea pigs (*4, 5*). However, the mechanisms underlying these effects are unknown.

Normal thermoregulation apparently is controlled by a variety of putative mediators. Initially, the monoamine neurotransmitters were implicated in thermoregulation, but this view is incompatible with empirical findings that have shown that the effect of monoamines on body temperature varies from species to species (*6*). Prostaglandins of the E series, on the other hand, induce an increase in body temperature in all the mammalian species investigated so far (*7, 8*). In addition, a variety of endog-

0033-7587/88 $3.00

enous peptides capable of producing opiate-like effects have been isolated from brain tissue and have been implicated in thermoregulation (*9–12*).

Exposure to ionizing radiation has been reported to increase blood levels of histamine in humans undergoing radiation therapy, as well as in dogs following irradiation (*13–15*). Histamine has been implicated in radiation-induced hypotension (*16*), reductions in cerebral blood flow (*17*), and performance decrements (*18*). Histamine is present in high concentration in the hypothalamus (*19, 20*) and is localized in nerve terminals (*21*). Also, ascending histamine tracts are found in the median forebrain bundle (*22*); histidine decarboxylase, the enzyme that converts histidine to histamine, is localized in different regions of the brain (*23*); histamine activates adenylate cyclase in the brain (*24*); and brain histamine turnover is increased by stress (*25*). Administration of histidine systemically (*26*) or histamine centrally (*27–29*) evokes hypothermia due to both H_1 and H_2 receptor activation (*30*). These neurochemical and pharmacological studies suggest that histamine may be a central neurotransmitter involved in many physiological functions including thermoregulation and could underlie radiation-induced hypothermia.

The purpose of the present study was to characterize the effect of exposure to ionizing radiation on body temperature in the rat (a) by determining the effect of variable doses of radiation on body temperature, (b) by determining whether radiation is acting on the brain or peripheral sites, and (c) by then elucidating possible mechanisms involved in these temperature responses.

MATERIALS AND METHODS

Drugs used Indomethacin and serotonin creatinine sulfate (Sigma Chemical Co., St. Louis, MO); naloxone (National Institute on Drug Abuse, Washington, DC); mepyramine maleate (Mallinckrodt, Inc., St. Louis, MO); methysergide maleate (Sandoz Pharmaceuticals, E. Hanover, NJ); 2-methylhistamine dihydrochloride, 4-methylhistamine dihydrochloride, and cimetidine (Smith Kline French Laboratory, Philadelphia, PA); ketamine hydrochloride (Parke-Davis, Detroit, MI); xylazine (Hayer-Lockhart, Shawnee, KS); acepromazine (Ayerst Laboratories, NY). 2-methylhistamine, 4-methylhistamine, mepyramine, naloxone, and serotonin were dissolved in sterile, nonpyrogenic saline. Indomethacin was dissolved in a mixture of 1% sodium hydroxide and saline, while methysergide was dissolved in 10% dimethyl sulfoxide (DMSO) and pyrogen-free distilled water. Cimetidine was dissolved in 0.1 ml of 1 *N* HCl and diluted to the final volume with saline.

Animals Male Sprague-Dawley Crl:CD(SD)BR rats (Charles River Breeding Laboratories, Kingston, NY) weighing 200–300 g were used in these experiments. Rats were quarantined on arrival and screened for evidence of disease by serology and histopathology before being released from quarantine. The rats were housed individually in polycarbonate isolator cages (Lab Products, Maywood, NJ) on autoclaved hardwood contact bedding (Beta Chip Northeastern Products Corp., Warrensburg, NY) and acidified water (pH 2.5 using HCl) *ad libitum*. Animal holding rooms were kept at 21 ± 1°C with 50 ± 10% relative humidity on a 12-h light:dark lighting cycle with no twilight.

Radiation exposure Male Sprague-Dawley rats weighing 200–300 g were used in these experiments. The rats were placed in clear plastic containers for approximately 5 min before irradiation or sham exposure. The animals were exposed bilaterally to varying doses of γ photons using a ^{60}Co source at a rate of 10 or 20 Gy/min. Shielding of the head or body was accomplished using lead bricks. Dosimetry was performed using paired 50-ml ion chambers. Delivered dose was expressed as a ratio of the dose measured in a tissue-equivalent plastic phantom enclosed in a restraining tube to that measured in air.

Central administration of drugs Rats were anesthetized with 1 ml/kg, im of a mixture of ketamine (50 mg/kg), xylazine (5 mg/kg), and acepromazine (1 mg/kg), and were placed in a rat stereotaxic apparatus (David Kopf Instruments, No. 320). A single cannula was inserted into the lateral ventricle according to coordinates derived from the atlas of Pelligrino *et al.* (*31*): 0.8 mm posterior to bregma, 2.5 mm lateral.

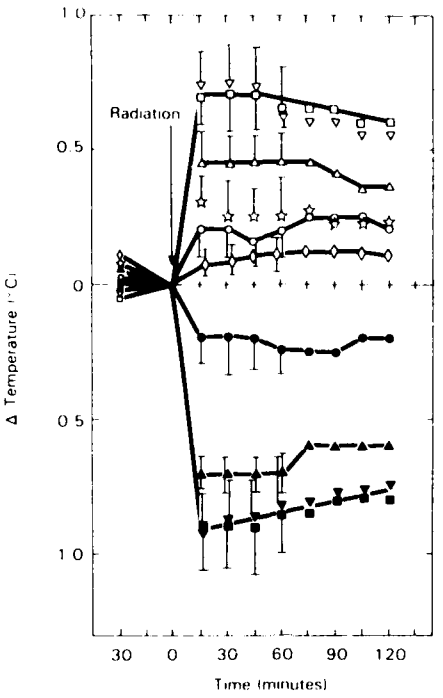

FIG. 1. Changes in rectal temperature of rats exposed to variable doses of ionizing radiation: Sham radiation (—), 1 Gy (○), 3 Gy (☆), 5 Gy (△), 10 Gy (□), 15 Gy (▽), 20 Gy (●), 50 Gy (▲), 100 Gy (▼), 150 Gy (■). Each point represents the mean ± SE of five observations except (—) and (□) which represent 15 observations. Zero on the abscissa represents body temperature at the time of injection.

The cannula was lowered until cerebrospinal fluid rose in the cannula. Dental acrylic was used to secure the cannula. After the end of an experiment, injection sites were histologically verified. The volume of injection was always 10 μl. At least 1 week was allowed for recovery before animals were used for experiments. Injections/radiation were done at the same time of day (0900) to avoid diurnal variation in temperature. The antagonists (indomethacin, naloxone, mepyramine, cimetidine, and methysergide) were given 30 min before the administration of the radiation/agonists (2-methylhistamine, 4-methylhistamine, or serotonin).

Measurement of body temperature. The animals were placed in cages 1 h before the beginning of experiments that were carried out at an environmental temperature of 22 ± 1°C. Body temperature was measured every 15 min over 2 h with thermistor probes inserted approximately 6 cm into the rectum and connected to a datalogger (Minitrend 205).

Statistics. Statistical evaluations were undertaken using Student's *t* test with a significance level of $P < 0.05$.

RESULTS

Exposure of rats to 1–15 Gy γ radiation induced hyperthermia, whereas 20 to 200 Gy induced hypothermia (Fig. 1). The onset of these effects was rapid and they reached their maximum effect within 15 min. The exposed rats normally did not show any significant behavioral changes up to 100 Gy but started circling (two of six

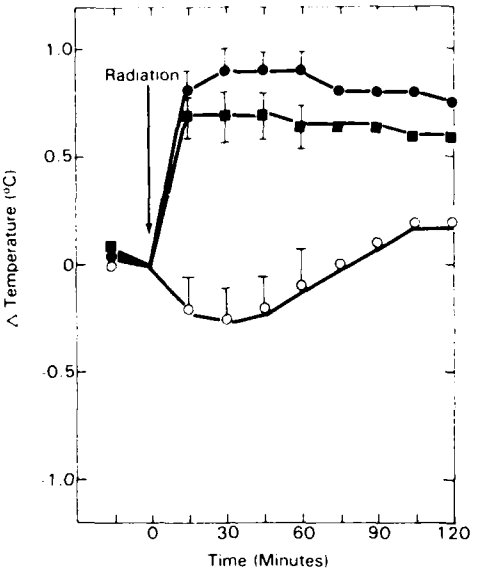

FIG. 2. Effect of 10 Gy ionizing radiation on body only (○), whole body (■), and head only (●). Each point represents the mean ± SE of six observations. Zero on the abscissa represents body temperature at the time of irradiation.

rats) when they were exposed above 100 Gy. On the basis of these results, a 10-Gy dose of radiation was used to determine the site of action of the effects of radiation on body temperature.

As can be seen in Fig. 2, hyperthermia induced by a 10-Gy dose of γ radiation occurred only after whole-body or head-only exposure, not when the head was shielded. Since whole-body exposure resulted in the same effect as head-only exposure, subsequent studies used whole-body exposure to ionizing radiation.

Experiments were then undertaken to determine what mechanisms may underlie radiation-induced changes in body temperature by comparing to radiation the effects of drugs with known actions and by determining if antagonists to these drugs could block the effects of radiation.

Since prostaglandins induced hyperthermia (*7, 8*), the effect of indomethacin, an inhibitor of prostaglandin synthesis, on hyperthermia induced by ionizing radiation was examined. Pretreatment with 1–5 mg/kg (ip) of indomethacin inhibited in a dose-dependent manner the hyperthermia induced by 1–15 Gy γ photons (Fig. 3 and Table I). Indomethacin alone had no effect on body temperature (Fig. 3). In addition, 1 mg/kg, ip, of indomethacin (given immediately after determination of body temperature 15 min after irradiation) rapidly reversed the fever produced by irradiation (Fig. 4).

The effect of pretreatment of naloxone on hyperthermia induced by ionizing radiation was also determined. Naloxone (10–50 μg, icv) had no significant effect on the body temperature in control animals but attenuated the hyperthermia only at doses

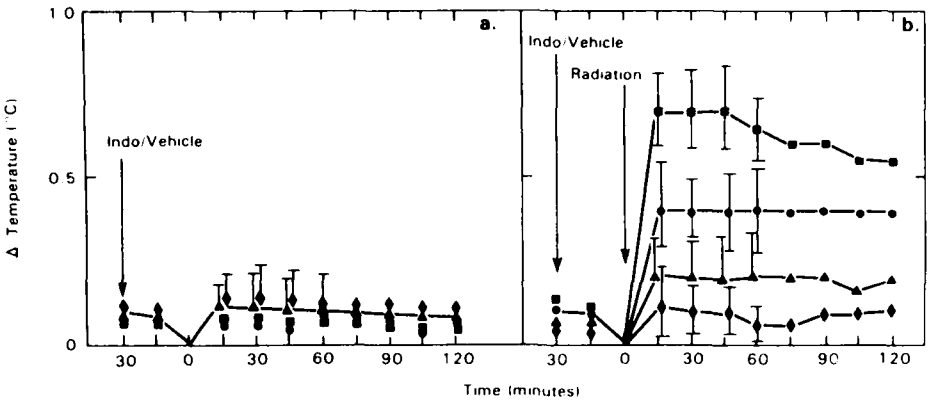

FIG. 3. Effect of intraperitoneal injection of indomethacin on hyperthermia induced by 10 Gy ionizing radiation. (a) Indomethacin (Indo) 1 mg/kg (▲), 3 mg/kg (■), 5 mg/kg (●), vehicle (◆); (b) 10 Gy ionizing radiation alone (■) and in the presence of Indo 1 mg/kg (●), 3 mg/kg (▲), and 5 mg/kg (◆). Each point represents mean ± SE of five observations. Zero on the abscissa represents temperature at the time of second injection.

of 1–3 Gy (Table II). The hyperthermia due to 5 to 15 Gy radiation was resistant to 10–100 μg, icv, of naloxone (Fig. 5 and Table II). Doses of naloxone above 100 μg were not used, since they induce hyperthermia in control animals.

Since histamine is released after exposure to radiation, its possible role in the thermoregulatory effects of radiation was examined. To differentiate between actions on

TABLE I

Effect of Indomethacin on the Hyperthermia Induced by Exposure to Ionizing Radiation

Treatment		*Mean change temperature (°C)*
Vehicle	+ 1 Gy ionizing radiation	0.3 ± 0.10 (n = 8)[a]
Indomethacin, 1 mg/kg	+ 1 Gy ionizing radiation	0.1 ± 0.10 (n = 5)
Indomethacin, 3 mg/kg	+ 1 Gy ionizing radiation	−0.1 ± 0.15 (n = 5)
Indomethacin, 5 mg/kg	+ 1 Gy ionizing radiation	0.2 ± 0.20 (n = 5)
Vehicle	+ 5 Gy ionizing radiation	0.6 ± 0.12 (n = 8)
Indomethacin, 1 mg/kg	+ 5 Gy ionizing radiation	0.1 ± 0.12 (n = 5)*
Indomethacin, 3 mg/kg	+ 5 Gy ionizing radiation	−0.1 ± 0.20 (n = 5)*
Indomethacin, 5 mg/kg	+ 5 Gy ionizing radiation	0.2 ± 0.15 (n = 5)*
Vehicle	+ 15 Gy ionizing radiation	0.8 ± 0.15 (n = 5)
Indomethacin, 1 mg/kg	+ 15 Gy ionizing radiation	0.3 ± 0.20 (n = 5)**
Indomethacin, 3 mg/kg	+ 15 Gy ionizing radiation	0.2 ± 0.10 (n = 5)**
Indomethacin, 5 mg/kg	+ 15 Gy ionizing radiation	0.1 ± 0.20 (n = 5)**

[a] n = number of animals.

* Significantly different from 5 Gy ionizing radiation; $P < 0.05$.

** Significantly different from 15 Gy ionizing radiation; $P < 0.05$.

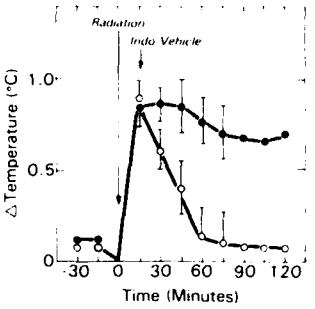

FIG. 4. Effect of intraperitoneal injection of indomethacin on hyperthermia induced by 10 Gy ionizing radiation: ionizing radiation alone (●) and in the presence of indomethacin (Indo) 1 mg/kg (○). Each point represents the mean ± SE of five observations. Zero on the abscissa represents temperature before radiation. At the second arrow Indo/vehicle was administered.

H_1 and H_2 receptors, agonists and antagonists specific for these receptors were used. Mepyramine (10–30 μg, icv), an H_1 antagonist, and cimetidine (10–30 μg, icv), an H_2 antagonist, both of which were previously found to antagonize hypothermia in-

TABLE II

Effect of Naloxone on the Hyperthermia Induced by Exposure to Ionizing Radiation

Treatment		*Mean change temperature (°C)*
Saline	+ 1 Gy ionizing radiation	0.3 ± 0.05 (n = 10)
Naloxone, 10 μg	+ 1 Gy ionizing radiation	0.1 ± 0.10 (n = 7)*
Naloxone, 30 μg	+ 1 Gy ionizing radiation	−0.1 ± 0.15 (n = 7)*
Naloxone, 50 μg	+ 1 Gy ionizing radiation	−0.1 ± 0.10 (n = 7)*
Saline	+ 3 Gy ionizing radiation	0.4 ± 0.10 (n = 8)
Naloxone, 10 μg	+ 3 Gy ionizing radiation	0.2 ± 0.10 (n = 7)**
Naloxone, 30 μg	+ 3 Gy ionizing radiation	0.1 ± 0.10 (n = 7)**
Naloxone, 50 μg	+ 3 Gy ionizing radiation	0.1 ± 0.15 (n = 7)**
Saline	+ 5 Gy ionizing radiation	0.5 ± 0.15 (n = 6)
Naloxone, 10 μg	+ 5 Gy ionizing radiation	0.7 ± 0.25 (n = 5)
Naloxone, 30 μg	+ 5 Gy ionizing radiation	0.7 ± 0.15 (n = 5)
Naloxone, 50 μg	+ 5 Gy ionizing radiation	0.6 ± 0.10 (n = 5)
Saline	+ 10 Gy ionizing radiation	0.7 ± 0.15 (n = 5)
Naloxone, 100 μg	+ 10 Gy ionizing radiation	0.9 ± 0.25 (n = 5)
Saline	+ 15 Gy ionizing radiation	0.8 ± 0.15 (n = 5)
Naloxone, 10 μg	+ 15 Gy ionizing radiation	0.9 ± 0.20 (n = 5)
Naloxone, 30 μg	+ 15 Gy ionizing radiation	0.8 ± 0.10 (n = 5)
Naloxone, 50 μg	+ 15 Gy ionizing radiation	1.0 ± 0.15 (n = 5)
Naloxone, 100 μg	+ 15 Gy ionizing radiation	1.1 ± 0.20 (n = 5)

* Significantly different from 1 Gy ionizing radiation: $P < 0.05$.
** Significantly different from 3 Gy ionizing radiation: $P < 0.05$.

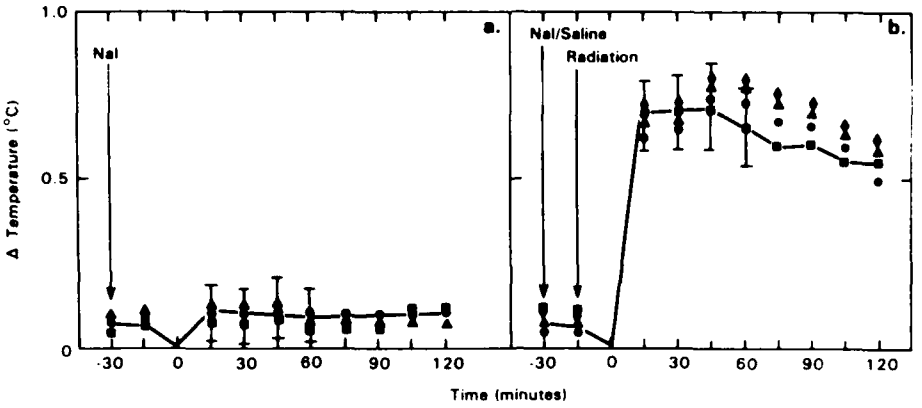

FIG. 5. Effect of icv naloxone on hyperthermia induced by 10 Gy ionizing radiation. (a) Naloxone (Nal) 10 μg (▲), 30 μg (●), and 50 μg (■); (b) 10 Gy ionizing radiation alone (■) and in the presence of Nal 10 μg (◆), 30 μg (▲), and 50 μg (●). Each point represents mean ± SE of five observations. Zero on the abscissa represents temperature at the time of second injection.

duced by histamine in guinea pigs (32), significantly antagonized in a dose-dependent manner hypothermia induced by exposure to 50 Gy radiation (Figs. 6 and 7). In addition, mepyramine antagonized hypothermia induced by 2-methylhistamine (10 μg, icv), an H_1 agonist, but did not antagonize the hypothermia induced by 4-methylhistamine (50 μg, icv), an H_2 agonist (Fig. 6 and Table III). Likewise, cimetidine significantly attenuated the hypothermia induced by 4-methylhistamine but not that induced by 2-methylhistamine (10 μg, icv) (Fig. 7 and Table III).

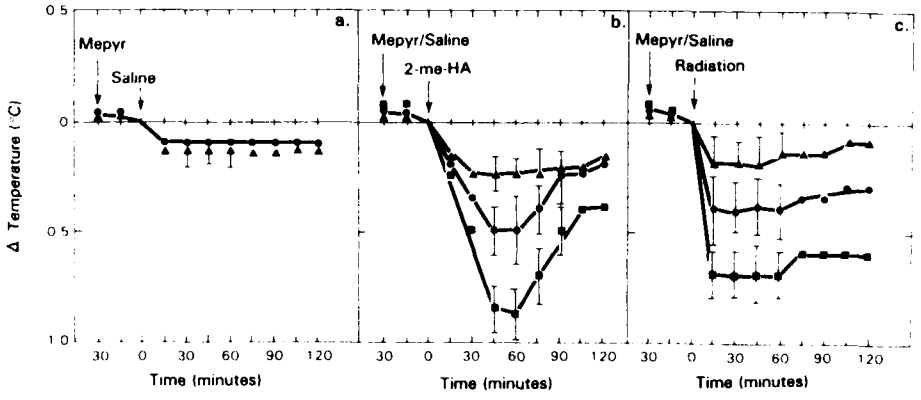

FIG. 6. Effect of icv mepyramine on hypothermia induced by 2-methylhistamine and ionizing radiation. (a) Mepyramine (Mepyr) 10 μg (●) and 30 μg (▲); (b) 10 μg of 2-methylhistamine (2-me-HA) alone (■) and in the presence of Mepyr 10 μg (●) and 30 μg (▲); (c) 50 Gy ionizing radiation alone (■) and in the presence of Mepyr 10 μg (●) and 30 μg (▲). Each point represents the mean ± SE of five observations. Zero on the abscissa represents temperature at the time of second injection.

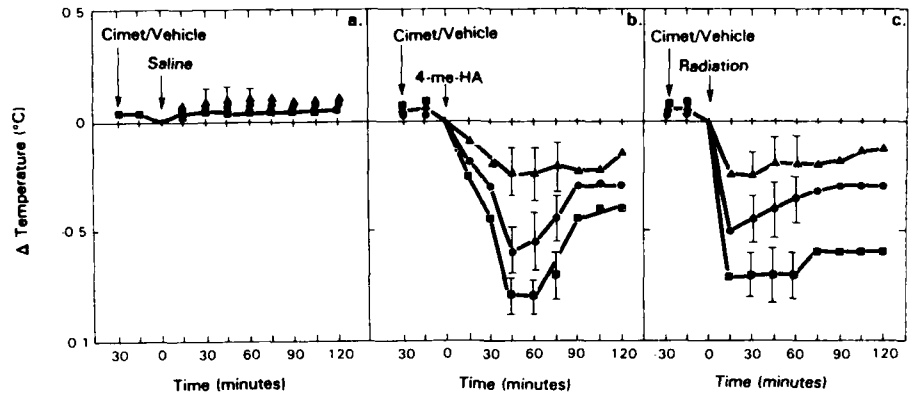

FIG. 7. Effect of icv cimetidine on hypothermia induced by 4-methylhistamine and ionizing radiation. (a) Cimetidine (Cimet) 10 μg (●), 30 μg (■), and vehicle (▲); (b) 30 μg of 4-methylhistamine (4-me-HA) alone (■) and in the presence of Cimet 10 μg (●) and 30 μg (▲); (c) 50 Gy ionizing radiation alone (■) and in the presence of Cimet 10 μg (●) and 30 μg (▲). Each point represents the mean ± SE of five observations. Zero on the abscissa represents temperature at the time of second injection.

Serotonin has also been shown to be involved in thermoregulation (*6*). Serotonin-induced hypothermia (30 μg, icv) can be blocked by pretreatment with the serotonin antagonist methysergide (Fig. 8). However, methysergide had no effect on radiation-induced hypothermia.

DISCUSSION

Exposure of rats to ionizing radiation induced either hyperthermia or hypothermia depending on the dose. Doses of 1–15 Gy γ photons induced hyperthermia, while doses of 20–200 Gy induced hypothermia. Radiation-induced hyperthermia appears to be centrally mediated, since body-only exposure resulted in hypothermia.

Ionizing radiation induces prostaglandin synthesis (*32, 33*). The observations that prostaglandins are potent pyretic agents (*8*) and that various anti-inflammatory

TABLE III

Effect of Mepyramine and Cimetidine on the Hypothermia Induced by 4-Methylhistamine and 2-Methylhistamine

Treatment		*Mean change temperature (°C)*
Saline	+ 4-Methylhistamine	0.8 ± 0.15 (n = 6)
Mepyramine, 10 μg	+ 4-Methylhistamine	0.7 ± 0.20 (n = 5)
Mepyramine, 30 μg	+ 4-Methylhistamine	0.5 ± 0.25 (n = 5)
Saline	+ 2-Methylhistamine	0.9 ± 0.10 (n = 5)
Cimetidine, 10 μg	+ 2-Methylhistamine	1.1 ± 0.25 (n = 5)
Cimetidine, 30 μg	+ 2-Methylhistamine	0.8 ± 0.18 (n = 5)

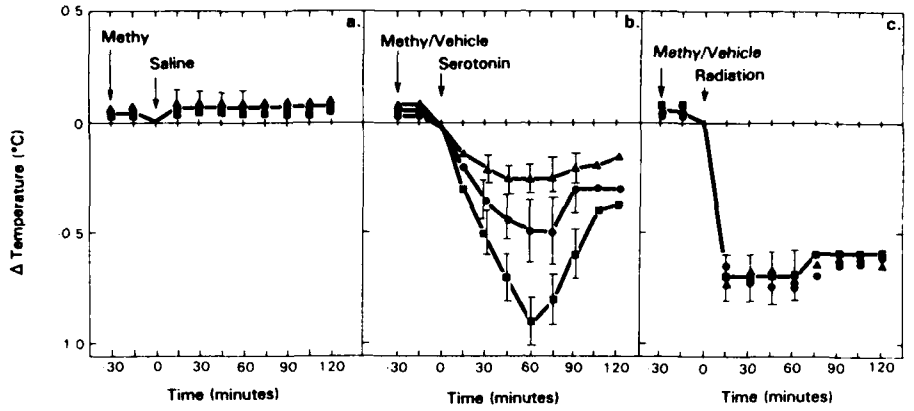

FIG. 8. Effect of icv methysergide on hypothermia induced by serotonin and ionizing radiation. (a) Methysergide (Methy) 10 μg (▲), 30 μg (■), and vehicle (●); (b) 10 μg of serotonin alone (■) and in the presence of Methy 10 μg (●) and 30 μg (▲); (c) 50 Gy ionizing radiation alone (■) and in the presence of Methy 10 μg (●) and 30 μg (▲). Each point represents the mean ± SE of five observations. Zero on the abscissa represents temperature at the time of second injection.

agents blocked their synthesis in tissue (*34*) have implicated prostaglandins in thermoregulation. Indomethacin attenuated the hyperthermia due to low doses of ionizing radiation, indicating that this effect may be mediated by prostaglandins.

Ionizing radiation alters β-endorphin-like immunoreactivity in the brain but not in blood (*35*). β-Endorphin induces hyperthermia. When β-endorphin is injected centrally to different species, varying the ambient temperature and dose, the effect is similar to that observed after central or peripheral administration of morphine (*36, 37*). Relatively low doses of morphine and β-endorphin raise the level about which temperature is regulated in rats, cats, mice, rabbits, guinea pigs, and fish (*38–40*). If radiation induces the release of β-endorphin, naloxone and similar antagonists ought to lower temperature. In our experiments, naloxone attenuated only the hyperthermia induced by 1- and 3-Gy doses of radiation and had no antagonistic effect on higher doses (5 to 15 Gy).

Since indomethacin attenuated the hyperthermia induced by all the lower doses studied, there may be a possible interrelationship between the opioid peptides and prostaglandins. Opioids have been reported to increase the synthesis of prostaglandins in the central nervous system (*41*). If radiation exposure resulted in the release of central β-endorphin, the resulting synthesis and release of prostaglandins would be blocked by indomethacin treatment.

The effect of indomethacin reversing radiation-induced hyperthermia may have some clinical utility. Clinical reports of radiation accidents have consistently indicated the rapid development of fever, lasting for many hours (*42–44*). Patients were generally given antibiotics to suppress infections. Anti-inflammatory drugs, such as indomethacin (a drug used in the treatment of arthritis), have not been used and might be useful adjuncts to therapy. Vomiting and diarrhea are common in accident victims, possibly making indomethacin difficult to administer by the normal oral

route. However, indomethacin could be included in an intravenous drip along with electrolytes and antibiotics.

The hypothermic effect of high doses of radiation appears to involve the release of histamine. Central administration of 2-methylhistamine (a relatively specific H_1 receptor agonist) and 4-methylhistamine (a relatively specific H_2 receptor agonist) caused hypothermia in rats that was selectively attenuated by both the H_1 receptor antagonist, mepyramine, and the H_2 receptor antagonist, cimetidine. Similar results have been reported in guinea pigs and rabbits (*45*, *46*). In the present experiments, both mepyramine and cimetidine specifically attenuated the hypothermia induced by 2-methylhistamine and 4-methylhistamine, respectively, and also antagonized radiation-induced hypothermia, indicating the involvement of histaminergic H_1 and H_2 receptors.

Central injection of serotonin in rats induces hypothermia and was specifically antagonized by the serotonin antagonist, methysergide (*47*). However, serotonin was not involved in radiation-induced hypothermia, since methysergide did not attenuate the hypothermia.

The present results indicate that ionizing radiation induces hyperthermia after low doses and hypothermia after high doses. Prostaglandins and to some extent opioid peptides may be involved in the hyperthermia, and histaminergic H_1 and H_2 receptors, but not serotonin, may be involved in the hypothermia.

ACKNOWLEDGMENTS

This research was supported by the Armed Forces Radiobiology Research Institute, Defense Nuclear Agency, under work unit B4157. Views presented in this paper are those of the authors; no endorsement by the Defense Nuclear Agency has been given or should be inferred. Research was conducted according to the principles enunciated in the "*Guide for the Care and Use of Laboratory Animal Resources, National* Research Council."

RECEIVED: February 27, 1987; REVISED: September 28, 1987

REFERENCES

1. D. J. KIMELDORF and E. L. HUNT, In *Ionizing Radiation: Neural Function & Behavior*, p. 125. Academic Press, New York, 1965.
2. T. S. VENINGA, Implication of bioamines in the X-ray-induced temperature response of cats and rabbits. *Radiat. Res.* **48**, 358–367 (1971).
3. H. FANGER and C. C. LUSHBAUGH, Radiation death from cardiovascular shock following a criticality accident. *Arch. Pathol* **83**, 446–460 (1967).
4. S. B. KANDASAMY, W. A. HUNT, and G. A. MICKLEY, Effects of ionizing radiation on the temperature of conscious rats. In *Proceedings of the International Conference on Prostaglandins and Lipid Metabolism in Radiation Injury* (T. L. Walden, Jr., and H. N. Hughes, Eds.), p. 79. Plenum, New York, 1986.
5. S. B. KANDASAMY, W. A. HUNT, and G. A. MICKLEY, Ionizing radiation induces hypothermia in guinea pigs. *Toxicologist* **7**, 1024 (1987).
6. W. FELDBERG and A. S. MILTON, In *Inflammation* (J. R. Vane and S. H. Ferreira, Eds.), pp. 617–656. Springer-Verlag, New York, 1978.
7. A. S. MILTON and S. WENDLANDT, A possible role for prostaglandin E, as a modulator for temperature regulation in the central nervous system of a cat. *J. Physiol.* **207**, 76–77 (1970).

8. A. S. MILTON and S. WENDLANDT, Effects on body temperature of prostaglandin of the A, E, and F series on injections into the third ventricle of unanaesthetized rats and rabbits. *J. Physiol* **218,** 325–336 (1971).
9. D. S. SEGAL, R. G. BROWNE, F. BLOOM, N. LING, and D. GUILLEMIN, Beta-endorphin: Endogenous opiate or neuroleptic. *Science* **198,** 411–414 (1977).
10. L. F. TSENG, H. H. LOH, and C. H. LI, Human beta-endorphin: Development of tolerance and behavioral activity in rats. *Biochem. Biophys. Res. Commun.* **74,** 390–396 (1977).
11. W. G. CLARK and G. L. BERNARDINI, β-Endorphin-induced hyperthermia in the cat. *Peptides* **2,** 371–373 (1981).
12. S. B. KANDASAMY and B. A. WILLIAMS, Peptide and non-peptide opioid-induced hyperthermia in rabbits. *Brain Res.* **265,** 63–71 (1983).
13. E. C. LASSER and K. W. STENSTROM, Elevation of circulating blood histamine in patients undergoing deep roentgen therapy. *Am. J. Roentgenol.* **72,** 985–988 (1954).
14. L. G. COCKERHAM, T. F. DOYLE, M. A. DONLON, and E. A. HELGESON, Canine post-radiation histamine levels and subsequent response to compound 48/80. *Aviat. Space Environ. Med.* **55,** 1041–1045 (1984).
15. L. G. COCKERHAM, T. F. DOYLE, M. A. DONLON, and C. J. GOSSETT-HAGERMAN, Antihistamines block radiation-induced intestinal blood flow in canines. *Fund. Appl. Toxicol.* **5,** 597–604 (1985).
16. W. A. ALTER III, R. N. HAWKINS, G. N. CATRAVAS, T. F. DOYLE, and J. K. TAKENAGA, Possible role of histamine in radiation induced hypotension in the rhesus monkey. *Radiat. Res.* **94,** 654 (1983).
17. L. G. COCKERHAM, T. J. CERVENY, and J. D. HAMPTON, Postradiation regional cerebral blood flow in primates. *Aviat. Space Environ. Med.* **57,** 578–582 (1986).
18. T. F. DOYLE, J. E. TURNS, and T. A. STRIKE, Effect of an antihistamine on early transient incapacitation of monkeys subjected to 4 rads of mixed gamma-neutron radiation. *Aerospace Med.* **42,** 400–403 (1971).
19. H. M. ADAM and H. K. A. HYE, Concentration of histamine in different parts of brain and hypophysis of cat and its modification by drugs. *Br. J. Pharmacol.* **28,** 137–152 (1966).
20. J. F. LIPINSKI, H. SCHAUMBURG, and R. J. BALDESSARINI, Regional distribution of histamine in human brain. *Brain Res.* **52,** 403–408 (1973).
21. S. H. SNYDER and K. M. TAYLOR, Histamine in the brain: A neurotransmitter. In *Perspectives in Neuropharmacology* (S. H. Snyder, Ed.), pp. 43–73. Oxford Univ. Press, New York, 1972.
22. J. C. SCHWARTZ, Histaminergic mechanisms in brain. *Annu. Rev. Toxicol.* **17,** 325–339 (1977).
23. M. BAUDRY, M. P. MARTRES, and J. C. SCHWARTZ, The subcellular localization of histidine decarboxylase in various regions of rat brain. *J. Neurochem.* **21,** 1301–1309 (1973).
24. M. BAUDRY, M. P. MARTRES, and J. C. SCHWARTZ, H_1 and H_2 receptors in the histamine-induced accumulation of cyclic AMP in guinea pig slices. *Nature* **253,** 362–364 (1975).
25. K. M. TAYLOR and S. H. SNYDER, Brain histamine. Rapid apparent turnover altered by restraint and cold stress. *Science* **172,** 1037–1039 (1971).
26. M. D. GREEN, B. COX, and P. LOMAX, Histamine H_1 and H_2 receptors in the central thermoregulatory pathways of the rat. *J. Neurosci. Res.* **1,** 353–359 (1975).
27. G. G. SHAW, Hypothermia produced in mice by histamine acting on the central nervous system. *Br. J. Pharmacol.* **42,** 205–214 (1971).
28. H. E. BREZENOFF and P. LOMAX, Temperature changes following microinjection of histamine into the thermoregulatory centers of the rat. *Experientia* **26,** 51–52 (1970).
29. C. H. SAWYER, Rhinencephalic involvement of pituitary activation by intraventricular histamine in the rabbit under nembutal anaesthesia. *Am. J. Physiol.* **180,** 37–46 (1955).
30. P. LOMAX and M. D. GREEN, In *Body Temperature: Regulation, Drug Effects, and Therapeutic Implications,* (P. Lomax and E. Schonbaum, Eds.), pp. 289–304. Dekker, New York, 1979.
31. L. S. PELLIGRINO, A. S. PELLEGRINO, and A. J. CUSHMAN, *A Stereotaxic Atlas of the Rat Brain.* Plenum, New York, 1979.
32. V. EISEN and D. I. WALKER, Effect of ionizing radiation on prostaglandin-like activity in tissues. *Br. J. Pharmacol.* **57,** 527–532 (1976).
33. E. PAUSESCU, R. CHIRVASIE, T. TEODOSIU, and C. PAUN, Effects of ^{60}Co gamma-radiation on the hepatic and cerebral levels of some prostaglandins. *Radiat. Res.* **65,** 163–171 (1976).

34. J. R. VANE, Inhibition of prostaglandin synthesis as a mechanism of action for aspirin-like drugs. *Nature* **231**, 232–235 (1971).

35. G. A. MICKLEY, K. E. STEVENS, G. H. MOORE, W. DEERE, G. A. WHITE, G. L. GIBBS, and G. P. MUELLER, Ionizing radiation alters beta-endorphin-like immunoreactivity in brain but not blood. *Pharmacol. Biochem. Behav.* **19**, 979–983 (1983).

36. W. G. CLARK and J. M. LIPTON, Changes in body temperature after administration of amino acids, peptides, dopamine, neuroleptics, and related agents. II. *Neurosci. Biobehav. Rev.* **18**, 299–371 (1985).

37. J. M. LIPTON and W. G. CLARK, Neurotransmitters in temperature control. *Annu. Rev. Physiol.* **48**, 613–623 (1986).

38. A. H. REZANI, C. J. GORDON, and J. E. HEATH, Action of preoptic injections of β-endorphin on temperature regulation in rabbits. *Am. J. Physiol.* **243**, R104–111 (1982).

39. S. B. KANDASAMY and B. A. WILLIAMS, Hyperthermic responses to central injection of some peptide and non-peptide opioids in the guinea pig. *Neuropharmacology* **2**, 621–628 (1983).

40. M. KAVALIERS, Pineal mediation of the thermoregulatory and behavioral activating effects of β-endorphin. *Peptides* **3**, 679–685 (1982).

41. H. O. J. COLLIER, W. J. MCDONALD-GIBSON, and S. A. SNEED, Morphine and apomorphine stimulate prostaglandin production by rabbit brain homogenate. *Br. J. Pharmacol.* **52**, 116P (1974).

42. T. L. SHIPMAN, C. C. LUSHBAUGH, D. F. PETERSEN, W. H. LANGHAM, P. S. HARRIS, and J. N. P. LAWRENCE, Acute radiation death resulting from an accidental nuclear excursion. *J. Occup. Med.* **3**, 146–192 (1961).

43. J. S. KARAS and J. B. STANBURY, Fatal radiation syndrome from an accidental nuclear excursion. *N. Engl. J. Med* **272**, 755–761 (1965).

44. R. GALE, Witness to disaster: An American doctor at Chernobyl. *Life*, August, 20–28 (1986).

45. P. N. KAUL, S. B. KANDASAMY, and W. G. KIRLIN, Hypothermia following centrally administered histamines in guinea pigs. In *Environment, Drugs, and Thermoregulation*, pp. 55–57. Karger, Basel, 1983.

46. K. K. TANGRI, G. PALIT, N. MISRA, and K. P. BHARGAVA, Histamine and thermoregulation in the rabbit. In *Thermoregulatory Mechanisms and Their Therapeutic Implications*, pp. 224–228. Karger, Basel, 1980.

47. S. B. KANDASAMY and B. A. WILLIAMS, Hypothermic and antipyretic effects of ACTH (1-24) and α-melanotropin in guinea pigs. *Neuropharmacology* **23**, 49–53 (1984).

Breathing 100% Oxygen After Global Brain Ischemia in Mongolian Gerbils Results in Increased Lipid Peroxidation and Increased Mortality

Hubert S. Mickel, Yashesh N. Vaishnav, Oliver Kempski, Dag von Lubitz, Joseph F. Weiss, and Giora Feuerstein

Exposure of Mongolian gerbils to a 100% oxygen atmosphere after 15 minutes of global brain ischemia resulted in a marked increase in the production of pentane, an in vivo product of lipid peroxidation. Much less pentane production occurred in animals subjected to global brain ischemia then exposed to an air atmosphere and in animals exposed to a 100% oxygen atmosphere without ischemia. Gerbils placed in 100% oxygen for 3–6 hours after 15 minutes of ischemia also had a threefold increase in 14-day mortality compared with gerbils subjected to ischemia and then placed in an air atmosphere. These findings raise a serious question about the use of oxygen-enriched atmospheres during reperfusion following ischemia. (*Stroke* 1987;18:426–430)

BREATHING oxygen-enriched atmospheres is a usual and customary emergency procedure for patients suffering from an acute ischemic injury to the brain. Clinicians show little concern that the resulting arterial Po_2 is elevated. Instead, concern is focused on whether hypoxia is occurring as a consequence of respiratory complications.

Production of free radicals of oxygen or reactive oxygen species occurs during reperfusion following ischemia.[1] Lipid peroxidation also occurs in the brain during ischemic injury,[2] possibly related to the presence of endogenous iron.[3] In postischemic brain, iron ion delocalization is thought to promote lipid peroxidation by the production of free radicals of oxygen.[4–6] Xanthine oxidase is also a source of reactive oxygen species damage in ischemia.[7–9] Allopurinol, a xanthine oxidase inhibitor, has been shown to prevent free-radical-induced reperfusion injury.[10] However, following ischemia, mitochondrial respiration is impaired[11] so that an increase in substrate, i.e., molecular oxygen, could result in a dramatic increase in reaction product, i.e., oxygen free radicals. The increase in reactive oxygen species as a consequence of increased tissue Po_2 could result in the tissue injury and lipid peroxidation.[12]

There are many products of lipid peroxidation,[13] including those that result from cleavage of the hydrocarbon chain of polyunsaturated fatty acids. Among these products are the alkanes pentane and ethane.[14, 15] Pentane is produced from peroxidative cleavage of the *cis* double bond 6 carbons from the hydrocarbon end of ω-6 fatty acids such as linoleic or arachidonic acids. Ethane is produced in a similar manner from ω-3 fatty acids such as linolenic or eicosapentaenoic acids. These volatile hydrocarbons are eliminated into the expired air and reflect in vivo peroxidation. When collected and measured, alkane production is more indicative of lipid peroxidation than the measurement of thiobarbituric-acid-reactive substances, which is most often used.[16]

To our knowledge, no studies measuring pentane production in relation to brain ischemia have been published.

Materials and Methods

Male Mongolian gerbils (Tumblebrook Farms), weighing 55–65 g were subjected to 15 minutes of global brain ischemia by bilateral carotid occlusion under anesthesia with 2% halothane (2-bromo-2-chloro-1,1,1-trifluoroethane, Halocarbon Laboratories, Hackensack, N.J.). *Control animals* were subjected to anesthesia and sham surgery but not ischemia. At the end of 15 minutes of ischemia and/or anesthesia, each animal was placed in an atmosphere of either pure 100% oxygen (UN 1072, Air Products) or breathing quality air (Air Products). To reduce the amount of halothane present in the closed atmosphere, each animal breathed the atmosphere flowing through a closed container measuring 20 × 14 × 6 in. for 30 minutes. At the end of 30 minutes, the animal was placed in a closed system to measure pentane produc-

From the Neurobiology Research Division, Department of Neurology, Uniformed Services University of the Health Sciences (H.S.M., G.F.), the Armed Forces Radiobiology Research Institute (Y.N.V., J.F.W.), the National Institutes of Health (D.v.L.), Bethesda, Maryland, and Institut fuer Chirurgische Forschung, Klinikum Grosshadern, Munich, Federal Republic of Germany (O.K.).

The opinions or assertions contained herein are the private ones of the authors and are not to be construed as official or as necessarily reflecting the views of the Department of Defense or the Uniformed Services University. There is no objection to its presentation and/or publication.

Supported by the Uniformed Services University of the Health Sciences Protocol G19218

Address for reprints: Hubert S. Mickel, MD, P.O. Box 41046, Bethesda, MD 20814

Received July 4, 1986, accepted October 14, 1986

tion. To decrease environmental hydrocarbon contamination of the expired atmospheric sample, a 10-minute washout period of the closed system was required. The experiments were conducted according to the principles set forth in the "Guide for Care and Use of Laboratory Animals," Institute of Laboratory Animal Medicine, National Research Council, Department of Health, Education, and Welfare, publication no. (NIH) 80-23, 1980.

The animal holding chamber used for sampling volatile compounds was similar to that described by Lawrence and Cohen[17] and Hafeman and Hoekstra,[18] with some modifications. Figure 1 represents the closed system used in these studies. A 2-liter Nalgene vacuum-type dessicator was used as the animal chamber. Oxygen or air was introduced through a polypropylene Y tube into the air or O_2 reservoir. The reservoir was connected with another polypropylene Y tube to the inlet of the chamber to allow oxygen or air to enter from the reservoir. A water seal maintained the closed system at ambient pressure. The expired chamber air was cycled through a series of 3 traps: 5% H_2SO_4 to remove NH_3, 10% KOH to remove CO_2, and a cold finger ice bath to condense water vapors. As NH_3 and CO_2 were removed from the chamber air, equal volumes of oxygen or air entered the chamber through a stopcock to maintain a constant atmospheric pressure. Before sampling, the pump was turned off. Forty-ml samples were removed with a gastight syringe at a three-way stopcock, and an equal volume of oxygen or air entered the chamber through another stopcock to maintain constant atmospheric pressure.

The sample was passed through a stainless steel cartridge (3.2 × 70 mm) filled with activated alumina, kept at −32° C during filling and before analysis. A Varian 3700 gas chromatograph was equipped with a Chemical Data System Model 310 concentrator. The cartridge was inserted in the desorber probe, and the desorber was flash-heated to 210° C for 3 minutes to desorb and transfer the hydrocarbons from the alumina cartridge to the concentrator trap (3.2 mm × 60 cm, leading half filled with charcoal, the other half with Tenax[19]). On flash-heating the trap desorbed the hydrocarbons onto the gas chromatographic column (3.2 mm × 2 m filled with Porasil B). The column was heated at 60° C for 3 minutes, and then the temperature was increased to 75° C at 1° min. The injection port was maintained at 220° C and the flame ionization detector at 250° C.

Areas of hydrocarbon peaks and standard samples were determined by triangulation, and the quantity of pentane evolved was calculated.[2]

Activated charcoal (nutshell type SK-4, 60/80 mesh), activated alumina (Alcoa type F-1, 60/80 mesh), Porasil B (80/100 mesh), Tenax (2,6-diphenyl-*p*-phenyleneoxide polymer, 80/100 mesh) were all purchased from Applied Science Laboratories, State College, Penn. Hydrocarbon standards (approximately 100 ppm in helium) were obtained from Scott Specialty Gases, Plumsteadville, Penn. Air, helium, hydrogen, and oxygen (scientific grade) for gas chromatography were purchased from MG Industries, Valley Forge, Penn. Teflon tubing with Luer adapters was obtained from Hamilton, Reno, Nev., and Tygon tubing, type R-3603, from Fisher Scientific Company.

A sample of the atmosphere was taken at the time the system was closed. This became the zero time (30 minutes postischemia) sample. Subsequent samples were taken at 60, 90, 120, and 180 minutes after ischemia or anesthesia. There were 4 groups, each with 7 animals: 2 ischemic groups (air and oxygen) and 2 control groups (air and oxygen).

Mortality was assessed for 14 days after ischemia in gerbils exposed to oxygen for 3 or 6 hours.

The results were analyzed by analysis of variance (ANOVA) followed by the Student-Newman-Keuls test for multiple comparisons using an HP-85 microcomputer. Fisher's exact test was used to analyze mortality.

Results

After 3 hours of oxygen exposure following ischemia, a total of 581.3 ± 77.1 (mean ± SEM) pmol of

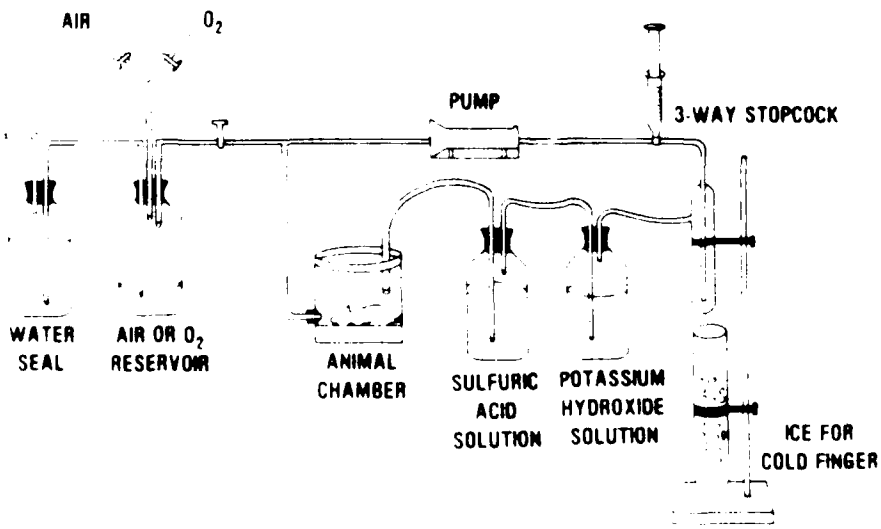

FIGURE 1 *Diagram of closed system used*

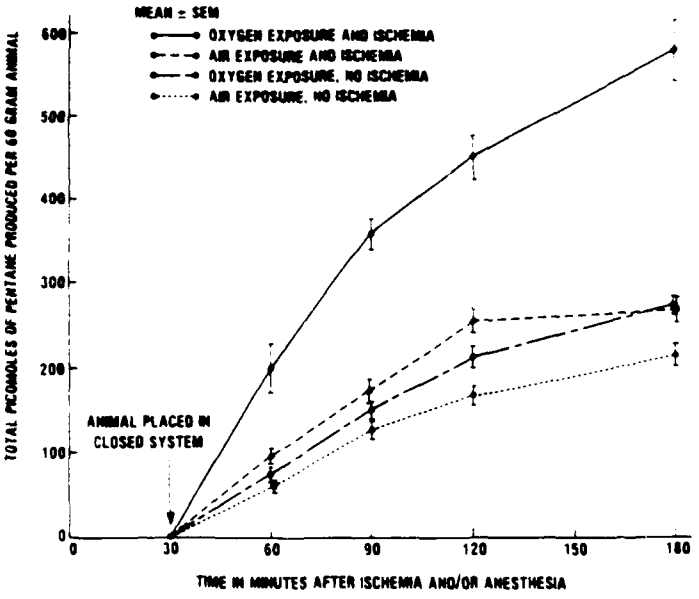

FIGURE 2. *Production of pentane by Mongolian gerbils after brain ischemia and/or anesthesia with reperfusion in air or a 100% oxygen atmosphere.*

pentane per 60-g animal was collected during a 150-minute collection period. Ischemic animals placed in air produced only 271.5 ± 26.2 pmol of pentane per 60-g animal. Control animals placed in 100% oxygen produced 276.7 ± 15.7 pmol of pentane per 60-g animal, and control animals placed in air produced 213.2 ± 28.4 pmol of pentane per 60-g animal. The total amount of pentane produced by the ischemic animals exposed to oxygen was about twice that produced by the other groups and is significantly different from each of the other groups ($p < 0.01$). Although differences in pentane production were noted between the ischemic animals placed in air and the control groups, these differences were not significant at all times sampled (Figure 2). Although the values for 60 minutes were marginally significant, the increases in the amount of pentane formed by ischemic animals exposed to oxygen at 90, 120, and 180 minutes were significant ($p < 0.01$) by the Student-Newman-Keuls test. The amount of peroxidation measured by pentane production is essentially 3 times as much as that expected at 180 minutes by the sum of the individual contributions of ischemia and of oxygen alone over the values for control gerbils exposed to air. Since the only difference between animals exposed to oxygen after anesthesia and animals exposed to oxygen after occlusion is a 15-minute period of brain ischemia, the increased tissue oxygen content from breathing 100% oxygen during brain reperfusion is assumed to result in a marked increase in lipid peroxidation. However, at this time we have no direct experimental evidence demonstrating that the increase in pentane production occurs only in the brain.

Furthermore, exposure to 100% oxygen for 3–6 hours following global brain ischemia results in a threefold increase in 14-day mortality when compared with animals exposed to air following ischemia. In fact, oxygen-treated animals displayed significantly higher mortality ($p < 0.001$) throughout the 14 days following the ischemic insult. [In a subsequent experiment, exposure of ischemic animals to 100% oxygen for 30 minutes resulted in no difference in mortality compared with ischemic animals exposed to air ($n = 16$ in each group).] There was no significant difference between exposure to 100% oxygen for 3 or 6 hours (Figure 3).

Discussion

Pentane is a reliable parameter for measuring in vivo lipid peroxidation.[19] Pentane is also a more sensitive index for ethanol-induced lipoperoxidation than ethane.[20] A problem in measuring pentane production in a closed system is that pentane is metabolized by the monooxygenase cytochrome P-450 at a rate 5–10 times faster than ethane,[21] resulting in a decrease in the total amount of pentane recovered due to metabolic elimination.[22] For that reason, the actual amount of pentane produced is probably higher than that measured in these studies. However, the total volume of our system is larger than of systems used by others, and perhaps there is a lesser proportion of pentane metabolized.

Since all factors were the same for our control and ischemic animals except the occurrence of ischemia, it is most unlikely that a gastrointestinal or bacterial origin for the measured pentane is of any consequence in this study,[23] and, most likely, the brain is the site of the increased pentane production during oxygen exposure following global brain ischemia.

The basal rate of pentane production in control animals exposed to air was 24 pmol pentane/kg body wt/min. This compares with 16 pmol pentane/kg body wt/min in human infants.[24] Pentane production in control animals breathing 100% oxygen was 31 pmol pentane/kg body wt/min. If one assumes that the increase in production of pentane by animals subjected to brain ischemia and then exposed to 100% oxygen is derived from the brain itself, it is possible to derive the follow-

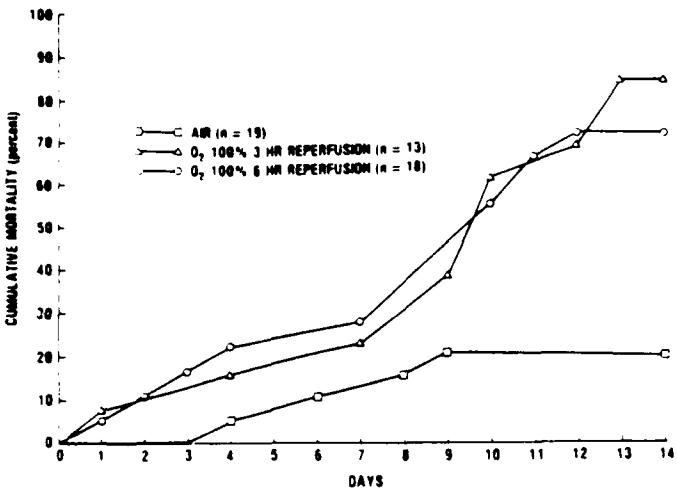

FIGURE 3. *Cumulative mortality in gerbils following 15-minute bilateral carotid occlusion.*

ing calculations. Assuming that the brain of a gerbil weighs 1 g and that the increase in pentane production following global brain ischemia represents lipid peroxidation in the brain, there is a production of pentane in the brain of ischemic animals exposed to air of 389 pmol/min/kg brain wt. Calculated from the difference between the ischemic and control animals exposed to 100% oxygen, pentane production from the brain of ischemic animals exposed to oxygen, however, is 2,031 pmol/min/kg brain wt, or 2 pmol/min from the gerbil brain. This is almost 100 times the basal rate of pentane production occurring in the control gerbil breathing air. However, we cannot state that this dramatic increase in lipid peroxidation caused the marked increase in mortality occurring in these animals.

The fact that giving supplemental oxygen is an unquestioned standard practice in clinical medicine for ischemia affecting the brain or heart makes the questions created by our observations of major importance. Whether lipid peroxidation is the only pathogenetic mechanism that is operative in the oxygen effect on reperfusion was not demonstrated in this study. The threshold of oxygen concentration and the duration of exposure needed to produce the deleterious oxygen effect have not yet been determined. Our findings also suggest the possibility that drugs which block peroxidation of lipids might have a potential beneficial effect in the reperfusion injury following ischemia.

Since supplementation with 100% oxygen is a common standard practice in the clinical management of acute myocardial ischemia and stroke, this study suggests that its value should be reassessed, especially in cases where no obvious respiratory difficulties occur and where no deficiency of oxygen is present in perfused tissue.

References

1. McCord JM: Oxygen-derived free radicals in post-ischemic tissue injury. *N Engl J Med* 1985;312:159–163
2. Watson BD, Busto R, Goldberg WJ, Santiso M, Yoshida S, Ginsberg MD: Lipid peroxidation in-vivo induced by reversible global ischemia in rat brain. *J Neurochem* 1984;42:268–274
3. Zaleska MM, Floyd RA: Regional lipid peroxidation in rat brain in vitro: Possible role of endogenous iron. *Neurochem Res* 1985;10:397–410
4. White BC, Krause GS, Aust SD, Eyster GE: Postischemic tissue injury by iron-mediated free radical lipid peroxidation. *Ann Emerg Med* 1985;14:804–809
5. Nayini NR, White BC, Aust SD, Huang RR, Indrieri RJ, Evans AT, Bialek H, Jacobs WA, Komara J: Post resuscitation iron delocalization and malondialdehyde production in the brain following prolonged cardiac arrest. *J Free Radicals Biol Med* 1985;1:111–116
6. Babbs CF: Role of iron ions in the genesis of reperfusion injury following successful cardiopulmonary resuscitation: Preliminary data and a biochemical hypothesis. *Ann Emerg Med* 1985;14:777–783
7. Chambers DE, Parks DA, Patterson G, Roy R, McCord JM, Yoshida S, Parmley LF, Downey JM: Xanthine oxidase as a source of free radical damage in myocardial ischemia. *J Mol Cell Cardiol* 1985;17:145–152
8. McCord JM, Roy RS, Schafler SW: Free radicals and myocardial ischemia. The role of xanthine oxidase. *Adv Myocardiol* 1985;5:183–189
9. Parks DA, Granger DN: Ischemia-induced vascular changes: Role of xanthine oxidase and hydroxyl radicals. *Am J Physiol* 1983;245:G285–G289
10. Stewart JR, Crute SL, Loughline V, Hess ML, Greenfield LJ: Prevention of free radical-induced myocardial reperfusion injury with allopurinol. *J Thorac Cardiovasc Surg* 1985;90:68–72
11. Hartung KJ, Jung K: Mitochondrial respiratory function as an indicator of the ischemic injury of the rat kidney. *Biomed Biochim Acta* 1985;44:1435–1443
12. Halliwell B, Gutteridge JMC: Lipid peroxidation, oxygen radicals, cell damage, and antioxidant therapy. *Lancet* 1984;1:1396–1397
13. Estabauer H: Aldehyde products of lipid peroxidation, in McBrien DCH, Slater TF (eds): *Free Radicals, Lipid Peroxidation, and Cancer*. London-New York, Academic Press, 1982, pp 101–128
14. Riely CA, Cohen G, Lieberman M: Ethane evolution: A new index of lipid peroxidation. *Science* 1974;183:208–210
15. Wade CR, van Rij AM: *In vivo* lipid peroxidation in man as measured by the respiratory excretion of ethane, pentane, and other low-molecular-weight hydrocarbons. *Anal Biochem* 1985;150:1–7
16. Gavino VC, Dillard CJ, Tappel AL: Release of ethane and pentane from rat tissue slices. Effect of vitamin E, halogenated hydrocarbons, and iron overload. *Arch Biochem Biophys* 1984;233:741–747
17. Lawrence GD, Cohen G: Ethane exhalation as an index of *in*

vivo peroxidation: Concentrating ethane from a breath collection chamber. *Anal Biochem* 1982;122:283–290
18. Hafeman DG, Hoekstra WG: Protection against carbon tetrachloride-induced lipid peroxidation in the rat by dietary vitamin E, selenium and methionine as measured by ethane evolution. *J Nutr* 1977;107:656–665
19. Dumelin EE, Tappel AL: Hydrocarbon gases produced during in vitro peroxidation of polyunsaturated fatty acids and decomposition of preformed hydroperoxides. *Lipids* 1977;12:894–900
20. Moscarella S, Laffi G, Buzzelli G, Mazzanti R, Carmelli L, Gentilini P: Expired hydrocarbons in patients with chronic liver disease. *Hepatogastroenterology* 1984;31:60–63
21. Remmer H, Hintze T, Frank H, Mueh-Zange M: Cytochrome P-450 oxidation of alkanes originating as scission productions during lipid peroxidation. *Xenobiotica* 1984;14:207–219
22. Frank H, Hintze D, Bimboes D, Remmer H: Monitoring lipid peroxidation by breath analysis. Endogenous hydrocarbons and their metabolic elimination. *Toxicol Appl Pharmacol* 1980;56:337–344
23. Gelmond D, Stein RA, Mead JF: The bacterial origin of rat breath pentane. *Biochem Biophys Res Commun* 1981;102:932–936
24. Wispe JR, Bell EF, Roberts RJ: Assessment of lipid peroxidation in newborn infants and rabbits by measurements of expired ethane and pentane: Influence of parenteral lipid infusion. *Pediatr Res* 1985;19:374–379

KEY WORDS • brain ischemia • reperfusion injury • pentane production • lipid peroxidation • oxygen free radicals

0022-1767/88/1407-2260$02.00/0
THE JOURNAL OF IMMUNOLOGY

Vol. 140, 2260-2266, No. 7, April 1, 1988
Printed in U.S.A.

INTERACTION OF RECOMBINANT IL-1 AND RECOMBINANT TUMOR NECROSIS FACTOR IN THE INDUCTION OF MOUSE ACUTE PHASE PROTEINS[1]

RICHARD F. MORTENSEN,[2]* JOHN SHAPIRO,* BIH-FEN LIN,* SUSAN DOUCHES,† AND RUTH NETA†

*From the *Department of Microbiology, The Ohio State University, Columbus, OH 43210, and †Department of Experimental Hematology, Armed Forces Radiobiology Research Institute, Bethesda, MD 20814*

Recombinant mouse and human IL-1 (α and β forms), as well as rTNF-α when administered in vivo, induced the production of the mouse acute phase reactants: serum amyloid P-component (SAP), C3, and fibrinogen. The SAP response to all three rIL-1 proteins reached a maximum at a dose of 10^4 U/mouse, which corresponds to 1 to 10 μg of protein. The maximum in vivo response consisted of a 10-fold increase in SAP levels, a 2-fold increase in C3 levels, and a 3-fold increase in fibrinogen concentration. By contrast, rTNF-α induced a much smaller acute phase (AP) protein response (4-fold increase in SAP) when administered in vivo. Administration of a combination if rIL-1 and rTNF resulted in an AP response that was additive for SAP, synergistic for fibrinogen, but resulted in only the same amount of C3 induced by IL-1 alone. Both recombinant monokines induced new SAP synthesis by isolated hepatocytes in vitro with an optimal response occurring with either 1 U of rIL-1/ml per 2×10^5 hepatocytes or 10^{-3} U/ml of rTNF. The hepatocyte response to IL-1 was of the same magnitude as the response of intact mice; however, the response to TNF was approximately 10^4 times more efficient in vitro. A mixture of the monokines induced an in vitro SAP response that was additive when suboptimal doses of rIL-1 were combined with optimal amounts of rTNF-α. Overall, the findings indicate that both monokines directly trigger hepatocyte synthesis of SAP and that their combined effect probably accounts for a substantial portion of the synthesis of these AP proteins in mice.

During the early stages of an inflammatory response, Mϕ[3] release a variety of polypeptides that are thought to be responsible for some of the characteristics of systemic inflammation (1, 2). Two of these monokines or cytokines are IL-1 and TNF-α which have been implicated as mediators of a variety of inflammatory events, including the induction of synthesis of APR and AP proteins (reviewed in References 3–5). The induction mechansim of the major AP protein of humans, CRP, has long been thought to depend on blood-borne mediators, inasmuch as the liver parenchymal cells are progressively "recruited" into CRP synthesis beginning in the periportal areas as shown with rabbits (6). The earliest experimental evidence indicating that a leukocyte product induced an AP protein was based on the induction of a group of APR in rabbits in response to purified leukocyte endogenous mediator (7), later shown to be IL-1 (1, 3). Evidence documenting the induction of de novo synthesis of an APR by liver hepatocytes in response to either biochemically purified IL-1 or rIL-1 has been limited to such APR as fibrinogen and the C proteins, C3 and factor B (8), minor APR which increase in concentration by only 2-fold, and to one major APR that increases by >100-fold, serum amyloid A protein, the precursor protein for secondary amyloid deposits (9–11).

SAP, which increases in concentration by up to 40-fold in mice in response to a noninfectious stimulus (12, 13), is homologous to CRP (reviewed in Ref. 1). SAP and CRP are members of the Pentraxin family of proteins which are composed of identical, noncovalently linked subunits and share a 66% amino acid and nucleotide sequence homology (14–16). In general, the numerous biologic activities assigned to both CRP and SAP are consistent with their role as effectors of nonspecific host resistance (12), especially those dependent on monocyte/Mϕ (17, 18). In addition, amyloid P component has recently been shown to be a structural component of several tissues, and may be a constituent of connective tissue microfibrils (19, 20). We have previously reported that mouse SAP synthesis is driven by biochemically purified mouse IL-1 both in *vivo* (21) and in *vitro* (22).

The studies described here were designed to compare the requirement for the in vivo and in vitro induction of SAP by rmoIL-1 and rhIL-1 (23–25), as well as rhTNF-α (26), a mediator of many of the same inflammatory events as IL-1 (27). Inasmuch as IL-1 and TNF-α are induced coordinately by the same stimuli from cells of the monocyte lineage, we have also investigated the effect of their combined administration. These experiments were done in vivo and included measurements of three AP proteins to determine whether they are coordinately expressed: SAP, C3, and fibrinogen. Similarly, an IL-1 and TNF interaction was also studied directly in vitro by measuring SAP synthesis by isolated mouse hepatocytes. Our findings show that IL-1 is a more potent inducer of APR

Received for publication August 10, 1987.
Accepted for publication December 30, 1987.
The costs of publication of this article were defrayed in part by the payment of page charges. This article must therefore be hereby marked *advertisement* in accordance with 18 U.S.C. Section 1734 solely to indicate this fact.
[1] Supported by United States Public Health Service, National Institutes of Health Grant CA30015 and a grant from The Johns Hopkins Center for Alternatives to Animal Testing.
[2] To whom correspondence and requests for reprints should be addressed.
[3] Abbreviations used in this paper: Mϕ, macrophage; CRP, C-reactive protein; SAP, serum amyloid P-component; APR, acute phase reactant(s); AP, acute phase; rhIL-1 and rhTNF, human rIL-1 and rTNF; rmoIL-1, mouse rIL-1.

than TNF-α, but that the expression of the acute phase proteins differ in response to combinations of IL-1 and TNF. The results also show that both monokines act directly on hepatocytes, rather than via additional mediators, to induce the coordinated increase in production of these AP proteins.

MATERIALS AND METHODS

Mice. Female C57BL/6N, C3H/HeN, and C3H/HeJ mice were obtained from Harlan Sprague Dawley (Indianapolis, IN) or the Animal Genetics and Production Branch (National Institutes of Health, Bethesda, MD) and were used at 5 to 8 wk of age in all experiments. Mice were housed in a Bioclean model PCS-80 filter chamber (Hazelton Laboratories, Bethesda, MD) with an air flow of 0.7 m^3/min.

Monokines. rmoIL-1 was a generous gift from Dr. Steven B. Mizel and Dr. Peter M. LoMedico (Hoffmann-La Roche, Nutley, NJ) and had a sp. act. of 2×10^8 U/mg protein by the thymocyte co-stimulation assay (23, 28). A goat anti-serum specific for the moIL-1 was also obtained from Dr. Steven Mizel (29). rhIL 1α was obtained from Dainippon Ltd. (Japan) and Hoffmann LaRoche. rhIL-1β was obtained from the Upjohn Co. through the courtesy of Dr. Daniel Tracey. The specific activity of rhIL-1-α was 1×10^7 U/mg protein and for rhIL-1β, 1×10^8 U/mg. The activity of the rhIL-1 was based on the LBRM-33 1A5 proliferation assay (28). rhTNF-α was obtained through Dr. H. Michael Shepard (Genentech, South San Francisco, CA) and had a sp. act. of 5×10^7 U/mg protein (lot 3056-55) and was stored at 4°C. The rTNF-α was tested for biologic activity at the time it was diluted (5×10^5 U/ml) for injection or addition to to hepatocyte cultures by the L-929 cytotoxicity assay in the presence of 1 μg/ml of actinomycin D (26). The activity was 50 to 90% of the sp. act. of the original material and was used within 2 mo of receipt. Rabbit antibody to rTNF-α (Endogen, Inc.) was capable of neutralizing 10^4 U/ml antiserum. The endotoxin content of all the recombinant monokines was <0.1 ng/mg protein by the Limulus amoebocyte lysate assay (M. A. Bioproducts, Walkersville, MD).

Induction of APR in vivo by monokines. Mice were bled (retro-orbitally) and serum or plasma concentrations of the APR determined before beginning each experiment to ensure that the levels of the APR were within the range of endogenous concentrations for the strain (13). Recombinant cytokines were diluted in Dulbecco's PBS containing 0.2% defined HyClone FBS (Logan, UT), the latter contained <0.005 ng/ml endotoxin. The same volume of 0.5 ml was injected i.p. into each mouse. For each dose of the recombinent protein five mice were used per experiment. At 20 h after injection, the mice were bled and the serum or plasma collected and stored at −20°C.

Fibrinogen assay. Assays for fibrinogen in diluted citrated plasma were performed by measuring the rate of conversion of fibrinogen to fibrin in the presence of thrombin excess. The calibration was made using the Sigma Diagnostic Kit (Sigma Chemical Co., St. Louis, MO). Measurements of fibrin clot formation were performed on a Fibrometer (Becton Dickinson, Mountain View, CA). The data is expressed as milligrams of fibrinogen/100 ml of plasma.

Measurement of SAP and C3. Serum levels of SAP and C3 were measured by rocket immunoelectrophoresis. Rabbit antibody to mouse SAP was prepared as described elsewhere (13, 21) and a monospecific goat anti-mouse C3 was purchased from Cappel Labs (Cooper Biomedical, Malvern, PA). The rabbit anti-mouse SAP and anti-mouse C3 were used at a 1/120 and a 1/150 dilution, respectively, in 1.0% agarose in low ionic strength Tricine-buffer (pH 8.6). The sensitivity of the assay was approximately 2 μg/ml for each Ag. A single acute phase mouse serum from A/J mice containing 1800 μg/ml SAP and 1200 μg C3 served as the standard.

Isolation and culture of mouse hepatocytes. Mice were lightly anesthetized with sodium pentobarbital and a retrograde liver perfusion was done as described by Klaunig et al. (30). Briefly, microtubing was inserted into a small cut made in the hepatic portal vein and sutured into place. The lower abdominal vena cava was then ligated and the perfusate allowed to run to waste through a cut made in the subhepatic inferior vena cava. The liver was perfused first with 30 ml of Ca^{2+} and Mg^{2+} free HBSS containing 10 mM D-glucose, 50 ng/ml insulin, 0.5 mM EGTA, and 0.4 mM HEPES which was kept at 37°C. This was followed by perfusion with type IV collagenase (Worthington Biochemicals) at 175 U/ml in L-15 Leibowitz medium (GIBCO, Grand Island, NY) until the liver lobes had noticeably disintegrated. Throughout the perfusion, the subhepatic inferior vena cava was periodically clamped to increase the intrahepatic pressure. The entire perfusion was carried out at 37°C at a flow rate of 5 ml/min. The perfused liver was removed, placed in 25 ml of the collagenase solution, and gently tweezed until most of the cells were released from the capsule. After pipetting this suspension two or three times, the cells were passed through sterile gauze, mixed with an equal volume of L-15 containing 10% FBS and 20 mM HEPES, and spun down at only 50 × *g* to remove Kuppfer cells. The cells were resuspended in L-15 medium containing 10% FBS (HyClone), 1.5 mg/ml D-glucose, 0.45 mg/ml BSA, 10 ng/ml insulin, 10^{-6} M dexamethasone, and 10 mM HEPES and plated at 2×10^6 cells/well in 24-well plates (Corning No. 25820). After 3 h, the medium and nonadherent cells were removed and the same medium without dexamethasone was added for another 24 h. After this incubation period, various amounts of rhIL-1-δ and/or rTNF-α were added to the cells along with fresh medium of L-15 plus 5% mouse serum depleted of SAP, 1.5 mg/ml D-glucose, 0.45 mg/ml BSA, 10 ng/ml insulin, and 20 mM HEPES. After 24 h of incubation, the supernatants were removed and assayed for SAP levels by a competitive ELISA using reagents prepared as described elsewhere (22). An Immulon-II plate (Dynatech, Cambridge, MA) was coated at 4°C overnight with 200 ng/well of purified mouse SAP. Dilutions of the culture supernatants were incubated overnight with a 1/2000 dilution of IgG rabbit anti-mouse SAP. The supernatants were then added to the coated wells and incubated for 4 h at room temperature. A 1/5000 dilution of horseradish peroxidase-IgG (goat) anti-rabbit IgG (Kirkegard and Perry, Gaithersburg, MD) was added for 2 h, followed by the substrate o-phenylenediamine at 1 mg/ml in 0.1 M citric acid (pH 4.5) and 0.012% hydrogen peroxide. A purified preparation of mouse SAP was used to generate a standard curve over the range of 10 to 2000 ng/ml. The sensitivity of the assay was approximately 10 ng/ml.

RESULTS

Induction of SAP in vivo by rIL-1. We tested both mouse and human rIL-1 preparations for their SAP-inducing capacity in the C57BL/6 mouse since this strain is a high SAP responder to many inflammatory stimuli (13, 21). A dose-response relationship between SAP levels 24 h after injection of rmoIL-1 was observed with a maximum response occurring in response to 10^4 U/mouse (Fig. 1). The 10^4 U of rmoIL-1 corresponds to 5.0 μg of protein based on a sp. act. of 2×10^6 U/mg protein. A goat antiserum specific for the rmoIL-1 neutralized most of its SAP-inducing capacity when used at a dilution sufficient to neutralize all of the IL-1 activity in the

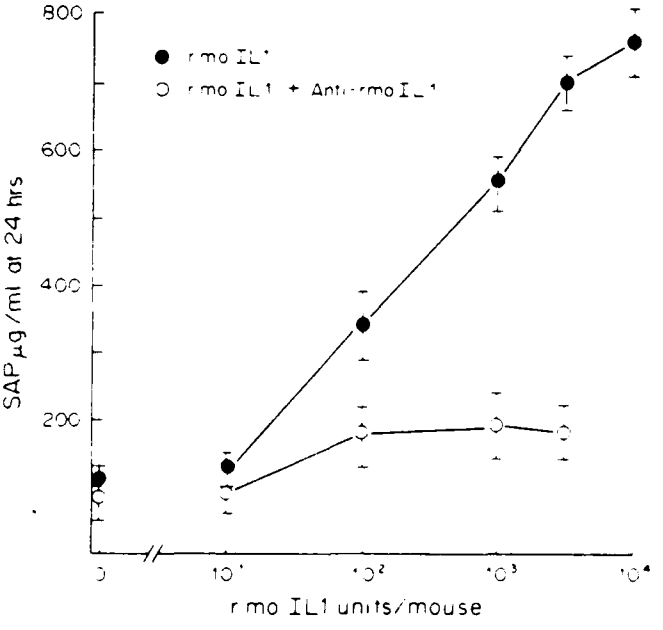

Figure 1 Production of SAP by C57BL/6 mice in response to rmoIL-1. Female mice were injected i.p. with various amounts of rmoIL-1 (●) diluted in Dulbecco's PBS containing 0.2% FBS. Controls received the vehicle alone (0 U). The rmoIL-1 was allowed to react with a sufficient amount of goat antiserum specific for rmoIL-1 to neutralize the IL-1 activity in the thymocytic assay. Groups of five mice per dose were used. Data represents the mean (±SD) from three experiments.

thymocyte bioassay (29) (Fig. 1). There was only a slight (2.0-fold) response to the vehicle itself which contained <0.005 ng LPS in the amount injected which is below the threshold amount for inducing a change in SAP levels (13).

Both the α and β forms of human rIL-1 were also active in vivo; however, the α form was slightly more active at submaximal doses (Fig. 2). The maximum SAP response occurred in response to approximately 10^4 U of each form of IL-1 which corresponds to 1 μg of rIL-1α and 10 μg of rIL-1β, respectively. Heat inactivation of the rhIL-1 preparations destroyed >95% of their activity in the LBRM-33-1A5 assay for IL-2 production (data not shown), and also most of the SAP-inducing activity (Fig. 2). A significant in vivo SAP response occurred with as little as 10^2 U of either mouse or human rIL-1 which corresponds to 10 to 100 ng of protein. The amount of IL-1 eliciting the maximum response is equivalent to blood concentrations of $\sim 10^{-11}$ M concentration, an estimate based on the uptake of all of the IL-1 injected into the circulation. This concentration has been associated with several other reported biologic activities of IL-1 (3, 5, 27).

Kinetics of mouse SAP induction. The mouse SAP response to a stimulus such as LPS reaches a maximum level 30 to 36 h after challenge with a single dose of LPS (21). If IL-1 is a mediator of SAP induction, then the kinetics of the SAP response to IL-1 should be more rapid than to the inflammatory agent. Measurements at 6-h intervals after injection of rhIL-1-β indicated that the maximum levels of SAP occurred 12 to 18 h later and rapidly declined thereafter to the endogenous levels of 30 to 50 μg/ml for C57BL/6 mice by 48 h (Fig. 3).

In vivo induction of SAP by rTNF-α. TNF-α is another cytokine that mediates several inflammatory events including the induction of APR (31). An increase in SAP levels in response to rTNF-α occurred only at doses >10^4 U/mouse and the maximum response was a fourfold increase (Fig. 4). The maximum response required 5 × 10^4 U/mouse, or approximately 1 μg protein (Fig. 4). The

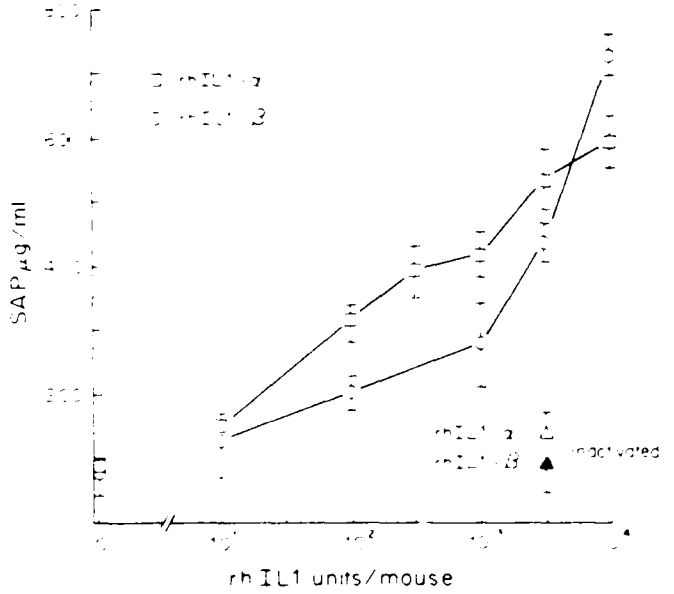

Figure 2. Induction of SAP in C57BL/6 mice in response to either rhIL-1α or rhIL-1β. The 20-h level of SAP (μg/ml ±SD) was measured. Controls received either the vehicle alone (0 U) or heat (80°C, 5 min) inactivated rhIL-1 preparations (△, ▲).

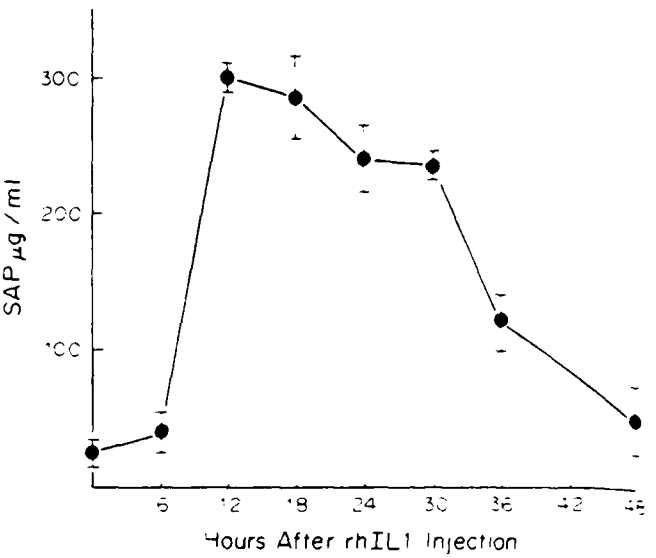

Figure 3. Kinetics of the in vivo induction of mouse SAP synthesis by rhIL-1β. C57BL/6 mice were infused with 10^3 U of rhIL-1β and serum samples monitored every 6 h for SAP levels. Two groups of six to eight mice were bled alternatively every 12 h (four samples/mouse) for 48 h. Data are the mean (±SD) of two experiments.

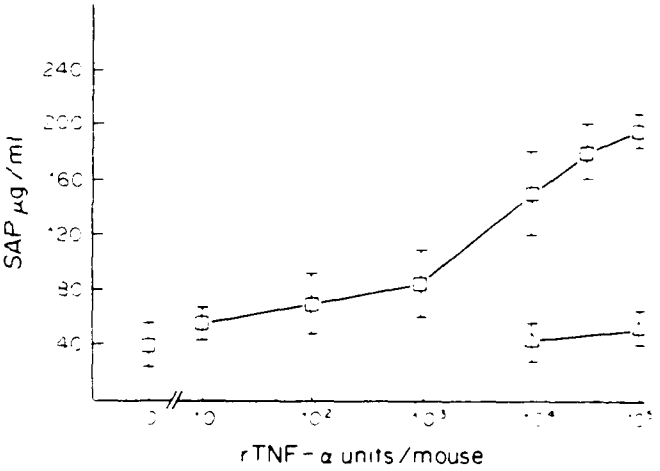

Figure 4. In vivo induction of SAP by rhTNF-α. Various amounts of rTNF-α were injected into mice and SAP levels measured 24 h later. Heat inactivated (70°C, 1 h) rTNF-α was also used (△). Mean SAP concentration (±SD) for three experiments with five mice per dose in each experiment.

activity of the rTNF-α is based on the L cell assay of the diluted protein (26). Heat inactivation for 1 h at 70°C, which destroys the activity of TNF in other assays (26, 27), was found to abolish most of its SAP-inducing activity (Fig. 4).

Effect of a mixture of rIL-1 and rTNF on SAP production. Since each of the monokines is likely to be present simultaneously (27, 32), we tested whether TNF and IL-1 administered together resulted in a response that was either additive or synergestic. Only at the lower doses of IL-1 (10^1 and 10^2 U), coupled with an optimal dose of TNF, was there evidence for an additive effect of the two monokines on the SAP response (Fig. 5). The SAP response of mice to a mixture of several relatively high doses (10^3 to 10^5) of TNF and a relatively low dose of IL-1 (10 U) also generated an additive response (data not shown). Thus, it appears that once the maximal SAP response is obtained, there is no further increase in response to a mixture of cytokines.

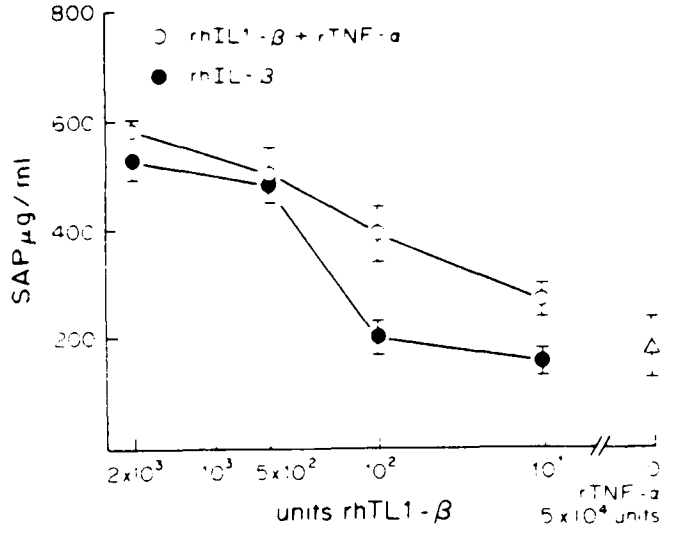

Figure 5. Effect of a mixture of rhIL-1 and rTNF-α on the in vivo induction of SAP. Mice received various doses of rhIL-1β along with an optimal dose of rTNF-α (5×10^4 U) (○) and the SAP levels measured 20 h later. Controls consisted of mice receiving rhIL-1β alone (●) or rTNF-α alone (△). Groups of five mice/treatment were examined. The mean (±SD) of two identical experiments is shown.

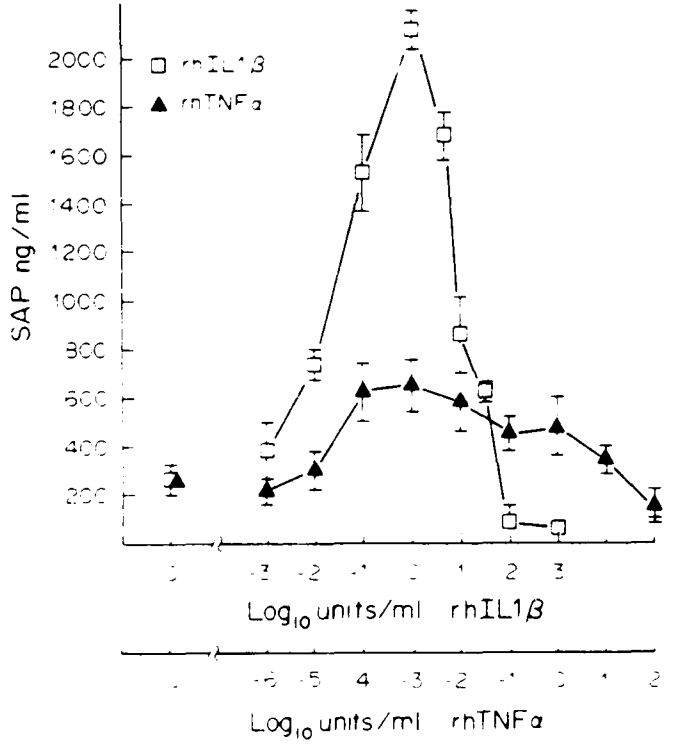

Figure 6. Effect of rhIL-1β and rhTNF-α on in vitro synthesis of SAP by mouse hepatocytes. Isolated hepatocytes (2×10^5/ml per well) were incubated 24 h with various amounts of the cytokines and the amount of SAP secreted into the culture measured by a competitive ELISA. Results are the mean (±SD) of four experiments.

Induction of hepatocyte synthesis by rIL-1 and rTNF in vitro. To test whether the recombinant cytokines act directly on hepatocytes to trigger new synthesis of SAP, we tested isolated mouse hepatocytes in vitro for SAP production. The optimal increase in SAP synthesis occurred with 1.0 U/ml of rhIL-1-β per 2×10^5 hepatocytes (Fig. 6). This response was induced by 1.0 ng of IL-1 (~10^{-11} M). Significant responses were detected over the range of 0.01 U/ml to 20 U/ml; however, concentrations >50 U/ml were inhibitory, but not cytotoxic when tested by protein synthesis ([^{3}H]leucine incorporation) of the hepatocytes vs untreated cells. The magnitude of the SAP response was ~10-fold and is therefore of the same magnitude as the in vivo response to the rhIL-1 preparation.

The in vitro hepatocyte production of SAP in response to rTNF-α was also examined. The optimal response occurred at concentrations of only 10^{-2} to 10^{-4} U/ml of rTNF-α and was approximately a three-fold increase (Fig. 6), which is similar to the fourfold increase in the SAP response in vivo (Fig. 4). The addition of $>10^2$ U/ml of rTNF-α resulted in cytotoxicity as detected by dye exclusion and protein synthesis. The addition of a mixture of optimal amounts of rTNF-α and suboptimal amounts of rhIL-1β to the isolated hepatocytes resulted in a SAP response that was additive, but clearly not synergistic (Table I). Subsequent testing of various mixtures of rhIL-1β and TNF-α at concentrations less than optimal for each monokine always generated SAP responses that were additive. The results suggests that the two cytokines probably regulate SAP synthesis independently.

Induction of C3 by rIL-1 and rTNF-α. Increased production of C3 by rIL-1 and rTNF-α in mice has been associated with the accumulation of mRNA (8, 31). We measured plasma levels of C3 and observed an increase in response to rhIL-1-α which did not appear to be dose-dependent (Table II). A high dose of rTNF-α (7.5 μg) that induced maximal SAP production also generated a small increase in the C3 level. The plasma levels of amyloid P-component and fibrinogen from the same mice are shown for comparison. Although the SAP and fibrinogen responses increase in a dose-dependent manner, the C3 levels did not. A single combination of the cytokines did not result in any further increase in SAP or C3, but induced a significant increase in fibrinogen (Table II).

Induction of fibrinogen with rhIL-1 and rhTNF-α and their combination. The fibrinogen levels in plasma of C57BL/6 mice receiving the two monokines was also determined. The results in Figure 7 show that IL-1 alone induced higher levels of fibrinogen than TNF-α on a weight basis for each monokine. Administration of IL-1α and a large dose (7.5 μg) of TNF-α in combination resulted in a synergistic induction of fibrinogen as judged by the increased slope of the dose-response curve and by the more than additive response to the combination of cytokines (Fig. 7). This contrasts with the lack of a synergistic

TABLE I

Effect of addition of both rhIL-1β and rTNF-α on SAP production by mouse hepatocytes in vitro

rhIL-1β (U/ml)	rTNF-α (U/ml)	SAP (ng/ml ±SD)
0.10		1055 (97)
	10^{-2}	1447 (122)
	10^{-3}	1506 (254)
	10^{-4}	1601 (139)
0.01		1152 (291)
	10^{-2}	1516 (268)
	10^{-3}	1673 (163)
	10^{-4}	1402 (199)
0		242 (44)
	10^{-2}	625 (98)
	10^{-3}	521 (125)
	10^{-4}	610 (27)

[illegible] both monokines added to 2×10^5 hepatocytes and culture supernatants assayed for SAP [illegible]

TABLE II

Comparison of level of acute phase proteins in C57BL/6 mice 24 h after receiving rhIL-1α and rTNF-α[a]

Treatment		SAP	Fibrinogen[b]	Serum C3
Monokine	Dose	(μg/ml)	(% of control)	(μg/ml)
rhIL-1α	1.0 ng	29 (12)	111 (3)	833 (117)
	10 ng	88 (7)	168 (4)	1007 (179)
	75 ng	251 (75)	234 (18)	1029 (110)
	150 ng	294 (111)	232 (17)	1170 (178)
	500 ng	327 (97)	273 (25)	1183 (150)
	1000 ng	357 (130)	303 (10)	1083 (160)
rTNF-α	7.5 μg	257 (121)	198 (29)	809 (143)
rhIL-1α and rTNF-α	150 ng 7.5 μg	347 (59)	332 (7)	1014 (144)
Saline		35 (17)	100 (9)	747 (142)

[a] Data obtained from three experiments, each of which used three mice/dose of monokine. Data are the mean (SD) of duplicate measurements on each serum or plasma sample.

[b] Percent of control calculated vs saline injection (control) value of 118 (11) mg/100 ml.

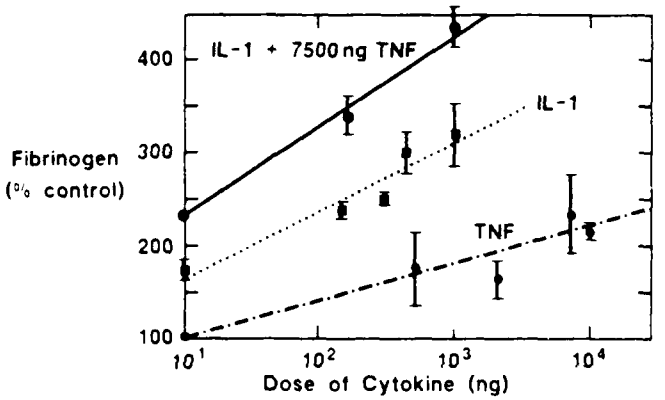

Figure 7. In vivo production of fibrinogen in response to rhIL-1α and rhTNF-α. C57BL/6 mice received various doses of rhIL-1α or rTNF-α alone or in combination. The results are from three experiments. In each experiment, plasma from three individual mice per dose was assayed. The background level of plasma fibrinogen ranged from 95 to 120 mg/100 ml.

response of SAP and C3 to the combined administration of cytokines at the same doses (Table II).

DISCUSSION

The experiments described here show the induction of increased mouse SAP production in vivo and synthesis in vitro in response to the recombinant monokines, IL-1 and TNF-α. In addition, two other AP proteins C3 and fibrinogen that increase to a lesser extent than SAP, were also induced in vivo by IL-1 and TNF. In general, the magnitude of the SAP response generated by the rIL-1 proteins is similar to both the previously reported in vivo response to a variety of inflammatory stimuli in mice, and also the in vitro response of hepatocytes to culture supernatants of activated mouse Mϕ (11, 13, 22, 33). Since Mϕ are the major source of both IL-1 and TNF-α, and each has been shown to be capable of inducing the other (27, 32), it seems likely that these polypeptide cytokines are released together during the very early stages of a systemic inflammatory response, and in turn directly trigger hepatic synthesis of several AP proteins in a coordinated fashion. In these studies, two inflammatory monokines induced the production of three distinct AP proteins. The coordinated synthesis of several AP proteins with different biologic functions may occur in response to more than a single mediator provided that the inducing molecules (mediators) are released rapidly by cells that recognize alterations (damage) in a variety of tissues (1–3).

Earlier work from one of our laboratories reported that activated Mϕ products and biochemically purified mouse IL-1 induced hepatocyte synthesis and secretion of mouse SAP (22, 33). The IL-1 for the earlier studies was purified from the supernatants of superinduced P388D$_1$ mouse monocytic cell line (34), the source of rmoIL-1 used in the present experiments (23). The possibility that other monokines such as TNF were present in the IL-1 preparation from P388D$_1$ could not have been excluded at that time. However, the results with the various forms of rIL-1 described herein support our earlier conclusion that this cytokine is a direct inducer of de novo synthesis of SAP by hepatocytes (33). The rIL-1 preparations induced a detectable AP protein response with as little as 10 to 100 ng amounts per mouse, whereas a detectable response to rTNF-α required at least a 10- to 100-fold greater quantity. Although the response to IL-1α was greater than that to IL-1β at some of the lower doses tested, the overall increase in the response was similar for both forms of IL-1, a result that might be expected since both forms of IL-1 have been shown to bind to the same receptor (35, 36). It is worth noting that the mRNA content for IL-1β in human monocytes is at least 10-fold greater than that of IL-1α (24), suggesting that the β-form may be more abundant in circulation. Like humans, mice also have recently been shown to have two distinct genes for IL-1 (37); however, the rmoIL-1 used in this study was the pI5 form, which is equivalent to human IL-1α (23).

Experiments were performed to determine whether IL-1 and TNF induce an AP protein response as a consequence of the direct binding of each monokine to distinct receptors on cells within the target tissue (38, 39). An additive effect of a combination of the monokines on the SAP response in vivo was observed only at suboptimal doses of one of the monokines; however, a synergistic response over a broad range of IL-1 doses and a maximal dose of TNF was detected only when fibrinogen levels were measured. The level of C3 also increased but was too limited to show a dose-response. The in vitro SAP response to a combination of monokines was also additive. Whether the differences in the blood levels of AP proteins reflect differences in their rate of utilization, altered clearance, or differences in the rate of synthesis remains to be determined for each protein. Studies of CRP and serum amyloid A protein gene expression clearly show that the blood levels primarily reflect the rate of new synthesis, rather than altered consumption (40, 41). The circulating level of mouse SAP is known to be independent of its rate of clearance or catabolism and therefore the level is probably governed by synthesis and/or secretion (42).

Inasmuch as TNF has been shown to stimulate IL-1 release in vivo (27), it is difficult to determine the independent effects of each cytokine. Both IL-1 and TNF have been reported to have regulatory effects on the production of the AP proteins C3, factor B and α-1-antichymotrypsin (increase) and albumin and transferrin (decrease) (31). The results of the experiments herein show that rTNF-α is a less potent inducer of SAP in vivo than IL-1. The same rTNF-α used in these studies has been shown to be

rapidly cleared in mice with almost one-third of the rTNF-α taken up by the liver (43). Although TNF-α may exert some inflammatory effects localized to the site of production, it has also been detected in the plasma of animals with systemic inflammation by bioassays (43). The chemotactic activity of TNF for monocytes and polymorphonuclear neutrophils (44) may serve to amplify the AP protein response by recruiting cells to provide additional mediators for hepatic stimulation.

Induction of SAP synthesis by isolated mouse hepatocytes in vitro permits the identification of inflammatory mediators that act directly on the target cell, an experimental system that will be critical for eventually determining the molecular mechanisms of IL-1 and TNF triggering and regulation of SAP synthesis. The mouse hepatocyte cultures procedure described earlier by us (22, 23), results in single cell preparations free of Kuppfer and endothelial cells, an important aspect since both of the latter might serve as a source of additional IL-1 and/or TNF (27, 32). The SAP response of hepatocytes to rhIL-1β in vitro correlated well with the in vivo SAP response, i.e., 10^4 U (10 μg) per 100×10^6 hepatocytes/liver for an optimum response which calculates to an in vitro dose of 10 U (0.01 μg)/10^5 hepatocytes, a dose only slightly greater than the one generating an optimal response (1.0 U/2×10^5 cells). The response to TNF-α in vitro did not correlate with the in vivo response since the isolated hepatocytes are at least 10^4-fold more responsive to TNF-α. An explanation for this dissociation is not obvious, but may be related to the interaction of TNF-α with blood proteins and/or cells other than the target tissue, which might lower its in vivo activity. Comparisons between the in vivo and in vitro responses must be made with caution, since not all of the hepatocytes respond in vitro (33).

Although SAP is a molecular homologue of human CRP, the finding that mouse SAP can be induced by IL-1 and TNF does not imply that CRP is induced by the same monokines. Goldman and Liu (45) have recently reported that neither rIL-1 nor rTNF-α were capable of inducing human CRP synthesis from a human hepatoma cell line, but a distinct monocyte derived hepatocyte stimulating factor was active. A similar hepatocyte-stimulating monocyte product has been reported by other groups examining the induction of rat nonpentraxin acute phase proteins (46, 47). However, Darlington et al. (48) have shown that both rhIL-1 and rhTNF-α were capable of inducing several AP proteins from human hepatoma cell lines including CRP. There is no reason to exclude the possibility of multiple inducing signals for AP proteins and events.

The biologic significance of the coordinate induction and expression of AP proteins is most readily appreciated on the basis of the need for a rapid, nonspecific host defense response. The three proteins measured here serve this function. Mouse SAP has been shown to heighten listericidal activity of mouse Mϕ (17), and to increase IL-1 production by elicited Mϕ in vitro (49). C3 is an effective opsonin and in the form of C3b directly mediates uptake via activated Mϕ and polymorphonuclear neutrophils (50). Fibrinogen would be consumed during clot formation and the fibrinopeptides generated amplify the cellular component of the inflammatory response (2). Inasmuch as AP proteins are not the same even in closely related species, it seems likely that selective pressures exerted on each vertebrate species dictate the nature of the AP proteins and may also influence the cytokines mediating their induction.

Acknowledgments. We thank the following individuals for their generous gifts of recombinant monokines and/or antibody: Dr. Steve Mizel (Bowman-Gray Medical School, Winston-Salem, NC), Dr. Peter LoMedico (Hoffmann-La Roche, Nutley, NJ), Dr. Dan Tracey (Upjohn Co., Kalamazoo, MI), and Dr. H. Michael Shepard (Genentech, South San Francisco, CA).

REFERENCES

1. **Kampschmidt, R. F.** 1984. The numerous postulated biological manifestations of interleukin-1. *J. Leukocyte Biol. 36:341.*
2. **Koj, A.** 1985. In *The Acute-Phase Response to Injury and Infection* (Research Monograph in Cell and Tissue Physiology). A. H. Gordon and A. Koj, eds. Elsevier, Amsterdam, pp. 181–220.
3. **Dinarello, C. A.** 1984. Interleukin-1 and the pathogenesis of the acute phase response. *N. Engl. J. Med. 311:1413.*
4. **Old, L. J.** 1985. Tumor necrosis factor (TNF). *Science 230:630.*
5. **Oppenheim, J. J., E. J. Kovacs, K. Matsushima, and S. K. Durum.** 1986. There is more than one interleukin 1. *Immunol. Today 7:45.*
6. **Kushner, I., and G. Feldmann.** 1978. Control of the acute phase response. Demonstration of CRP synthesis and excretion by hepatocytes in the rabbit. *J. Exp. Med. 148:466.*
7. **Merriman, C. R., L. A. Pulham, and R. F. Kampschmidt.** 1975. Effect of leukocytic emdogenous mediator on C-reactive protein in rabbits. *Proc. Soc. Exp. Biol. Med. 149:782.*
8. **Perlmutter, D. H., G. Goldberger, C. A. Dinarello, S. B. Mizel, and H. R. Colten.** 1986. Regulation of class III major histocompatibility complex gene products by interleukin 1. *Science 232:850.*
9. **Ramadori, G., J. D. Sipe, C. A. Dinarello, S. B. Mizel, and H. R. Colten.** 1985. Pretranslational modulation of acute phase hepatic protein synthesis by murine recombinant interleukin-1 (IL-1) and purified human IL-1. *J. Exp. Med. 162:930.*
10. **Ramadori, G., J. D. Sipe, and H. R. Colten.** 1985. Expression and regulation of the murine serum amyloid A (SAA) gene in extrahepatic sites. *J. Immunol. 135:3645.*
11. **Pepys, M. B., and M. L. Baltz.** 1983. Acute phase proteins with special reference to C-reactive protein and related proteins (Pentraxins) and serum amyloid A protein. *Adv. Immunol. 34:141.*
12. **Gewurz, H., C. Mold, J. Siegel, and B. Fiedel.** 1982. C-reactive protein and the acute phase response. *Adv. Intern. Med. 27:345.*
13. **Mortensen, R. F., K. Beisel, N. J. Zeleznik, and P. T. Le.** 1983. Acute phase reactants of mice. II. Strain dependence of SAP levels and response to inflammation. *J. Immunol. 130:885.*
14. **Oliveria, E. B., E. C. Gotschlich, and T.-Y. Liu.** 1979. Primary structure of human C-reactive protein. *J. Biol. Chem. 254:489.*
15. **Woo, P., J. R. Korenberg, and A. S. Whitehead.** 1985. Characterization of genomic and cDNA sequence of human C-reactive protein and comparison with the cDNA sequece of serum amyloid P-component. *J. Biol. Chem. 260:13384.*
16. **Lei, K.-J., T. Liu, G. Zon, E. Soravia, T.-Y. Liu, and N. D. Goldman.** 1985. Genomic DNA sequence for human C-reactive protein. *J. Biol. Chem. 260:13377.*
17. **Singh, P. P., F. Gervais, E. Skamene, and R. F. Mortensen.** 1986. Serum amyloid P-component-induced enhancement of macrophage listericidal activity. *Infect. Immun. 52:688.*
18. **Zahedi, K., and R. F. Mortensen.** 1986. Macrophage tumoricidal activity induced by human CRP. *Cancer Res. 46:5077.*
19. **Breathnach, S. M., S. M. Melrose, B. Bhogal, F. C. deBeer, R. F. Dyck, B. Tennent, M. M. Black, and M. B. Pepys.** 1981. Amyloid P component is located on elastic fiber microfibrils in normal human tissue. *Nature 293:652.*
20. **Inoue, S., C. P. Leblond, D. S. Grant, and P. Rico.** 1986. The microfibrils of connective tissues. II. Immunohistochemical detection of the amyloid P component. *Am. J. Anat. 176:139.*
21. **Le, P. T., M. T. Muller, and R. F. Mortensen.** 1982. Acute phase reactants of mice. I. Isolation of serum amyloid P-component (SAP) and its induction by a monokine. *J. Immunol. 129:665.*
22. **Le, P. T., and R. F. Mortensen.** 1984. *In vitro* induction of hepatocyte synthesis of the acute phase reactant mouse serum amyloid P-component by macrophages and IL 1. *J. Leukocyte Biol. 35:587.*
23. **Lomedico, P. T., U. Gubler, C. P. Hellmann, M. Durovich, J. G. Giri, Y.-C. E. Pan, K. Collier, R. Semionow, A. O. Chua, and S. B. Mizel.** 1984. Cloning and expression of murine interleukin-1 cDNA in *Escherichia coli*. *Nature 312:458.*
24. **Auron, P. E., A. C. Webb, L. J. Rosenwasser, S. F. Mucci, A. Rich, S. M. Wolff and C. A. Dinarello.** 1984. Nucleotide sequence of human monocyte interleukin 1 precursor cDNA. *Proc. Natl. Acad. Sci. USA 81:7807.*

25. **March, C. J., B. Mosley, A. Larsen, D. P. Cerretti, G. Braedt, V. Price, S. Gillis, C. S. Henney, S. R. Kronheim, J. D. Gradbstein, P. J. Conlon, T. P. Hopp, and D. Cosman.** 1985. Cloning, sequence, and expression of two distinct human interleukin-1 complementary DNAs. *Nature 315:641.*
26. **Pennica, D., G. E. Nedwin, J. S. Hayflick, P. H. Seeburg, R. Derynck, M. A. Palladino, W. J. Kohr, B. B. Aggarwal, and D. V. Goeddel.** 1984. Human tumor necrosis factor: precursor structure, expression and homology to lymphotoxin. *Nature 312:724.*
27. **Dinarello, C. A., J. G. Cannon, S. M. Wolff, H. A. Bernheim, B. Beutler, A. Cerami, I. S. Figari, M. A. Palladina, and J. V. O'Conner.** 1986. Fever, tumor necrosis factor/cachectin and interleukin-1. *J. Exp. Med. 163:1433.*
28. **Larrick, J. W., L. Brindley, and M. V. Doyle.** 1985. An improved assay for the detection of interleukin 1. *J. Immunol. Methods 79:39.*
29. **Mizel, S. B., M. Dukovich, and J. Rothstein.** 1983. Preparation of goat antibodies against interleukin 1: use of an immunoadsorbent to purify interleukin 1. *J. Immunol 131:1834.*
30. **Klaunig, J. E., P. J. Goldblatt, D. E. Hinton, M. M. Lipsky, and B. Trump.** 1981. Mouse liver cell culture. I. Hepatocyte isolation. *In Vitro 17:913.*
31. **Perlmutter, D. H., C. A. Dinarello, P. I. Punsal, and H. R. Colten.** 1986. Cachetin/tumor necrosis factor regulates hepatic acute phase gene expression. *J. Clin. Invest. 78:1349.*
32. **Bachwich, P. R., S. W. Chensue, J. W. Larrick, and S. L. Kunkel.** 1986. Tumor necrosis factor stimulates interleukin-1 and prostaglandin E_2 production in resting macrophages. *Biochem. Biophys. Res. Commun. 136:94.*
33. **Le, P. T., and R. F. Mortensen.** 1986. Induction and regulation by monokines of hepatic synthesis of mouse serum amyloid P-component (SAP). *J. Immunol. 136:2526.*
34. **Mizel, S. D., and K. Mizel.** 1981. Purification to apparent homogeneity of murine interleukin 1. *126:834.*
35. **Gubler, U., A. O. Chua, A. S. Stern, C. P. Hellmann, M. P. Vitek, T. M. DeChiara, W. R. Benjamin, K. G. Collier, M. Dukovich, P. C. Familletti, C. Fiedler-Nagy, J. Jenson, K. Kaffka, P. Kilian, D. Stremlo, B. H. Wiettreich, D. Woehle, S. B. Mizel, and P. T. Lomedico.** 1986. Recombinant human interleukin 1: purification and biological characterization. *J. Immunol. 136:2492.*
36. **Dower, S. K., S. R. Kronheim, T. P. Hopp, M. Cantrell, M. Deeley, S. Gillis, C. S. Henney, and D. L. Urdal.** 1986. The cell surface receptors for IL-1α and IL-1β are identical. *Nature 324:266.*
37. **Gray, P. W., D. Glaister, E. Chen, D. V. Goddel, and D. Pennica.** 1986. Two interleukin 1 genes in the mouse: cloning and expression of the cDNA for murine IL-1β. *J. Immunol. 137:3644.*
38. **Rubin, B. Y., S. L. Anderson, S. A. Sullivan, B. D. Williamson, E. A. Carswell, and L. J. Old.** 1985. High affinity binding of ^{125}I-labeled human tumor necrosis factor to specific cell surface receptors. *J. Exp. Med. 162:1099.*
39. **Aggarwal, B. B., T. E. Eessalu, and P. E. Hass.** 1985. Characterization of receptors for human tumor necrosis factor and their regulation by gamma-interferon. *Nature 318:665.*
40. **Chelladuri, M., S. S. Macintyre, and I. Kushner.** 1983. *In vivo* studies of serum C-reactive protein turnover in rabbits. *J. Clin. Invest. 71:6041.*
41. **Goiberger, G., D. H. Bing, J. D. Sipe, M. Rita, and H. R. Colten.** 1987. Transcriptional regulation of genes encoding the acute-phase proteins CRP, SAA, and C3. *J. Immunol. 138:3967.*
42. **Baltz, M. L., R. F. Dyck, and M. B. Pepys.** 1985. Studies on the *in vivo* synthesis and catabolism of serum amyloid P component (SAP) in the mouse. *Clin. Exp. Immunol. 59:235.*
43. **Beutler, B. A., I. W. Milsark, and A. Cerami.** 1985. Cachectin/tumor necrosis factor: production, distribution and metabolic rate *in vivo*. *J. Immunol. 135:3972.*
44. **Ming, W. J., L. Bergani, and A. Mantovani.** 1987. Tumor necrosis factor is chemotactic for monocytes and polymorphonuclear leukocytes. *J. Immunol. 138:1469.*
45. **Goldman, N. D., and T. Y. Liu.** 1987. Biosynthesis of human CRP in cultured hepatoma cells is induced by a monocyte factor(s) other than interleukin-1. *J. Biol. Chem. 262:2363.*
46. **Koj, A., J. Gauldie, E. Regoeczi, D. N. Sauder, and G. D. Sweeney.** 1984. The acute-phase response of cultured rat hepatocytes. System characterization and the effect of human cytokines. *Biochem. J. 224:505.*
47. **Wolosky, B. N., and G. M. Fuller.** 1985. Identification and partial characterization of hepatocyte-stimulating factor from leukemic cell lines: comparison with interleukin-1. *Proc. Natl. Acad. Sci. USA 82:1443.*
48. **Darlington, G. J., D. R. Wilson, and L. B. Lachman.** 1986. Monocyte-conditioned medium, IL-1 and tumor-necrosis factor stimulate the acute phase response in human hepatoma cells *in vitro*. *J. Cell. Biol. 103:787.*
49. **Sarlo, K. T., and R. F. Mortensen.** 1985. Enhanced IL 1 production mediated by mouse SAP. *Cell. Immunol. 93:398.*
50. **Fearon, D. T., and W. W. Wong.** 1983. Complement ligand-receptor interactions that mediate biological significance. *Annu. Rev. Immunol. 1:243.*

Mem. Inst. Oswaldo Cruz, Rio de Janeiro, Vol. 82, Suppl. II: 29-38, 1987
Intern. Symp. on Immunomodulators

POTENTIAL THERAPEUTIC APPLICATIONS FOR INTERLEUKIN 1: ANTI-TUMOR AND HEMATOPOIETIC EFFECTS

JOOST J. OPPENHEIM*, KOUJI MATSUSHIMA*, KIKUO ONOZAKI**
& RUTH NETA***

*National Cancer Institute, Biological Response Modifiers Program, Frederick, MD 21701-1031, USA
**Department of Microbiology, University of Tsukuba, Institute of Basic Medical Sciences, Sakura, Ibaraki 305, Japan ***Department of Experimental Hematology, Armed Forces Radiobiology Research Inst., Bethesda, MD, 20814, USA

Interleukin 1 (IL 1), a major immunoregulatory monokine, was originally defined by its ability to act as a co-mitogenic factor for murine thymocytes (Gery et al., 1972). Since then IL 1 has been revealed to act as a mediator of host defenses that modulates inflammatory, immunological as well as hematological reactions (Oppenheim et al., 1986). In this report we will discuss two distinct effects of IL 1 with potential therapeutic applicability: First, antitumor cell activities and second, the bone marrow restorative activities that probably account for the radioprotective effects of IL 1 (Neta et al., 1986).

There is in vitro and in vivo evidence that IL 1 may play an important role in host defense against tumors by augmenting in vitro monocyte-mediated tumor cytotoxicity (Onozaki et al., 1985), by augmenting in vitro NK cell activity (Matsushima et al., 1985) by having direct in vitro antiproliferative and cytocidal effects for some tumor cells (Onozaki et al., 1985; Lovett et al., 1986) and by inducing in vivo tumor regression in mice (Nakamura et al., 1986).

In the course of investigations of the in vitro cytostatic effects of IL 1 (Onozaki et al., 1985), we established that IL 1 inhibited the incorporation of tritiated thymidine by the mouse myeloid leukemic cell line, M1 (Onozaki et al., 1986). Coincidentally, we observed that incubation of M1 cells with IL 1 in conjunction with lipopolysaccharide endotoxin (LPS) resulted in both synergistic growth inhibitory effects and the differentiation of M1 cells into macrophage-like cells (Onozaki et al., 1986). We therefore examined the effects of combinations of IL 1, with IFN-β or TNF (which could be produced by M1 cells in response to LPS), on the growth and differentiation of M1 cells (Onozaki et al., 1987).

We have also shown that administration of IL 1 protects mice from death (Neta et al., 1986). This increased survival was paralleled by the recovery of hematopoietic system from radiation damage. In the course of investigating the reasons for the marrow (BM) restorative effects of IL 1, we have observed that administration of IL 1 to normal mice markedly increases cycling of bone marrow cells. These observed properties of IL 1 induction of BM cell cycling, differentiation of leukemic cell and its cytostatic effect may have therapeutic utility.

MATERIALS AND METHODS

Reagents – RPMI 1640 was purchased from M. A. Bioproducts (Walkersville, MD). Fetal calf serum (FCS) was obtained from Hyclone Laboratories (Logan, UT). Lipopolysaccharide (LPS, E. coli 0127:B8, Westphal) and latex particles with a diameter of 0.81 μm were from Difco Laboratories (Detroit, MI). Ox erythrocytes were from Nippon Biotest Laboratory (Tokyo). Rabbit antibody, IgG, against ox erthrocytes was prepared from antiserum obtained by immunizing rabbits with ox erythrocytes. Concanavalin A (ConA) was from Pharmacia Fine Chemicals, Uppsala, Swede. [^{3}H] Thymidine ([^{3}H]TdR, 2 Ci/ml) was from New England Nuclear (Boston, MA). Preparation and purification of recombinant human TNF (pI 5.9, 17,000 dalton, 1.9 x 10^6 U/mg), production and purification of recombinant human IL 1α (pI 5.3, 18,000 dalton, 2 at 3 x 10^7 U/ml) and natural human IL 1-β (pI 7.0, 17,000 dalton, 2.3 x 10^7 U/mg) have been reported (Yamada et al., 1985; Furutani et al., 1986; Matsushima et al., 1985). Mouse recombinant IL 1-α was kindly provided by Dr. P. Lomedico of Hoffman-LaRoche (Lomedico et al., 1984). Mouse interferon-α (1.5 x 10^6 U/mg)-β (5.3 x 10^7 U/mg) and anti-mouse IFN-β immunoglobulin (rabbit) were from Lee Biomolecular Research Laboratories, Inc., San Diego, CA. Antiserum against human TNF was obtained by immunizing rabbits with purified TNF.

Purified human recombinant IL 1-α (specific activity 7.5 x 10^6 units/mg protein as assessed by the co-mitogenic effect in the thymocyte proliferation assay (Matsushima et al., 1985) and recombinant GM-CSF supplied in sucrose (Lot #344-061-47 specific activity of 4 x 10^7 units/mg protein) were a generous gift of Immunex Corp., Seattle, WA.

Cell cultures – The clone of M1 cells used was M2/436-7 that had been established by Dr. Ichikawa (Moore & Rouse, 1983) (Chest Disease research Institute, Kyoto University, Kyoto, Japan) and provided through Dr. K. Akagawa (Department of Cellular Immunology, NIH, Shinagawa, Tokyo, Japan). This clone is known to differentiate into macrophages but not into neutrophils. The cell line was recloned by limiting dilution, and was maintained in RPMI 1640, 100 μg/ml of Streptomycin and 10% heat activated FCS. To determine the effects of cytokines or LPS, one hundred μl of a cell suspension of M1 cells (2 x 10^5 cells/ml) in RPMI 1640 supplemented with antibiotics, 10% FCS, and test samples was cultured in wells of flat-bottomed microtiter plates (Sumitomo Bakelite, Tokyo) at 37°C in 5% CO_2 in air for varying periods. After culture, the viable cell number as judged by trypan blue dye exclusion was determined using a hemocytometer.

Assay for differentiation of M1 cells – One hundred μl of a suspension of M1 cell (2 x 10^5 cells/ml) in RPMI 1640 medium supplemented with antibiotics and 10% FCS was cultured in wells of flat-bottomed microtiter plates at 37°C in 5% air. Polymyxin-B (10 μg/ml) as indicated was added to cultures. Usually cells were cultured for 3 days, and their differentiation was determined by measuring development of FcR expression or phagocytic activity. The assay for FcR was performed by the modified method of (Bianco et al., 1970). Briefly, M1 cells were cultured with 0.4% EA (ox erythrocytes sensitized with IgG of rabbit anti-ox erythrocytes antiserum) at 37°C for 3hr. After cultures, the percentage of M1 cells with more than three erythrocytes attached was determined by counting at least 200 M2 cells in an hemocytometer. To assess phagocytic activity, M1 cells were cultured with 4% polystyrene latex particles for 8hr, and the percentage of cells ingesting more than 10 latex particles was determined in a hemocytometer by counting at least 200 cells.

Assay for IL 1 activity – IL 1 activity was determined by measuring the incorporation of [^{3}H]TdR by C3H/HeJ mouse thymocytes cultured for 3 days in the presence of 0.5 μg/ml ConA and serially diluted IL 1 as described (Matsushima et al., 1985). One unit per milliliter was defined as the reciprocal of the dilution at which 50% of the maximum thymocyte proliferation response was obtained.

Assay for IFN activity – The antiviral activity of an IFN sample was assayed by inhibition of the cytopathic effect of vesicular stomatitis virus on mouse L929 fibroblast cells (provided by Dr. Y Ito of NIH, Tokyo) Antiviral activity expressed in IFN units was determined from the reciprocal of the highest dilution of the sample that reduced the viral cytopathic effect by 50%

Assay for TNF activity – The activity of TNF was determined by a L929 fibroblast cell lytic assay. Briefly, one hundred μl of a suspension of TNF-sensitive mouse L929 fibroblast cells (4 x 10^5 cells/ml) were cultured with serially diluted test samples in wells of flat-bottomed microtiter plates at 37°C for 18 hr in 5% CO_2 in air in the presence of actimomycin D (1 μg/ml). After culture, the plates were washed, and cells lysis was determined by staining the plates with crystal violet (0.5%) in methanol/water (1:4 V/V). After solubilizing the dye-stained cells with 0.1 ml of 0.1% SDS, the dye uptake was calculated by an automatic micro ELISA autoreader (Immuno Reader NJ-2000, Inter-Med). One unit of TNF activity was defined as the reciprocal of the dilution of samples that lysed 50% of the test cells.

Preparation of conditioned medium of M1 cells – M1 cells suspended in RPMI 1640 medium supplemented with 10% FCS at a density of 1 x 10^6 cells/ml were cultured with or without cytokines or LPS for 2 days. The culture supernatants were dialysed against RPMI 1640 medium, and IL 1, IFN and TNF activities were measured.

Mice – Inbred strains of mice, C57BL/6J, C3H/HeJ, and B6D2F1 were obtained from Jackson Laboratories, Bar Harbor, ME. C3H/HeN mice were also used (Animal Genectics and Production Branch, NCI, Frederick, MD). The mice were housed in the Veterinary Department Facility at the Armed Forces Radiobiology Research Institute in cages of 10-12 mice with filter lids. Female mice, 8-12 weeks of age were used for all experiments. Standard lab chow and HCL acidified water (pH 2.4) were given ad libitum. All cage cleaning procedures and injections were carried out in a microisolator.

Administration of cytokines and hydroxyurea – IL 1 administered to three or four mice per experimental group which were sacrificed by cervical dislocation. Lymphokines were diluted in 0.5% bovine serum albumin in normal saline (sterile-filtered) to a concentration of 10 μg/ml and 100 μg/ml, respectively and stored at -20°C until just prior to intrapentoneal (IP) injection into mice. The lymphokines were diluted in pyrogen-free saline and administered at doses of 100ng/0.5 ml per mouse for IL 1-α and 5 μg/0.5 ml per mouse for GM-CSF. All preparations contained less than 0.06ng of LPS per injection as assessed by the Limulus amebocyte assay. In some experiments hydroxyurea (HU) was injected (900 mg/kg body weight IP) 2 hours prior to sacrifice of the mice.

Recovery of bone marrow cells – Femurs were removed and placed on ice in Hanks' Balanced Salt Solution (HBSS) containing 100 units/ml of penicillin and 100 μg/ml of streptomycin (Gibco, Grand Island, NY). Single cell suspensions were prepared by washing each cavity of the femur with 3 ml of HBSS with a sterile syringe and 26 gauge needle. Cell counts were obtained using a haemocytometer. Viability, as assessed by trypan blue exclusion was always >95%. Cytospin slides were prepared on a Shannon Cytospin II (250g., 6 minutes) using 10^5 cells and 0.1 fetal calf serum per slide. They were stained with a modified Wright's Giemsa stain (Diff-Quick, CMS, ILL), and evaluated by light microscopy.

In vitro bone marrow cell proliferation assay – GM-CSF was diluted in complete media containing RPMI 1640, 10% fetal calf serum (Hyclone), 100 units/ml penicillin, 100μg/ml streptomycin, 10^{-5} M 2-mercaptoethanol, and 2 mM L-glutamine. GM-CSF was added to 96 well microtiter plates (Falcon) in 0.1 ml volumes to yield final concentrations of 10, 1, and 0.1 ng/ml. Next, the bone marrow cells were added in 0.1 ml volumes at concentrations of 1×10^5 and 5×10^4 cells/well. The cultures were incubated for 2 days at 37°C with 5% CO_2 in air. The cells were then pulsed with 1 μCi [^{3}H] thymidine per well and harvested 18 hrs later (Skatron Cell harvester, Sterling, VA) onto glass fiber filters which were then counted in Betacount scintillation fluid on a Mark III scintillation counter.

Cell sizing procedure – The bone marrow cells were resuspended at a 1:100 dilution of the original cell concentration in Isoton II, an isotonic solution specific for the Coulter sizing system. Cell profiles were obtained at several cell concentration (ranging from 1:500 to 1:10), using different media and at different time points (1,2, or 4 hrs after recovery) with similar results.

The cells were collected by the Coulter sampling stand equipped with a manometer. Since the bone marrow cells range in diameter from 1μ-10μ a manometer with 70μ diameter aperture was utilized. The relevant Coulter ZM settings were amplification – 8 and current – 100. For the Coulter channelyzer C-1000, the base channel threshold was set at 15 to exclude red blood cells and the count range switch was set at 4K. (Similar results were obtained at 1K and 10K). These settings were determined after calibrations of the manometer with 10μ beads. Using a shape correction factor of 1.38 for lymphocytes, the size or the threshold factor of each channel was found to be 5.39 μm and the range of volumes analyzed was 80.87 to 620 μm.

After a sample of cells was sized, the frequency distribution, as determined by the channelyzer, was stored and analyzed using the Accucomp software package and an Apple III personal computer.

Flow cytometric analysis of DNA content and cell size – Flow cytometric analysis of DNA content was performed using the propidium iodine (PI) staining technique (Crissman & Stein kamp, 1982). Statistical analysis of the results were performed using the Mann Whitney and Wilcoxon Sign Ranks tests.

RESULTS AND DISCUSSION

In vitro regulation of M1 tumor cell growth and differentiation by cytokines – First it was established that incubation of M1 cells with LPS had cytostatic effects and induced the cell line to produce IL 1, IFN and TNF activities (Onozaki et al., 1987). All three cytokines by themselves (human recombinant IL 1-α at 10 U/ml, murine IFN-β at 10^3 U/ml and human recombinant TNF at 10^3 U/ml) also reduced the number of M1 cells recovered after 2 days and more markedly after 3 days of culture. Combinations of IL 1-α and IFN-β or TNF revealed that paired cytokines had more than additive growth inhibitory effects. Incubation of M1 cells with combinations of IL 1-α and IFN-β or IL 1-α and TNF almost completely suppressed cell replication (Onozaki et al., 1987). We established that all the cytokine preparations and culture

media did not contain LPS as assessed by limulus amoebocyte assay (sensitivity limit of 0.125 ng/ml).

We then investigated the hypothesis that the cytostatic effects of cytokines on M1 cells were accompanied by increased cell differentiation. The effect of cytokines on differentiation was evaluated by assaying FcR expression by M1 cells. Cells that attached more than 3 erythrocytes were considered FcR positive. IL 1-α (10 U/ml), IFN-β (10^3 U/ml) and TNF (10^3 U/ml) by themselves did not induce FcR expression. In contrast, FcR expression was induced by combinations of IL 1-α and IFN-β or IL 1-α and TNF (Onozaki et al., 1987). FcR expression became evident after 2 days of culture, and became more pronounced after 3 days of incubation. Combinations of cytokines increased not only the percentage of cells that bind 3-10 erythrocytes, but also the percentage of cells that bound more than 10 erythrocytes. Concentrations equal to or greater than 10 μ/ml IFN-β and >100 μ/ml TNF in combination with IL 1-α induced FcR expression in a dose dependent manner (Fig. 1). IL 1-α and IFN-β or TNF also synergistically stimulated another indicator of differentiation namely phagocytosis. Again,, although none of the cytokines by themselves enhanced the phagocytic activity of M1 cells, IL 1-α with IFN-β or IL 1-α with TNF increased phagocytic activity. The concentration of IL 1-α needed to induce FcR expression or phagocytic activity was determined by culturing cells with varying doses of IL 1-α with or without IFN-β or TNF. Concentrations equal to or greater than 1 U/ml IL 1-α synergized in inducing differentiation. By morphological criteria cells treated with IL 1-α and IFN-β or IL 1-α and TNF after 3 days of culture developed the characteristics of macrophages such as increased adherence and spreading, enlargement, increased vacuolization, and more nonspecific esterase activity.

All IL 1 preparations tested including human recombinant IL 1-α, natural IL 1-β and mouse recombinant IL 1-α, behaved similarly and synergized with murine IFN-β or human recombinant TNF in inducing differentiation as assessed by either FcR expression or by phagocytic activity. Dose response studies revealed that at 1 U/ml all three preparations of IL 1 exhibited optimal activity.

The combination of IFN-β and TNF resulted in enhanced growth inhibition. However, mixtures of IFN-β and TNF failed to induce FcR expression or phagocytosis by M1 cells. Consequently, the cytostatic effects of these two cytokines could be dissociated from differentiative effects.

The cytostatic and differentiative effects of TNF and LPS are mediated by IFN-β – We previously observed that TNF as well as LPS, but not IL 1, stimulated M1 myelomonocytic cells to produce detectible supernatant IFN activity after 2 days of incubation (Onozaki et al., 1987). This IFN activity was almost completely neutralized by a rabbit anti-mouse IFN-β, but not by a control antiserum. In order to determine whether the elaborated IFN-β mediated the differentiation-inducing activity of TNF and LPS, the effect of anti-mouse IFN-β antibody on M1 cell differentiation was studied. The phagocytic activity induced by IFN-β, or TNF in conjunction with IL 1-α, or LPS by itself was inhibited by the anti IFN-β antibody, but not by control rabbit serum (Fig. 2). The antibody also inhibited FcR induction by IL 1-α and IFN-β, IL 1-α and TNF or by LPS by itself (data not shown). IFN-α alo induced phagocytic activity only if added with IL 1-α. Thus, IFN-α like IFN-β in conjuction with IL 1 can induce cell differentiation. The activity of IF- α was not inhibited by anti-IFN-β antibody, suggesting that IFN-α is also capable of inducing M1 cell differentiation. The role of IFN-β in the cytostatic effects of the cytokines was also investigated. The results on Fig. 3 show that anti-IF-β partly blocked the growth inhibitory activity of TNF and LPS, but not that of IL 1, suggesting that the cytostatic effect of TNF on M1 cells also are mediated by IFN-β.

A number of tumor cell lines have been reported to have varying degrees of sensitivity to the antiproliferative effect of IL 1, including a human melanoma cell line, A375, a clone of mouse fibroblast cell line, L929, a human myeloid cell line, K562, and a mouse T lymphoma cell line, Eb (Onozaki et al., 1985; Lovett et al., 1986). The present study demonstrates enhanced in vitro cytostatic effects of IL 1 in combination with IFN or TNF on an immature myeloid M1 cell line. Our study suggests that even when the cytostatic effects of a cytokine such as IL 1 are modest, the growth inhibitory effect of cytokines can be strikingly accentuated by interactions with other cytokines. The in vitro synergistic tumoricidal effect of the combination of TNF and IFN-gamma has been well documented for several tumor cell lines (Williamson et al., 1983; Tsujimoto et al., 1986). It

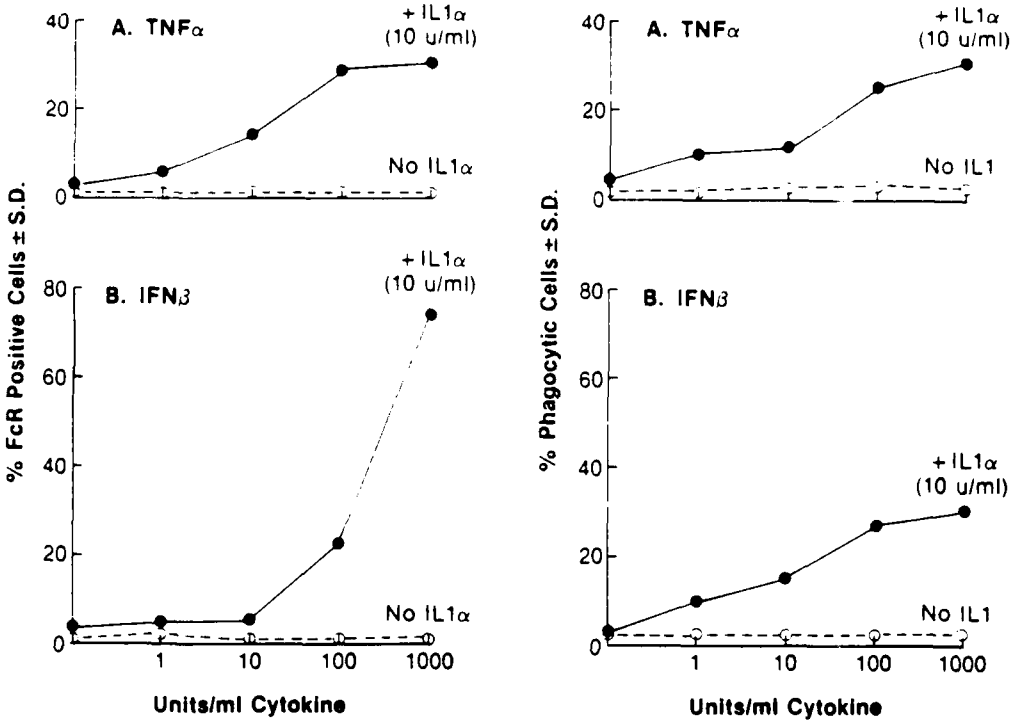

Fig. 1: Synergistic effect of IL 1α and IFNβ or TNFα on the induction of FcR expression and phagocytic activity of M1 cells. *The % of FcR positive cells ± SD and the % phagocytic cells ± SD of triplicate cultures are shown.* M1 cells were treated with varying doses of IFNβ or TNF with or without IL 1 for 3 days.

has been hypothesized that IFN-gamma may synergize with TNF by up-regulating the expression of receptors for TNF (Tsujimoto et al., 1986). Similarly, IL 1 may induce the expression of IFN and/or TNF receptors on M1 cells.

To effectively induce differentiation required the continuous presence of two cytokines, IL 1-α and IFN-β, or IL 1-α and TNF during the entire course of incubation. Therefore, cells probably require two distinct but concomitant signals provided by IL 1 and IFN-β or TNF. Although IL 1 by itself did not induce the production of IFN activity by M1 cells, both TNF and LPS induce the production of IFN activity. The differentiation inducing activity of TNF and LPS could be completely neutralized by specific antibody to IFN-β. IFN-β itself could induce differentiation of M1 cells in combination with IL 1. Consequently, IFN-β appears to mediate the induction of M1 cell differentiation into macrophages by TNF and LPS. Recently, Resnitsky et al. (1986) reported that IFN-β also mediates the differentiation of M1 cells induced by phorbol myristic acid or colony stimulating factor 1, since such differentiation can be blocked using specific antibody to IFN-β (Resnitzky et al., 1986). Therefore, IFN-β along with IL 1 may be essential mediators of M1 cell differentiation.

The relationship of differentiation to cytostasis is not clear cut. Although the induction of differentiation of M1 cells is always associated with growth inhibition, the reverse is not always the case. Based on our results we certainly cannot claim that antiproliferative effects of cytokines are necessarily associated with differentiative events. However, use of more sensitive assays of differentiation might establish a direct correlation between differentiative and cytostatic events.

In conclusion, combinations of cytokines act synergistically both to inhibit tumor growth and to enhance cell differentiation. Our study also shows that minimal non-toxic doses of IL 1 suffice for obtaining anti-proliferative effects of IL 1 provided it is used in conjunction with IFNβ or TNF. Thus, combinations of these cytokines may prove useful in treatment of some types of tumors in vivo.

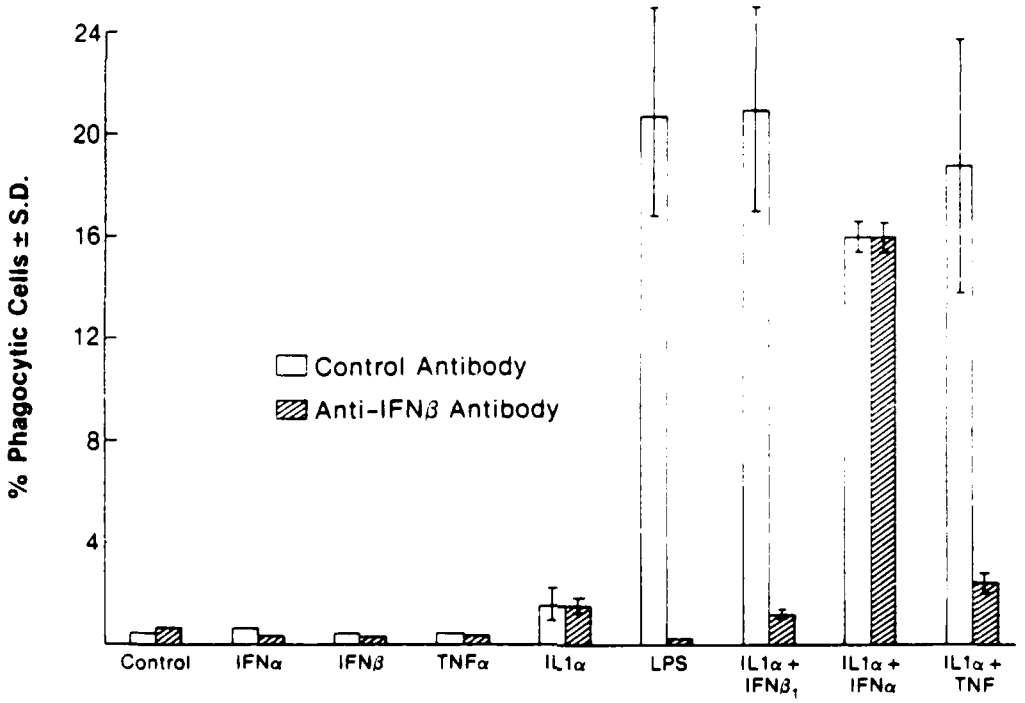

Fig. 2: Effect of anti-mouse IFNβ antibody on induction of phagocytic activity of MI cells by cytokines and LPS. MI cells were treated with cytokines or LPS in the presence of control rabbit antibody or anti-IFNβ antibody for 3 days, and the % of phagocytic cells determined. All the cultures except for those with LPS were incubated in the presence of polymyxin-B (10 μ/ml). IFNα, β and TNF were used at 10^3 U/ml, and IL 1α at 10 U/ml. The % phagocytic MI cells ± SD of triplicate cultures induced by cytokines or LPS in presence or absence of anti-IFNβ is shown.

Bone marrow restorative effects of IL 1 – Administration of LPS to mice 1 day prior to lethal doses of irradiation reduces the suppression of hematopoiesis (Smith et al., 1958). Intraperitoneal (IP) administration of IL 1, 20 hrs before a lethal dose of radiation, increases the survival of mice in association with hematopoietic recovery as indicated by the production of increased numbers of nucleated bone marrow cells by 5 – 13 days following irradiation (Neta et al., 1986). As observed with LPS, the number of endogenous splenic colonies (EFUs) was also greatly enhanced in IL 1 treated irradiated mice (Neta et al., 1986).

To evaluate further the myelopoietic consequences of IL 1, the effect of IL 1 on normal murine bone marrow was evaluated (Neta et al., 1987). Although 20 hrs after an IP injection of 100 ng IL 1 there was no increase in the number of bone marrow cells, the numbers of enlarged bone marrow cells were increased by 25.3 ± 4.1% as determined by Flow cytometry.

The cause of the bone marrow cell enlargement was investigated by giving IL 1 treated mice hydroxyurea (HU); an agent that arrests cells at the G1/S interphase of the cell cycle and is toxic to cells in the S phase. Treatment with HU eliminated the number of large bone marrow cells in IL 1 treated mice, but had no effect on the size distribution of cells from control mice (Table I). This result suggests that IL 1 induces bone marrow cells to enter the cell cycle. This hypothesis was further supported by data showing increases from 26.7 to 39.2% of large BM cells in the S+G1+M phases of the cell cycle in IL 1 treated over control mice as determined by flow cytometric analysis of cellular DNA content (data not shown).

Finally, we compared the capacity of control and IL 1 treated BM cells to proliferate in

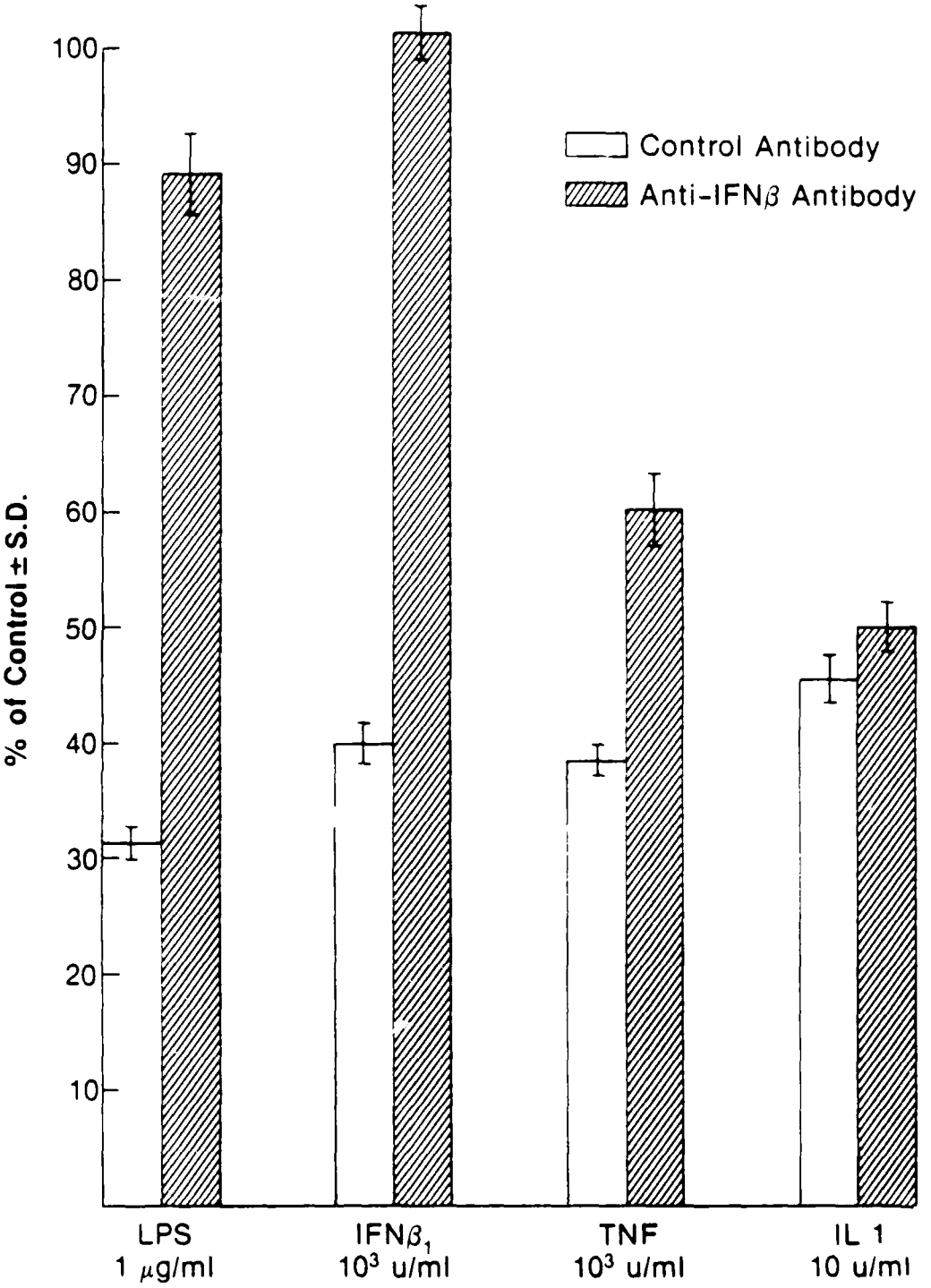

Fig. 3. Effect of anti-mouse IFNβ antibody on the growth inhibitory effects of cytokines and LPS for Ml cells. Ml cells were treated with varying doses of cytokines and LPS in the presence of control rabbit antibody or anti-IFNβ antibody for 3 days, and then the viable cell number determined. All the cultures except for LPS were conducted in the presence of polymyxin-B (10 μg/ml). Addition of polymyxin-B did not influence cell growth. The mean % of control ± SD of triplicate cultures is shown.

TABLE I

Effect of administration of Hydroxyurea (HU) on the size of bone marrow cells from IL 1 treated and control mice

		Cell Volume Distribution		
		Overall	Medium	Large
In vivo treatment		(80-620)*	(215-323)	(324-620)
IL 1	HU			
-	+	97 ± 5*	94 ± 3	88 ± 8
+	+	90 ± 6	79 ± 10**	74 ± 4**

*Range of cell volume in MM^3.

**Mean % change in cell number in different cell size compartment in saline or IL 1 treated mice w/wo subsequently administrated HU. Mean ± SEM of 20 experiments is shown utilizing 3-4 mice in each group. BM from 4 different inbred mouse strains was assessed 20 hrs following IL treatment and 2 hrs following HU or saline administration, using a Coulter channelyzer.

**$p = < 0.01$

culture for 72 hr in response to GM-CSF; a growth factor for macrophage and granulocyte progenitor cell (Moore & Rouse, 1983). The results show that the proportion of GM-CSF responsive progenitor cells present in BM of IL 1 treated mice approximately doubled (Table II). Consequently, prior in vivo treatment with IL 1 does enrich the BM in progenitor cells with the capacity to subsequently proliferate in vitro in response to GM-CSF. This latter response to IL 1 as could be expected, was blocked by concomitant treatment of mice with HU. This indicates that IP administration of IL 1 induces an increased proportion of GM-CSF responsive BM cells to enter the S phase of the cell cycle.

We have demonstrated that administration of IL 1 to mice therefore has several stimulatory effects on bone marrow cells. IL 1 stimulates an increase in GM-CSF responsive macrophage and granulocyte progenitor cells in the bone marrow, increases the proportion of large bone marrow cells as measured by Coulter Volume channelyzer and by light scattering, increases the sensitivity to HU treatment and increases the proportion of cells in S and G_2 + M phases of cell cycle. Since, the late S phase of the cell cycle was reported in numerous studies to be the most radioresistant phase of the cell cycle (Denenkamp, 1986), the radioprotective effect of this cytokine may be related to the induction of larger number of bone marrow cells into the radioresistant late S phase.

However, based on this in vivo data we cannot conclude whether the effects of IL 1 on BM cell cycling are direct or indirect. For example, IL 1 has been documented to indirectly induce T cells to progress into the S phase of the cell cycle by stimulating the production of IL 2 (Smith et al., 1980). Our results show that IL 1 by itself is not a direct in vitro growth stimulant of bone marrow cells or of GM-CFU (Vogel et al., 1987). IL 1 presumably is acting indirectly as a co-stimulant. In fact, one of us has observed that following intraperitoneal administration of a single dose of recombinant IL 1, high titers, 1-2 x 10^3 units per ml of CSF, appeared in the circulation within 2 hr and persisted for up to 6 hr. (Vogel et al., 1987). Furthemore, there are reports that IL 1 can stimulate CSF production by stromal cells (Adamson, 1986). Similarly, fibroblasts stimulated with IL 1 release supernatant factors that support CFU-GM, BFU-E and CFU-GEMM colony formation (Zucali et al., 1987). It is therefore probable that in addition to CSF, IL 1 may stimulate the release of other hematopoietic growth factors.

As an endogenous pyrogen and mediator of the inflammatory response, IL 1 has been considered a noxious rather than a beneficial cytokine. However, IL 1 has been implicated as a differentiation and maturation-inducing agent for a variety of cells (Oppenheim et al., 1986). IL 1 has been proposed to participate in wound healing (Oppenheim, 1986) and to increase protection from infections (Kampschmidt & Pulliam, 1975). Our own studies demonstrated IL 1 to be a radioprotector (Neta et al., 1986). In addition, the enhanced levels of IL 1 detected the placenta and amniotic fluid (Flynn et al., 1985), in the circulation after exercise (Cannon & Kluger, 1983), and post ovulation (Cannon & Dinarello, 1985), suggest that this cytokine may play a constructive role in normal function, as well as in the recovery and repair of damaged BM cells.

IL 1 in synergy with CSF promotes the growth and differentiation of bone marrow progenitor cells into myeloid cells. IL 1 in conjunction with IFNβ also has cytostatic differentiative effects on MI cells. The differentiative effect of IL 1 on hematopoeitic cells resembles its effect on MI cells. Although the antitumor and restorative effects of IL 1 are apparently disparate, they may both be based on the capacity of IL 1 to synergistically enhance the effects of other induced cytokine signals. Consequently, IL 1, by initiating a number of cytokine cascades may have divergent in vivo beneficial effects.

TABLE II

Effect of IL 1 administration on subsequent in vitro GM-CSF induced proliferation of murine BM cells

In vitro GM-CSF (ng/ml)	Number of cells per well	In vivo IL 1 treatment	
		–	+
None	5×10^4	594 ± 83	556 ± 70
None	1×10^5	662 ± 98	869 ± 109
10.0	5×10^4	13,611 ± 1,145	20,456 ± 1,195
10.0	1×10^5	19,852 ± 1,911	33,360 ± 2,131

*Mean cpm ± SD of ^{3}HTdR incorporated by triplicate cultures of incubated for 72 hr. The experiment is representative of the 15 experiments performed using 4 different inbred mouse strains. BM was obtained 25 hrs following IP administration of 100 ng IL 1 or saline.

ACKNOWLEDGMENT

We are grateful for the critical discussion of this paper to Drs. Scott Durum and Tom Sayers and the editorial assistance of Ms. Beth Danner and Ms. Bobbie Unger.

REFERENCES

ADAMSON, J.W., 1986. Hematopoeitic growth factor production by mesenchymal cells. *Exp. Hemat., 14* :418 (abstr.).

BIANCO, C.; PATRIC, R. & NUSSENZWEIG, V., 1970. A population of lymphocytes bearing a membrane receptor for antigen-antibody-complement complexes. *J. Exp. Med., 132* :702.

CANNON, J.G. & DINARELLO, C.A., 1985. Increased plasma IL 1 activity in women after ovulation. *Science, 227* :1247.

CANNON, J.G. & KLUGER, M.J., 1983. Endogenous pyrogen activity in human plasma after exercise. *Science, 220* :617.

CRISSMAN, H.A. & STEIN KAMP, J.A., 1982. Rapid, one step staining procedures for analysis of cellular DNA and protein by single and dual laser flow cytometry. *Cytometry, 3* :84.

DENENKAMP, J., 1986. Cell kinetics and radiation biology. *Int. J. Radiat. Biol., 49* :357.

FLYNN, A.; FINKEL, J.Y. & LOFTUS, M.A., 1985. Comparison of interleukin-1 production of adherent cells and tissue pieces from human placenta. *Immunopharcology, 9* :19.

FURUTANI, Y.; NOTAKE, M.; FUKUI, T.; OHUE, M.; NOMURA, H.; YAMADA, M. & NAKAMURA, S., 1986. Complete nucleotide sequence of the gene for human interleukin 1 alpha. *Nucleic Acids Res., 14* (8) :3167.

GERY, I.; GERSHON, R. & WAKSMAN, G.H., 1972. Production of the T-lymphocyte response to mitogen I. The responding cell. *J. Exp. Med., 136* :128.

ICHIKAWA, Y., 1969. Differentiation of a cell line of myeloid leukemia. *J. Cell. Physiol., 74* :223.

KAMPSCHMIDT, R.F. & PULLIAM, L.A., 1975. Stimulation of antimicrobial activity in the rat with leukocytic endogenous mediator. *J. Reticuloendoth. Soc., 17* :162.

LOMEDICO, P.T.; GUBLER, U.; HELLMANN, C.P.; DUKOVICH, M.; GIRI, J.G.; PAY, Y.E.; COLLIER, K.; SEMINOW, R.; CHUA, A.O. & MIZEL, S.B., 1984. Cloning and expression of murine interleukin 1 cDNA in Escherichia coli. *Nature, 312* (29) :458.

LOVETT, D.; KOZAN, B.; HADMAN, M.; RESCH, K. & GEMSA, D., 1986. Macrophage cytotoxic: Interleukin 1 is a mediator of tumor cytostasis. *J. Immunol., 136* :340.

MATSUSHIMA, K.; DURUM, S.K.; KIMBALL, E.S. & OPPENHEIM, J.J., 1985. Purification of human interleukin 1 from human monocyte culture supernatants and identify of thymocyte co-mitogenic factor, fibroblast proliferation factor, acute phase protein inducing factor and endogeneous pyrogen. *Cell Immunol., 29* :290.

MATSUSHIMA, K.; ONOZAKI, K.; BENOZUR, M. & OPPENHEIM, J.J., 1985. Studies of the production of interleukin 1 (IL1) and potential antitumor activity of IL1. The physiologic, metabolic, and immunologic actions of interleukins 1. (ed. by Kluger, Oppenheim, and Powanda). Alan. R. Liss. Inc., p. 253.

MOORE, R.N. & ROUSE, B.T., 1983. Enhanced responsiveness of committed macrophage precursors to macrophage-type colony-stimulating factor (CSF-1) induced in vitro by interferons alpha/beta. *J. Immunol., 131* :2374.

NAKAMURA, S.; NAKATA, K.; KASHIMOTO, S.; YOSHIDA, H. & YAMADA, M., 1986. Antitumor effect of recombinant human interleukin 1 in alpha against murine synergistic tumors. *Japanese J. Cancer Res.* (Gann), *77* :767.

NETA, R.; DOUCHES, S.D. & OPPENHEIM, J.J., 1986. Interleukin 1 is a radioprotector. *J. Immunol., 136* :2483.

NETA, R.; DOUCHES, S.D. & OPPENHEIM, J.J., 1986. Radioprotection by interleukin 1. In immunoregulation by characterized polypeptides. (eds.) G. Goldstein, J.F. Bach and H. Wigzall. Proceedings of UCLA Symposia on Molecular and Cellular Biology 41 :429.

NETA, R.; OPPENHEIM, J.J.; DOUCHES, S.D.; GICLAS, P.C.; IMBRA, R.J. & KARIM, M., 1986. Radioprotection with Il 1. Comparison with other cytokines. In Progress in Immunology VI, Acad. Press, NY, p. 900

NETA, R.; SZTEIN, M.B.; OPPENHEIM, J.J.; GILLIS, S. & DOUCHES, S.D., 1987. The in vivo effects of Il 1. Bone marrow cells are induced to cycle following administration of Il 1. *J. Immunol., 139* : 1861.

ONOZAKI, K., MATSUSHIMA, K.; AGGARWAL, B. B. & OPPENHEIM, J.J., 1985. Human interleukin 1 is a cytocidal factor for several tumor cell lines. *J. Immunol., 135* :3962.

ONOZAKI, K., MATSUSHIMA, K.; KLEINERMAN, E.S.; SAITO, T. & OPPENHEIM, J.J., 1985. Role of interleukin 1 (IL1) in promoting human monocyte-mediated tumor cytotoxicity. *J. Immunol., 135* :314.

ONOZAKI, K.; TAMATANI, T.; HASHIMOTO, T. & MATSUSHIMA, K., 1986. Augmentation of mouse myeloid cell line differentiation by interleukin 1. *Proc. of Japanese J. Microbiol., 41* :157.

ONOZAKI, K.; URAWA, H.; TAMATANI, T.; IWAMURA, Y.; HASHIMOTO, T.; BABA, T.; SUZUKIM, H.; YAMADA, M.; YAMAMOTO, S.; OPPENHEIM, J.J. & MATSUSHIMA, K., 1988. Synergistic interactions of interleukin 1, interferon-and tumor necrosis factor in terminally differentiating a mouse myeloid leukemic cell line (M1). *J. Immunol., 140* :112.

OPPENHEIM, J.J., 1986. Interleukins and interferons in inflamation. In Current Concepts. The Upjohn Co., Scope Publication, Kalamazoo, MI.

OPPENHEIM, J.J.; KOVACS, E.J.; MATSUSHIMA, K. & DURUM, S.K., 1986. There is more than one interleukin 1. *Immunology Today, 7* (2) :45.

RESNITZKY, D.; YARDEN, A.; ZIPORI, D. & KIMCHI, A., 1986. Autocrine – related interferon controls c-myc suppression and growth arrest during hematopoietic cell differentiation. *Cell, 46* :31.

SMITH, K.A.; LACHMAN, L.B.; OPPENHEIM, J.J.; FAVATA, M.F., 1980. The functional relationship of the interleukins. *J. Exp. Med., 151* :1551.

SMITH, W.W.; ALDERMAN, I.M. & GILLESPIE, R. F., 1958. Hematopoietic recovery induced by bacterial endotoxin in irradiated mice. *Am. J. Phys., 192* :549.

TSUJIMOTO, J.; YIP, Y.K. & VILCEK, J., 1986. Interferon-gamma enhances expression of cellular receptores for tumor necrosis factor. *J. Immunol., 136* :2441.

VOGEL, S.N.; DOUCHES, S.D.; KAUFMAN, E.N. & NETA, R., 1987. Induction of colony stimulating factor in vivo by recombinant interleukin 1 and recombinant tumor necrosis factor. *J. Immunol., 138* :2143.

WILLIAMSON, B.D.; CARSWELL, E.A.; RUBIN, B. Y.; PRENDERGAST, J.S. & OLD, L.J., 1983. Human tumor necrosis factor produced by human B-cell lines: Synergistic cytotoxic interaction with human interferon. *Proc. Natl. Acad. Sci.*, USA *88* :5397.

YAMADA, M.; FURUTANI, F.; NOTAKE, M.; YAMAGISHI, J.; YAMAYOSHI, M.; FUJUI, T.; NOMURA, H.; KOMIYA, M.; KUWASHINA, J.; NAKANO, K.; SOHMURA, Y. & NAKAMURA, S., 1985. Efficient production of human tumor necrosis factor in Escherichia coli. *J. Biotech., 3* :141.

ZUCALI, J. R.; BROXMEYER, H.E.; DINARELLO, C.A.; GROSS, M.A. & WEINER, R.S., 1987. Regulation of early human hematopoietic (BFU-E and CFU-6EHH) progenitor cells in vivo by interleukin 1 induced fibroblast conditioned medium. *Blood, 69* :33.

Histochemical Journal **19**, 413–418 (1987)

Mechanism of secretory granule exocytosis: Can granule enlargement precede pore formation?

ELSA A. SCHMAUDER-CHOCK[1] and STEPHEN P. CHOCK[2]*

[1]*Department of Experimental Haematology, Armed Forces Radiobiology Research Institute, Bethesda, Maryland 20814-5145*
[2]*Laboratory of Neurochemistry, NINCDS, NIH, Bethesda, Maryland 20892, USA*

Received 10 December 1986 and in revised form 24 March 1987

Summary

Secretory granules have been observed to swell during the process of exocytosis. Swelling is an indication of osmotic stress. The probable role of osmotic pressure in facilitating membrane fusion makes it necessary to determine whether granule membrane 'swelling' can occur prior to its fusion with the plasma membrane (pore formation) in the process of exocytosis. By subjecting adjacent thin and semi-thin sections of an activated granule to ultrastructural examination for membrane enlargement, and to metachromatic staining for verification of pore formation it is concluded that the perigranular membrane can indeed enlarge prior to pore formation. However, the degree of membrane enlargement can far exceed the limit of 2–3% stretching allowed under normal osmotic stress for a membrane bilayer. Such an extensive membrane enlargement, which takes place in the mechanism of exocytosis, cannot be achieved without being accompanied by the insertion of additional membrane.

Introduction

The symptoms of radiation sickness are consistent with those associated with mast cell degranulation (Conte *et al.*, 1956; Eisen & Wilson, 1957). In an effort to better understand how to control the mast cell-induced aspects of radiation injury, we have studied the mechanism of mast cell granule exocytosis, particularly the events involving granule activation prior to histamine release.

Granule swelling appears to be a prerequisite of mast cell granule release (Bloom & Haegermark, 1965; Bloom & Chakravarty, 1970; Padawer, 1970; Anderson *et al.*, 1973; Lawson *et al.*, 1977; Uvnas, 1982; Curran & Brodwick, 1985). Granule swelling is also implicated in other secretory systems such as the sea urchin egg cortical granule release (Zimmerberg & Whitaker, 1985), the catecholamine release from the adrenal chromaffin granules (Holz, 1986), the trichocyst release by *Paramecium* cells (Bilinski *et al.*, 1981), and the nematocyst discharge from the stinging cells of *Hydra* (Holstein & Tardent, 1984). This swelling may represent the onset of an osmotically-driven fusion event between the perigranular membrane and the plasma membrane, and may be analogous to the *in vitro* fusion of phospholipid vesicles with a planar membrane (Cohen *et al.*, 1982; Finkelstein *et al.*, 1986).

Uvnas has described the initial event in the mast cell degranulation process as an enlargement of the perigranular space, which is represented by the formation of a space between the granule matrix and its membrane (Uvnas, 1982). Many morphological changes associated with the mast cell granule activation have also been described by other investigators (Chi *et al.*, 1976; Caulfield *et al.*, 1980; Henriquez *et al.*, 1983). The term, 'altered granule', has been used to refer to a swollen granule with a dispersed matrix (Bloom & Haegermark, 1965). The degree of granule alteration and the number of granules showing morphological alteration also correlate well with the release of histamine (Bloom & Chakravarty, 1970; Rohlich *et al.*, 1971). When stained with a metachromatic dye such as Toluidine Blue, the altered granule appears pink while unaltered or quiescent granules stain dark blue or purple. The exhibition of metachromasy by the altered granule is the result of a dye spectral shift caused by an interaction between the uniquely arranged dye molecules bound to the anionic sites on the granule matrix previously occupied by histamine. Therefore, those granules which retain their histamine will stain dark blue or purple while those granules which have lost their histamine will stain

* Present address: 203 Cedar Avenue, Gaithersburg, Maryland 20877, USA

0018-2214/87 $03.00 + .12

pink with Toluidine Blue (Bloom & Haegermark, 1965; Anderson *et al.*, 1974; Uvnas, 1982). For a review on the principle of metachromasy, see Bergeron & Singer (1958). The pink colour of the metachromatically stained granule is an indication that its perigranular membrane has already fused with the plasma membrane. This fusion results in the formation of a pore through which the granule mediators are discharged and the granule histamine content is released via a cation exchange mechanism (Lagunoff *et al.*, 1964; Thon & Uvnas, 1967; Uvnas, 1982).

Additional evidence indicating that a swollen 'altered granule' has already fused with the plasma membrane and therefore already has a pore open to the cell exterior, came from the study by Rohlich *et al.* (1971). By using extracellular markers, they concluded that the swollen 'altered granules' contain pores, and are first found in the periphery of the mast cell following stimulation to secrete histamine. This contradicted earlier observations in which enlarged granules were also found deep within the mast cell when low concentrations of histamine liberators were used (Bloom & Haegermark, 1967; Bloom & Chakravarty, 1970). The important question here is not whether swollen activated granules can be found deep within a stimulated mast cell, but rather whether granule enlargement can precede pore formation.

As the concept of an osmotic gradient becomes more implicated in the mechanism of membrane fusion, it is evident that granule enlargement might reflect an increase in osmotic pressure within the granule. In an effort to define the role of an osmotic gradient in exocytosis, Finkelstein *et al.* (1986) recently posed the question whether granule swelling can occur prior to its fusion with the plasma membrane during exocytosis. This question cannot be clearly answered from the existing literature, partly due to the confusion between the use of the terms 'swollen granule' and 'altered granule'. The granule may be considered as having two components which function independently: the limiting perigranular membrane and the granule matrix. The condensed granule matrix is probably the site of high osmotic pressure which occurs as a result of decondensation during activation. The osmotic gradient is generated across the perigranular membrane.

We approached this question by simultaneously subjecting adjacent thin and semi-thin sections of the same granule to ultrastructural examination and to metachromatic light microscopy. This enables us to identify whether the perigranular membrane has fused with the plasma membrane. By applying the same technique to serial sections of an activated granule, we concluded that perigranular membrane enlargement can indeed precede pore formation. Furthermore, the degree of membrane enlargement can far exceed what is permitted by the simple stretching of a membrane bilayer. Such an extensive increase in surface area can only occur when accompanied by an insertion of additional bilayer into the perigranular membrane.

Materials and methods

Cell fractions enriched with connective tissue mast cells were obtained from low speed centrifugation (30*g*, 10 min) of peritoneal lavages from male Sprague-Dawley rats obtained through the NIH animal centre (Bethesda, MD, USA). After one wash in Hank's balanced salt solution (HBSS, Gibco, Grand Island, NY, USA), mast cells (about 2×10^6/ml) were activated by dispensing them into a 1/10 volume of compound A23187 solution (from Calbiochem, serially diluted in HBSS) such that the final concentration of compound A23187 in the reaction mixture equalled 0.5 μg/ml. After incubation at 20° C, the reaction was terminated by an addition of an equal volume of ice-cold 4% glutaraldehyde in 100 mM sodium cacodylate and 4 mM magnesium chloride. Unactivated mast cells (control) were obtained by adding the glutaraldehyde fixative solution prior to the A23187 treatment. Following glutaraldehyde fixation, samples were post-fixed with 1% osmium tetroxide. After a routine acetone and propylene oxide dehydration series, specimens were embedded in Epon 812 according to the standard procedure. Adjacent thin and semi-thin sections were obtained using a Reichert OM U3 ultramicrotome. Serial sections were picked up with slotted formvar coated grids with a carbon backing. After grid staining with Reynold's Lead Citrate and Uranyl Acetate, specimens were examined using a Philips 400 electron microscope. Metachromatic staining of the adjacent semi-thin section was done by exposing the section on a glass slide to several drops of 1% Toluidine Blue aqueous solution and warmed at about 50° C for about 1 min. After rinsing, the slide was mounted with a cover glass using Permount and examined under a Zeiss Ultrophot II microscope. Colour micrographs were obtained using Kodak Ektachrome 4 × 5 professional film.

Results

The ionophore A23187 has been used for studying mast cell granule exocytosis (Kagayama & Douglas, 1974). It has the advantage of having a slower time course for histamine release. Fig. 1 shows both an ultrastructural image and a light micrograph of corresponding adjacent thin and semi-thin sections of a quiescent rat peritoneal mast cell. The ultrastructural image (Fig. 1a) shows that the unactivated granules are amorphous and extremely electron dense. The perigranular membrane which surrounds each granule matrix is so tightly apposed to the surface of the granule matrix that it often cannot be distinguished from it. The adjacent semi-thin section of the same quiescent granule shown in Fig.

1a is seen in Fig. 1b stained with the metachromatic dye, Toluidine Blue. All quiescent granules stain dark purple. The absence of metachromasy in these granules indicates that they contain histamine, and therefore cannot have formed a pore with the plasma membrane to communicate with the cell exterior.

Fig. 2 shows images of adjacent thin and semi-thin sections of a cell after incubation with compound A23187 for 5 min. The ultrastructural image (Fig. 2a) shows many enlarged granule matrices, especially those near the plasma membrane. They take on the appearance of 'altered granules' similar to those reported in the literature (Bloom & Haegermark, 1965; Rohlich *et al.*, 1971; Anderson *et al.*, 1974; Uvnas, 1982). Many of the 'altered granules' with dispersed matrices also have their perigranular membranes fused with each other to form common membrane-lined vacuoles. Some of the vacuoles clearly have already fused with the plasma membrane. These same 'altered granules' also exhibit metachromasy and stain pink, as seen in the light microscopic image of the adjacent semi-thin section (Fig. 2b). Since only those granules which exhibit metachromasy have lost their histamine, it suggests that all the altered granules with dispersed matrices have established channels (pores) of communication with the cell exterior. In contrast, those granules which stained dark purple still retained their histamine, and therefore have not fused with the plasma membrane.

Fig. 3 shows several images from a series of serial sections of a cell incubated with compound A23187 for 30 s. The serial sections of the activated granule shown in this figure are composed of 15 thin sections of about 80 nm (silver section) and a semi-thin section of about 240 nm (blue section). Figs. 3b,d are thin sections (10th and 12th respectively) adjacent to the semi-thin section. The semi-thin section, the 11th section of the series (Fig. 3c), was stained with Toluidine Blue to see if the activated granule has developed a channel or pore which communicates with the outside. As can be seen, all the granules in this cell still stained dark purple, and even those showing their perigranular membranes already lifted from their matrices still have not fused with the plasma membrane. This strongly suggests that the perigranular membrane of the activated granules can enlarge prior to fusion with the plasma membrane. The extent of the perigranular membrane enlargement of the activated granule shown in Fig. 3 can be appreciated when the granule is reconstructed from the measurements of the granule diameters derived from each section in the series (Fig. 4). It is clear that during this early stage of granule activation, the perigranular membrane can nearly double in diameter, while the granule matrix remains relatively condensed. The fact that the condensed granule has been shown to retain its histamine content further supports our conclusion (Uvnas, 1982).

Discussion

It is well established that after a granule membrane fuses with the plasma membrane, a rapid cation exchange mechanism results in a decondensation or apparent swelling of the granule matrix with histamine release. In an effort to define the role of osmotic pressure in membrane fusion during exocytosis, the question has been raised as to whether a granule can also 'swell' prior to fusion with the plasma membrane. By applying both ultrastructural and metachromatic staining techniques to adjacent thin and semi-thin sections, we have demonstrated that the perigranular membrane can indeed enlarge prior to fusion with the plasma membrane (pore formation). This means that the perigranular membrane can also enlarge before granule matrix unravelling. This perigranular membrane enlargement may reflect a surge in intragranular osmotic pressure which triggers a rapid influx of water into the granule following granule activation. Evidence which supports this interpretation has already been suggested (Chock & Chock, 1985; Schmauder-Chock & Chock, 1985). Our findings can be partly taken as supporting evidence for the thesis of Finkelstein *et al.*, who proposed a role for osmotic pressure in facilitating membrane fusion (Cohen *et al.*, 1982; Finkelstein *et al.*, 1986). However, the extensive membrane enlargement observed here for the activated granule can not be explained by mere osmotic stretching of the perigranular membrane alone. As seen in Fig. 4, the size reconstruction of the serially sectioned activated granule shown in Fig. 3, the perigranular membrane diameter has enlarged from 0.72–1.2 μm. This represents a trebling of the perigranular membrane surface area. Since bilayer membrane cannot stretch beyond 2–3% of its original surface area (Kwok & Evans, 1981), this tremendous increase in surface area following granule activation requires additional membrane from another source. The evidence, which suggests the occurrence of a new membrane assembly as part of the mechanism for granule activation, has been previously reported (Chock & Schmauder-Chock, 1985). This rapid assembly of new membrane requires the storage of membrane precursor elements such as phospholipids, cholesterol and glycolipid within the quiescent granule. In support of this we have results which suggest that the average quiescent granule contains sufficient phospholipid to accomplish a four-fold expansion of its

surface area (Chock & Schmauder-Chock, 1987). Evidence which suggests the presence of phospholipid in other secretory granules has been reported before; however, their exact amounts were difficult to quantitate due to the difficulty in obtaining purified quiescent granules (Blaschko *et al.*, 1967; Helle, 1968; Marcus *et al.*, 1969; Simson *et al.*, 1973).

Confusion surrounding the term 'swollen' granule may stem from a lack of awareness that the granule consists of two components: the perigranular membrane and the granule matrix. They can enlarge independently except that the granule matrix can only enlarge (unravel) following pore formation. As a result of activation, the perigranular membrane rapidly enlarges. Initially, this event may represent membrane stretching due to increased intragranular osmotic pressure. However, this stretching can account for no more than 2–3% of the surface area increase. The tremendous membrane enlargement observed here can only be accomplished by the insertion of additional membrane which sustains the continous enlargement of the perigranular membrane until a fusion event occurs. During the period of membrane enlargement, the granule matrix remains quite condensed. Occasionally the matrix takes on a dappled appearance when examined ultrastructurally at this stage. This may represent a reorganization of matrix components. The fusion event is marked with a loss of histamine and a rapid unravelling and enlargement of the matrix.

The large degree of perigranular membrane enlargement observed here raises the question as to the purpose of such a mechanism in exocytosis. Since secretory granules do not undergo Brownian motion, and the cytoplasmic milieu might prevent their free movement, granule membrane expansion can serve as a mechanism by which the activated granule can approach and make contact with the plasma membrane in order for fusion to occur. Granule membrane expansion not only promotes contacts between the activated granule and the plasma membrane, it also increases the probability of its contact with neighbouring granules. The fusion between granules can result in the formation of a membrane-lined common vacuole which also has the advantage of rapid washout of granule mediators following pore formation. The insertion of new membrane which enables the granule to expand might also aid in the process of fusion, since the new membrane might be fusogenic.

Conclusion

By subjecting adjacent thin and semi-thin sections of an activated granule to ultrastructural examination and metachromatic staining, respectively, we have found that the perigranular membrane of an activated granule can enlarge prior to fusion with the plasma membrane. Since the extent of this membrane enlargement can far exceed that which is permitted by the physical stretching of a bilayer, it is postulated that insertion of additional membrane into the expanding perigranular membrane must have occurred during granule activation. This finding is consistent with our previous conclusion, that new membrane assembly is an inherent step in the mechanism of exocytosis.

Acknowledgements

This work represents continued evidence in support of the concept proposed in E.A.S-Cs' dissertation in the Department of Biology, George Washington University, Washington, D.C., USA. The authors would like to thank Mr Thomas K. Dalton and Mr Joe L. Parker, of AFRRI; Mrs Eunice L. Summers and Mr Alexander B. Wheaton of

Fig. 1. Images of the adjacent thin (a) and semi-thin (b) sections of an unstimulated mast cell. (a) Electron micrograph of the thin section of an unactivated mast cell reveals many dense osmophilic granules in the cytoplasm. The perigranular membranes of the quiescent granules are tightly apposed to their matrices and are often difficult to discern. The insert represents a × 2.6 magnification of the granule indicated by the arrow. (b) Light micrograph of the adjacent semi-thin section. The quiescent granules appear purple or dark blue when stained with Toluidine Blue. Scale bars: 1μm.

Fig. 2. Images of adjacent thin and semi-thin sections of a histamine-releasing mast cell. (a) Ultrastructural image of the thin section of a mast cell incubated with compound A23187 for 5 min. Many 'altered granules' with dispersed matrices are found in large vacuoles. One altered granule, at the lower right hand corner (arrow), is being extruded from the vacuole. (b) Light micrograph of the semi-thin section adjacent to the thin section shown in (a). All 'altered granules', as seen in (a) with dispersed matrices, are stained metachromatically pink with Toluidine Blue. This confirms that they have lost their histamine content and thus must possess pores communicating with the cell exterior. Scale bars: 1μm.

Fig. 3. Selected images from serial sections of an activated granule (arrow). The mast cell was activated by a 30 s incubation at 20° C in the presence of 0.5 μg/ml of compound A23187. (a) is the image of the 6th section of the series, while (b), (c) and (d) are images of the 10th, 11th and 12th sections of the series, respectively. The semi-thin section (c) was stained with Toluidine Blue. The fact that all granules, including the activated 'swollen' granule (arrow), stain purple suggests that fusion with the plasma membrane has not occurred. Scale bars: 1μm.

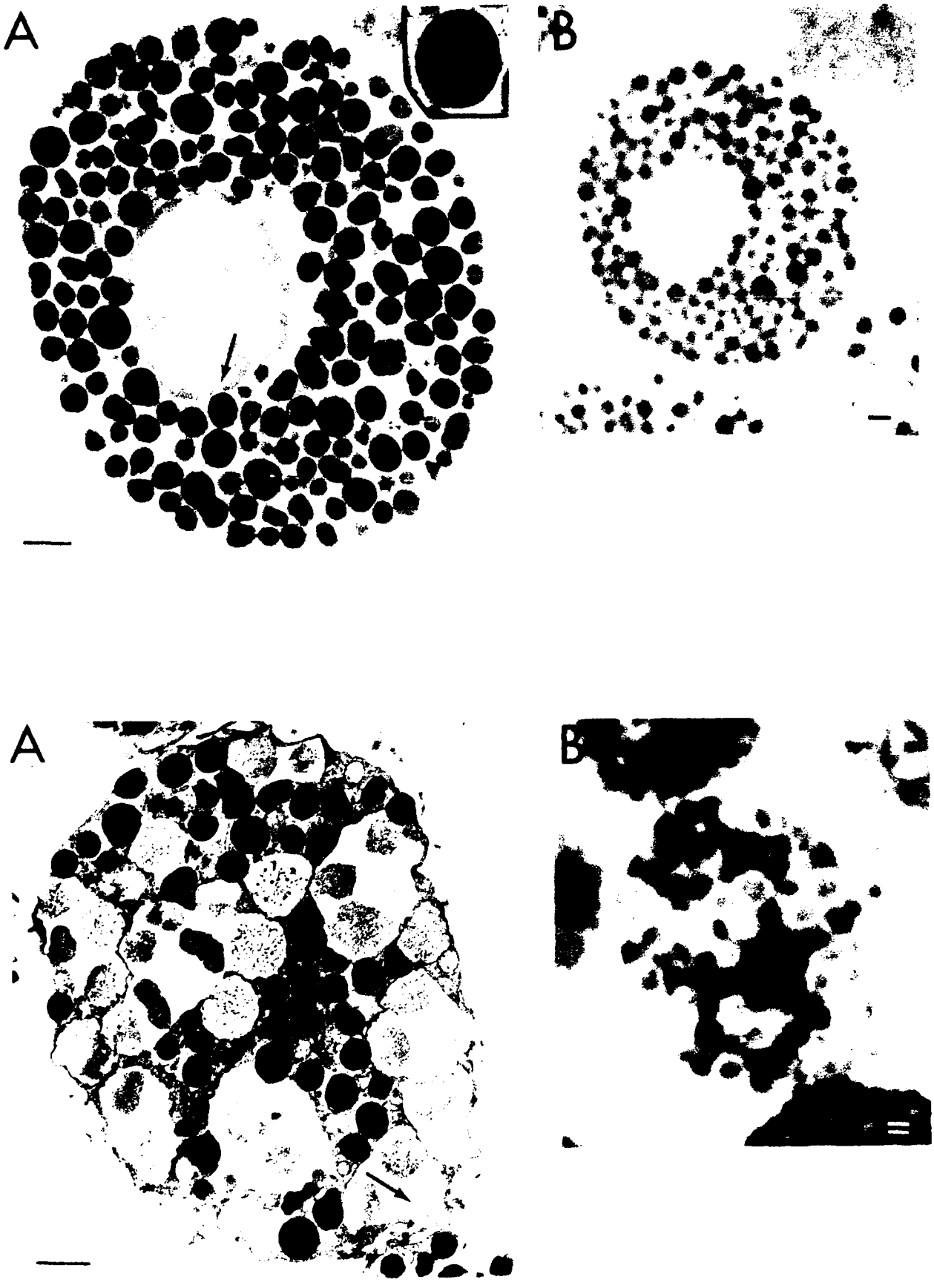
A
B
A
B

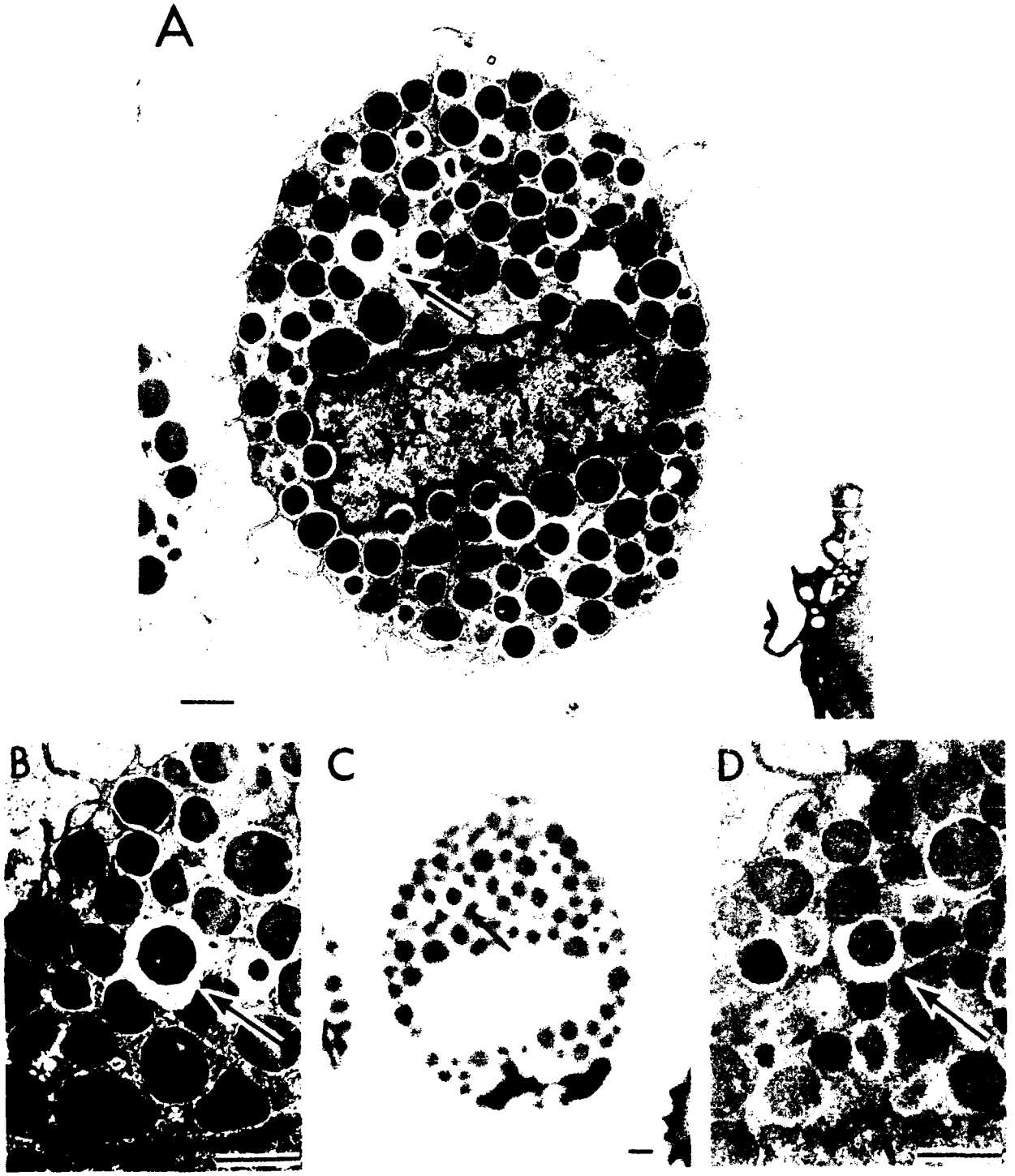
A
B
C
D

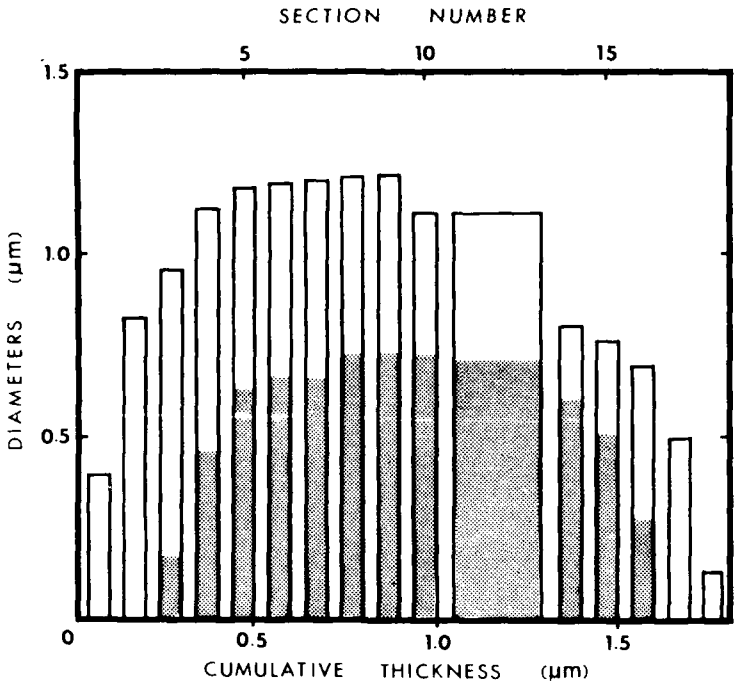

Fig. 4. Reconstruction of the activated granule shown in Fig. 3. The diameters of both the granule matrix (shaded area) and the perigranular membrane of the activated granule were measured from the electron micrograph of each section in the series and plotted as a function of the accumulated section thickness. Each thin section in the series was taken as 80 nm and the semi-thin section (section 11) as 240 nm. The maximum diameter of the matrix of this activated granule measured approximately 0.72 μm, while its perigranular membrane has enlarged to a diameter of about 1.2 μm.

LNC, NINCDS for their kind assistance and encouragement during the course of this work. Appreciation is also expressed to Dr Thomas McVittie of AFRRI and to Drs Wayne Albers and Janet Passonneau of LNC, NINCDS, NIH for support.

References

ANDERSON, P., SLORACH, S. A. & UVNAS, B. (1973) Sequential exocytosis of storage granules during antigen-induced histamine release from sensitized rat mast cells *in vitro*. An electron microscopic study. *Acta Physiol. Scand.* **88**, 359–72.

ANDERSON, P., ROHLICH, P., SLORACH, S. A. & UVNAS, B. (1974) Morphology and storage properties of rat mast cell granules isolated by different methods. *Acta Physiol. Scand.* **91**, 145–53.

BERGERON, J. A. & SINGER, M. (1958) Metachromasy: an experimental and theoretical reevaluation. *J. Biophys. Biochem. Cytol.* **4**, 433–57.

BILINSKI, M., PLATTNER, H. & MATT, H. (1981) Secretory protein decondensation as a distinct, Ca^{2+}-mediated event during the final steps of exocytosis in *Paramecium* cells. *J. Cell Biol.* **88**, 179–88.

BLASCHKO, H., FIREMARK, H., SMITH, A. D. & WINKLER, H. (1967) Lipids of the adrenal medulla: lysolecithin, a characteristic constituent of chromaffin granules. *Biochem. J.* **104**, 545–9.

BLOOM, G. D. & HAEGERMARK, O. (1965) A study on morphological changes and histamine release induced by compound 48/80 in rat peritoneal mast cells. *Expl. Cell Res.* **40**, 637–54.

BLOOM, G. D. & HAEGERMARK, O. (1967) Studies on morphological changes and histamine release induced by bee venom, *n*-decylamine and hypotonic solution in rat peritoneal mast cells. *Acta Physiol. Scand.* **71**, 257–69.

BLOOM, G. D. & CHAKRAVARTY, N. (1970) Time course of anaphylactic histamine release and morphological changes in rat peritoneal mast cells. *Acta Physiol. Scand.* **78**, 410–19.

CAULFIELD, J. P., LEWIS, R. A., HEIN, A. & AUSTEN, K. F. (1980) Secretion in dissociated human pulmonary mast cells. *J. Cell Biol.* **85**, 299–311.

CHI, E. Y., LAGUNOFF, D. & KOEHLER, J. K. (1976) Freeze-fracture study of mast cell secretion. *Proc. Natl. Acad. Sci. USA* **73**, 2823–7.

CHOCK, S. P. & CHOCK, E. S. (1985) A two-stage fusion model for secretion. *Fed. Proc.* **44** (4), 1324.

CHOCK, S. P. & SCHMAUDER-CHOCK, E. A. (1985) Evidence of *de novo* membrane generation in the mechanism of mast cell secretory granule activation. *Biochem. Biophys. Res. Commun.* **132**, 134–9.

CHOCK, S. P. & SCHMAUDER-CHOCK, E. A. (1987) The mast cell granules: a phospholipid source for prostaglandin synthesis. In *Prostaglandin and Lipid Metabolism in Radiation Injury*. (edited by WALDEN, T. L. and HUGHES, H. N.). New York: Plenum (in press).

COHEN, F. S., AKABAS, M. H. & FINKELSTEIN, A. (1982)

Osmotic swelling of phospholipid vesicles causes them to fuse with a planar phospholipid bilayer membrane. *Science* **217**, 458–60.

CONTE, F. P., MELVILLE, G. S. & UPTON, A. C. (1956) Effects of graded whole-body X-irradiation on mast cells in the rat mesentery. *Amer. J. Physiol.* **187**, 160–2.

CURRAN, M. & BRODWICK, M. S. (1985) Mast cell exocytosis and the gel-swell of granules. *Biophys. J.* **47**, 172a.

EISEN, V. D. & WILSON, C. W. M. (1957) The effects of beta-irradiation on skin histamine and vascular responses in the rat. *J. Physiol.* **136**, 122–130.

FINKELSTEIN, A., ZIMMERBERG, J. & COHEN, F. S. (1986) Osmotic swelling of vesicles: its role in the fusion of vesicles with planar phospholipid bilayer membranes and its possible role in exocytosis. *Ann. Rev. Physiol.* **48**, 163–74.

HELLE, K. B. (1968) The chromogranin of the adrenal medulla: a high-density lipoprotein. *Biochem. J.* **109**, 43–4.

HENRIQUEZ, A. S., BLOCH, K. J., KENYON, K. R., BAIRD, R. S., HANNINEN, L. A. & ALLANSMITH, M. R. (1983) Ultrastructure of mast cells in rat ocular tissue undergoing anaphylaxis. *Arch. Ophthalmol.* **101**, 1439–46.

HOLSTEIN, T. & TARDENT, P. (1984) An ultra-high speed analysis of exocytosis: nematocyst discharge. *Science* **223**, 830–33.

HOLZ, R. W. (1986) The role of osmotic forces in exocytosis from adrenal chromaffin cells. *Annu. Rev. Physiol.* **48**, 175–89.

KAGAYAMA, M. & DOUGLAS, W. W. (1974) Electron microscopic evidence of calcium induced exocytosis in mast cells treated with 48/80 or the ionophores A23187 and X-537A. *J. Cell Biol.* **62**, 519–26.

KWOK, R. & EVANS, E. (1981) Thermoelasticity of large lecithin bilayer membrane vesicles. *Biophys. J.* **35**, 637–52.

LAGUNOFF, D., PHILLIPS, M. T., ISERI, O. H. & BENDITT, E. P. (1964) Isolation and preliminary characterization of rat mast cell granules. *Lab. Invest.* **13**, 1331–44.

LAWSON, D., RAFF, M. C., GOMPERTS, B., FEWTRELL, C. & GILULA, N. B. (1977) Molecular events during membrane fusion: a study of exocytosis in rat peritoneal mast cells. *J. Cell Biol.* **72**, 242–59.

MARCUS, A. J., ULLMAN, H. L. & SAFIER, L. B. (1969) Lipid composition of subcellular particles of human blood platelets. *J. Lipid Res.* **10**, 108–14.

PADAWER, J. (1970) The reaction of rat mast cells to polylysine. *J. Cell Biol.* **47**, 352–72.

ROHLICH, P., ANDERSON, P. & UVNAS, B. (1971) Electron microscope observations on compound 48/80-induced degranulation in rat mast cells. *J. Cell Biol.* **51**, 465–83.

SCHMAUDER-CHOCK, E. A. & CHOCK, S. P. (1985) *De novo* membrane generation: implication of hydration forces in the mechanism of histamine release. In *Armed Forces Radiobiology Research Institute Annual Research Report, 1985*, pp. 21–3. Bethesda: AFRRI.

SIMSON, J. A. V., HALL, B. J. & SPICER, S. S. (1973) Histochemical evidence for lipoidal material in secretory granules of rat salivary glands. *Histochem. J.* **5**, 239–54.

THON, I. I. & UVNAS, B. (1967) Degranulation and histamine release: two consecutive steps in the response of rat mast cells to compound 48/80. *Acta Physiol. Scand.* **71**, 303–15.

UVNAS, B. (1982) Mast cell granules, in *The Secretory Granules* (edited by POISNER, A. M. and TRIFARO, J. M.) pp. 357–84. Amsterdam: Elsevier Biomedical.

ZIMMERBERG, J. & WHITAKER, M. (1985) Irreversible swelling of secretory granules during exocytosis caused by calcium. *Nature* **315**, 581–4.

7

PROTECTION AGAINST IONIZING RADIATION WITH EICOSANOIDS

LINDA K. STEEL AND GEORGE N. CATRAVAS

Department of Radiation Biochemistry and Chair of Science, Armed Forces Radiobiology Research Institute, Bethesda, MD 20814-5145.

INTRODUCTION

Prostaglandins (PGs) are extremely diverse in their pharmacological activities. They exhibit both antagonistic as well as cytoprotective properties in the pathogenesis of inflammation. Participation of PGs as chemical mediators in the regulation of immune responses and inflammation are increasingly apparent (1-3). The antagonistic properties of PGs have been implicated in a variety of symptoms resulting from exposure to ionizing radiation. Post irradiation increases in small bowel motility (4), diarrhea, flatulence, abdominal pain (5), mucositis (6), and esophagitis (7,8) have been attributed, in part, to excessive PG production.

In contrast, exogenous PGs, particularly of the E type, have been shown to be cytoprotective against a variety of damaging agents, and a deficiency of endogenous PG has been suggested to contribute to increase susceptibility to injury (9-17). These findings have provided much of the impetus to examine the potential cytoprotective effects of PGs in radiation injury.

Cells in Culture

Perhaps the earliest report of a cytoprotective effect of prostaglandins against ionizing radiation was demonstrated by Prasad (18). PGE_1 (10 μg/ml) added to Chinese hamster ovary (CHO) cells in cultures 1 or 4 hours before x-irradiation increased cell survival and colony forming ability approximately 2-fold, but was ineffective if added 1 or 4 hours after irradiation. He proposed that the observed radioresistance with PGE_1 pretreatment may be through stimulation of adenylate cyclase and subsequent elevation of cylic AMP. Several years later, Lehnert (19) investigated the possible relationship between agents known to elevate cyclic AMP and cell radiosensitivity. Addition of PGE_1 to the culture medium modified the survival of Chinese hamster V-79 cells after x-irradiation by increasing the shoulder portion of the survival curve. Since the compound was not present in the medium at the time of exposure, the possibility of a direct radioprotective effect was ruled out. It was concluded that the effects of PGE_1 are the result of elevated intracellular cyclic AMP, and that cell survival is, in part, dependent on the relationship between these levels and radiosensitivity.

Not all reports show PG induced radioprotection. Millar and Jinks (20) found that Chinese hamster cells (line V79-753B) exposed to 1 μg/ml PGE_1 or 10 μg/ml PGA_2 for 20 hours then subjected to gamma irrudiation from a ^{60}Co source were not altered in radiosensitivity. The authors did not observe any increase in radiation sensitivity with inhibition of PG synthesis by pretreatment of this cell line with nonsteroidal antiinflammatory drugs (21,22), but glucocorticoid pretreatment increased radiation resistance (22). Hanson and Ainsworth (23) reported that 16,16-dimethyl PGE_2 (2 μg/ml) added to CHO cells 2 hours prior to ^{60}Co gamma irradiation did not confer radioprotection. Similar results were obtained by Holahan and coworkers (24) using exponentially growing synchronous or asynchronous V79-A03 cells pretreated with 14 μM PGE_2 for 2 hours prior to x-irradiation, even though intracellular levels of cyclic AMP were elevated by PGE_2 pretreatment (E. V. Holahan, personal communication). However, PGE_2 did radioprotect asynchronous cells or cells irradiated in the G1 or S phase and exposed to N-ethylmaleimide, a nonspecific thiol-binding radiosensitizer. Recovery was not inhibited by incubation with buthionine-S,R-sulfoximime, a glutathione synthetase inhibitor. These results suggest that glutathione content is not associated with the radioprotective effect of PGE_2. (E. V. Holahan, personal communication). The studies of Millar and Jinks (21,22,25) also suggest a lack of a direct role for elevated glutathione content in the enhancement of radiation resistance of steroid, flurbiprofen or PG-treated cells.

Hinz and Dertinger (26) demonstrated that V-79 cells grown as spheroids could be protected from photon irradiation with PGE_1. However, if these cells were grown as monolayers, no PG-induced protection was conferred. Hanson and coworkers (27) also demonstrated PG-induced radioprotection with 16,16-dimethyl PGE_2 pretreatment of human melanoma (M-1) cells grown as spheroids and exposed to ^{137}Cs gamma radiation. No PG-induced radioprotection was seen in melanoma grown as single cells. These findings suggest a role for cell contact in the protection from radiation treatment and the possibility that membranes of cells in contact may be altered by PG treatment.

Walden and coworkers (28) recently demonstrated a decrease in cellular radiosensitivity of Chinese hamster lung fibroblast (V79A03) cells treated with leukotriene C_4 (LTC_4, 2.5 μM) for two hours prior to 10 Gy x-irradiation. Similar modification of radiosensitivity was demonstrated for LTE_4 but not for LTD_4. This is the first report of a derivative of the lipoxygenase pathway of arachidonic acid metabolism modifying the radiosensitivity of mammalian cells.

Local Irradiation

Clinical studies on the role of PG in radiotherapy are reviewed in another section of this volume. As with cells in culture, there is only tentative or scant evidence in the literature suggesting that PG treatment can protect against local radiation injury. Northway and colleagues (7) evaluated PGE_2 and indomethacin as potential cytoprotective agents of the esophageal mucosa against radiation injury. Opossums received subcutaneous (sc) injection of 5 or 10 μg/kg 16,16-dimethyl PGE_2 1 hour before irradiation and every 4 hours for 24 hours postirradiation; or indomethacin (sc) before or daily for one week postexposure. Animals received 2.25 Gy gamma radiation from a ^{60}Co source, delivered to the entire esophagus in a single dose. PG-treated animals had an increase in the severity of radiation esophagitis, while indomethacin treatment ameliorated the symptoms and severity. Similiar results were seen with aspirin or hydrocortisone treatment (8). They suggested that PG may mediate the inflammatory response resulting from radiation injury and that steroidal or nonsteroidal antiinflammatory drugs or other pharmacological modulation of endogenous PG synthesis may be of clinical prophylactic value.

In a preliminary report by Delaney (29) intraperitoneal administration of either 16,16-dimethyl PGE_2 or PGE_2 (100 or 250 μg/kg, respectively) to rats one hour prior to receiving 15 Gy abdominal x-irradiation did not alter the mortality curve. Uribe et al. (30) studied oral 16,16-dimethyl PGE_2 administration as a potential protective agent against the damaging effects of local x-irradiation to the abdomen. The mucosa from the small intestine was examined in rats administered PG at 24, 8 and 0.5 hours prior to exposure and 16 and 24 hours following abdominal exposure to 10 Gy. The mucosal crypts and villi, 3 days postirradiation, showed better preservation in rats treated with low doses of 16, 16-dimethyl PGE_2 (100-200 μg/kg). Mucosal damage was exacerbated in animals which received PG doses exceeding 400 μg/kg, similar to the increased severity of radiation esophagitis occurring in PG-treated opossums (7).

The effect of PGE_2 on radiation injury to the small intestine was also examined by Thomas-de la Vega and coworkers (31). Rats were administered 50 μg PGE_2 sc one hour before and 24 hours after 10 or 15 Gy gamma irradiation (^{137}Cs) of an exteriorized segment of the ileum. Morphometric and mitotic (recovery) measurements 3 and 5 days postirradiation demonstrated a cytoprotective effect of PGE_2 on exteriorized, irradiated ileal tissue. The authors suggested that the exogenous addition of PG may correct a postirradiation depletion. This mechanism appears unlikely in view of the reported increases in PG activity in the small

intestine following radiation exposure (4). A possible role of PG in intestinal cellular regeneration following radiation exposure has also been postulated (4).

Whole Body Irradiation

Investigators have only recently examined the use of PG as a potential radioprotectant against the effects of whole body exposure to ionizing radiation. In an earlier study, however, Gidali and Feher (32) examined the post-radiation effect of PGE_2 on the regeneration of hematopoietic cells (CFU-S). Gamma-irradiated mice were treated with 0.1 μg/g PGE_2 24 hours after whole body exposure to 350 rads. The kinetics of CFU regeneration were not improved, even with repeated PGE_2 administration postexposure. These findings suggested that exogenous PGE_2, after radiation insult, does not induce the proliferation of hematopoietic stem cells.

PG administration has been demonstrated to improve intestinal stem cell survival and renewal (33-35), bone marrow CFU-S survival (34,36) and animal survival, if given shortly before radiation exposure. Hanson and Thomas (33) examined the cytoprotective effect of PG on intestinal clonogenic cell survival. Mice were given 16,16-dimethyl PGE_2 sc to the dorsal neck region 1 hour before whole body dose of ^{137}Cs gamma rays. Four days after irradiation, a segment of the jejunum was evaluated for regenerative foci of epithelium. The intestinal clonogenic cells showed an increase in both the shoulder and the slope of the radiation survival curve. The radioprotective effect increased with PG doses ranging from 1 to 10 μg and plateaued at doses of 10-100 μg. Radioprotection was conferred within 5 minutes of PG administration; maximal protection was observed with administration 1 hour prior to irradiation. No radioprotection of intestinal microcolonies was seen if 16,16-dimethyl E_2 was given 4 or more hours prior to exposure, or given after irradiation. Natural PGE_2 also increased cell survival, but to a lesser degree. No radioprotection was seen with PGE_1 (1-100 μg) given before exposure. However misoprostol, a synthetic analog of PGE_1, exceeded the radioprotective activity of 16,16-dimethyl PGE_2 (35). Intestinal stem cell survival was increased nearly 600% with 25 μg misoprostol given two hours prior to exposure.

Hanson and Ainsworth (34) also demonstrated radioprotection of bone marrow stem cells (CFU-S) with PG pretreatment. Cell suspensions prepared from femurs of mice previously given 5 μg 16,16-dimethyl PGE_2 sc 1 hour prior to whole body ^{60}Co gamma radiation were injected via tail vein into lethally irradiated recipients. The CFU-S survival (estimated by spleen colony counts 8-10 days post-irradiation) showed an increase in both shoulder and slope of the curve from PG-treated animals. At 50% CFU-S survival, dimethyl PGE_2-induced radioprotection

gave a dose modification factor of 1.85. This protection was qualitatively similar to that seen for PG-induced radioprotection of intestinal stem cells (34). The 6-day radiation lethality ($LD_{50/6}$) was also increased 24% in PG-treated mice. The authors suggested that the mechanisms of PGE_2-induced radioprotection of the intestinal cell renewal system and bone marrow CFU-S survival may be through the induction or accumulation of elevated intracellular sulfhydryl compounds (33) and increased intracellular cyclic AMP levels (34). Higher in vivo intestinal radioprotection is conferred with misoprostol, compared to PGE_1, PGE_2 and 16,16-dimethyl PGE_2 (35). These results show that side chain modifications increase the radioprotective properties which contribute to enhanced cell survival.

Recently, Walden and colleagues have examined the radioprotective properties of 16,16-dimethyl PGE_2 on mouse survival (36,37). The extent of radioprotection was dependent on the dose and time of administration. Optimum protection was achieved with 40 µg PG given sc 30 minutes prior to whole-body exposure to gamma radiation from a ^{60}Co source. Under these conditions, a dose reduction factor of 1.72 was achieved. Lesser doses of PG, or earlier administration prior to irradiation were less effective. Similarly, postirradiation injection (5-60 minutes) of 10 µg PG was ineffective in increasing survival. Distribution and metabolism of 16,16-dimethyl PGE_2 in plasma, bone marrow and spleen at 5, 30 and 60 minutes postinjection were also examined. During this time plasma levels of PG remained constant, organ concentrations increased, and most of the 16,16-dimethyl PGE_2 remained unmetabolized. Dimethyl PGE_2 was also found to enhance splenic CFU-S survival in a dose-dependent manner. The authors suggest that the radioprotective benefits of 16,16-dimethyl PGE_2 result from physiologic changes (i.e., hypotension and extravasation) modulated by the synthesis or release of intermediary compounds such as erythropoietin, non-protein sulphydryls and cyclic AMP. Another noteworthy observation was the ineffectiveness of 16,16-dimethyl PGE_2 obtained as an oil dissolved in triacetin, compared to that obtained as an oil and subsequently dissolved in ethanol. Dimethyl PGE_2 dissolved in triacetin was substantially less radioprotective in both animal survival studies and CFU-S survival in spleen. The reasons for these differences are not known; however, they should be considered when interpreting the literature on PG-induced radioprotection.

Modulation of Substrate Availability

The exact mechanisms regulating the release of the 20-carbon essential fatty acid, arachidonate, upon cell stimulation (irradiation or otherwise) are not completely known. The essential fatty acids are precursors of the eicosanoids

(prostaglandins, leukotrienes, lipoxins and related substances). They also participate in membrane bilayer fluidity and viscosity, thereby exerting effects on membrane proteins and intrinsic enzymes and molecule translocation or channel formation across cell membranes. Modification or depletion of essential fatty acids has been shown to change phosopholipid fatty acid composition, inhibit cyclooxygenase activity and alter both cyclooxygenase and lipoxygenase products (reviewed in 38-41). The modulation of substrate availability by dietary fatty acid modification offers another approach to the evaluation of eicosanoid synthesis in the biological response to radiation exposure.

Cheng et al (42,43) examined the effect of a fat-free diet only, or a daily dietary supplement of 10 mg methyl linoleate or 2% cotton seed oil (approx. 50% linoleate), on fatty acid deficient rats subjected to repeated whole-body x-irradiation of 3 Gy. Fatty acid deficient animals were more radiosensitive than those whose diets were supplemented with linoleate. The authors suggested that the protective effect relates to the correction of the nutritional requirements of essential fatty acids by linoleic acid. Essential fatty acid deficiency has been shown to result in decreased PG production (44,45). Although dietary enrichment with linoleic acid may have effects unrelated to arachidonate metabolism, linoleate supplementation has been shown to increase PG production (46,47).

Intraperitoneal injection of 1 ml of olive oil (mixed glycerides, primarily oleic acid) 1 hour before or 30 minutes after lethal whole-body x-irradiation of mice was found to modestly increase animal survival over the $LD_{50/30}$ of controls (48). The authors speculated that the therapeutic effect of ip administered fats on lethally irradiated animals may partially overcome the malnutrition arising from the inability to utilize orally administered fatty acids. Oleic acid dietary supplements do not cause a change in eicosanoid levels (PGE_2, TxB_2 and LTB_4) in the rat (49).

In a preliminary report (29), Delaney suggests that essential fatty acid deficiency reduces radiation-induced mortality. Fatty acid deficient rats exposed to 14 Gy x-rays or 11 Gy from a 4 MeV linear accelerator in a single dose to the abdomen had increased survival compared to animals on the control diet. The author suggests that the enhanced survival is related to chronic PG depletion by a fatty acid deficient diet.

SUMMARY

More than a decade has past since the first reports suggested that exogenous eicosanoids modify cellular radiosensitivity and increase cell survival. Since then, it has become evident that cells, tissues, and whole organisms differ in radiosensitivity and in the capacity of PG to confer radioprotection. The majority of the studies indicate administration of PG postexposure does not modify radiosensitivity or enhance survival, and in fact may exacerbate symptoms of radiation injury. Exogenous PG administered prior to exposure to ionizing radiation has given mixed results in cell cultures or with local irradiation. Similiarly, studies on the effect of dietary fatty acid modification or depletion on animal radiosensitivity are inconclusive. More recently, whole body irradiation experiments have demonstrated significant PG-induced radioprotection of bone marrow, intestinal stem cells and animal survival. These studies have primarily focused on natural and synthetic PGs of the E series. However, newer synthetic analogues, such as misoprostol, with a longer duration of action (and possibly fewer adverse effects), suggest the potential for improving the radioprotective properties of PGs by side chain modifications.

The mechanism(s) of PG-induced radioprotection are postulated to be through biochemical and physiologic cell changes modulated by some intermediary compound(s). This intermediary substance is most frequently suggested to be cyclic AMP, however erythropoietin, superoxide dismutase, non-protein sulfhydryls, glutathione and others have been proposed. Although the mechanism remains unresolved, PG-induced radioprotection may have important implications for patients receiving radiation therapy for cancer. PGs are secreted by a number of tumors (50-54), and may contribute to radioprotection of malignant cells, reducing the therapeutic benefits of radiotherapy.

References

1. Goodwin, J. S. and Webb, D. R. Clin. Immunol. Immunpath. 15:106-122, 1980.
2. Kunkel, S. L., Chensue, S. W., Fantona, J. C., and Ward, P. A. In: The Reticuloendo-thelial System, A Comprehensive Treatise. Vol. VII: Immunology. (Eds. J. A. Bellanti and H. B. Herscowitz), Plenum Press, New York, 1984, p. 289-301.
3. Trang, L. E. Seminars Arth. Rheum. 9:153-190, 1980.
4. Borowska, A., Sierakowski, S., Mackowiak, J., and Wisniewski, K. Experientia 35: 1368-1370, 1979.
5. Mennie, A. T., Dalley, V. M., Dinneen, L. C. and Collier, H. O. J. Lancet 2:942-943, 1975.
6. Tanner, N. S. B., Stamford, I. F., and Bennett, A. Br. J. Cancer 43:767-771, 1981.
7. Northway, M. G., Libshitz, H. I., Osborne, B. M., Feldman, M. S., Mamel, J. J., West, J. H. and Szwarc, I. A. Gastroenterol. 78:883-892, 1980.
8. Northway, M. G., Eastwood, G. L., Libshitz, H. I., Feldman, M. S., Mamel, J. J. and Scwarc, I. A. Digest. Dis. Sci. 27:923-928, 1982.
9. Mann, M. S. Gastroenterol. 68:946-951, 1975.
10. Robert, A., Lancaster, J. P., Davis, J. P., Field, S. O., and Nezamis, J. E., Scand. J. Gastroenterol. 19:69-72, 1984.
11. Robert, A. Prostaglandins 6:523-531, 1974.
12. Robert, A., Nezamis, J. E., Lancaster, C., and Hanehar, A. J. Gastroenterol. 77:433-443, 1979.
13. Goodwin, J. S. Prog. Cancer Res. Ther. 16:393-415, 1981.
14. Papescu, C. M. Prostaglandins, Leukotrienes and Med. 21:97-105, 1986.
15. Karin, S. M. M. and Fung, W. P. Adv. in Prostaglandin Thromboxane Res. 2:109-111, 1976.
16. Kollberg, B., Nordemar, R., Samuelsson, K., and Bergstrom, S. Gastroenterol. 78:470-485, 1980.
17. Robert, A. Gastroenterol. 69: 1045-1047, 1975.
18. Prasad, N. K. Int. J. Radiat Biol. 22 187-189, 1972.
19. Lehnert, S. Radiat. Res. 62, 107-116, 1975.
20. Millar, B. C. and Jinks, S. Int. J. Radiat Biol. 46:367-373, 1984.
21. Millar, B. C. and Jinks, S. Br. J. Radiol. 54: 505-511, 1981.
22. Millar, B. C. and Jinks, S. Br. J. Radiat. 56: 201-206, 1983.
23. Hanson, W. R. and Ainsworth, E. J. 32nd Ann. Mtg. of Radiat. Res. Soc., Orlando, Florida, March 25-29, 1984, Abst. If-11, p.106.
24. Holahan, E. V., Hagan, M. P., D'Alesandro, M. and Blakely, W. F. 33rd Ann. Mtg. of Radiat. Res. Soc., Los Angeles, CA, May 5-9, 1985, Abst. Ib-11, p.117.
25. Millar, B. C. and Jinks, S. Int. J. Radiat Biol. 47: 539-552, 1985.
26. Hinz, G. and Dertinger, H. Radiat. Envir. Biophys. 21 255-264, 1983.
27. Hanson, W., DeLaurentiis, K. and Malkinson, F. 33rd Ann. Mtg. of Radiat. Res. Soc., Los Angeles, CA., May 5-9, 1985, Abst. He-8, p.97.
28. Walden, T. L. Jr., Holahan, E. V. Jr. and Catravas, G. N. Prog. Lipid Res. 25:587-590, 1986.
29. Delaney, J. Prostaglandins and radiation enteritis. Preliminary report of progress as of 5/1/86 Defense Nuclear Agency (DNA) contract # 001-85-C-0001. Armed Forces Radiobiology Research Institute.
30. Uribe, A., Johansson, C., Rubio, C. and Arndt, J. Acta Radiol. Oncol 23: 349-352, 1984.
31. Thomas-de la Vega, J. E., Banner, B. F., Hubbard, M., Boston, D. L., Thomas, C. W., Straus, A. K. and Roseman, D. L. Surg. Gynecol Obstetr. 158: 39-45, 1984.

32. Gidali, J. and Feher, I. Fifth International Congress of Radiation Research. Seattle, Washington, July 13-20, 1974. Abstract E-27-3 p.292.
33. Hanson, W. and Thomas, C. Radiat. Res. 96:393-398, 1983.
34. Hanson, W. and Ainsworth, E. J. Radiat. Res. 103: 196-203, 1985.
35. Hanson, W. R. and DeLaurentiis, K. Sixth International Conference on Prostaglandins and Related Compounds. Satellite Symposium, Prostaglandins in Gastroenterology: Focus on Misoprostol. Florence, Italy, June 4, 1986, (Abstr.).
36. Walden, T. L., Jr., Snyder, S. L., Patchen, M. L., and Steel, L. K. 34th Ann. Mtg. Radiation Res. Society. Las Vegas, Nevada, Apr. 12-17,1986. Abstr. CI-11, p. 41.
37. Walden, T. Jr., Patchen, M. and Snyder, S. L. personal communication (manuscript submitted).
38. Mathias, M. M. and Dupont, J. Lipids 14:247-253, 1979.
39. Willis, A. L. Nutrition Rev. 39:289-301, 1981.
40. Morita, I., Takahashi, R., Saito, Y. and Murota, S. J. Biol. Chem. 258: 10197-10199, 1983.
41. Croft, K. D., Codde, J. P., Barden, A., Vandongen, R., and Beilin, L. J. Biochem. Biophys. Acta 834: 316-323, 1985.
42. Cheng, A. L. S., Kryder, G. D., Berquist, L. and Deuel, H. J., Jr. Nutrition 48: 161-182, 1952.
43. Deuel, H. J., Jr., Cheng, A. L. S., Kryder, G. D., and Bingeman, M. E. Science 117: 254-255, 1953.
44. Hansen, H. S. Lipids 16: 849-854, 1981.
45. Dunham, E. W., Belasingham, M., Privett, O. S. and Nickell, E. C. J. Lipid Res. 13 458-467, 1978.
46. Nugteren, D. H., Van Evert, W. C., Soating, W. J., and Spuy, J. H. In: Adv. in Prostaglandins and Thromboxane Research (Ed. B. Samuelsson), Vol. 8, 1980, p. 1793-1796.
47. Epstein, M., Lifschitz, M. and Rappaport, K. Clin. Sci. 63: 565-571, 1982.
48. Ashikawa, J. K. and Anderson, O. K. Radiat. Res. 13: 99-107, 1960.
49. Terano, T., Salmon, J. A., Higgs, G. A., and Moncada, S. Biochem. Pharmacol. 35: 779-785, 1986.
50. Seyberth, H. W., Segre, G. V., Morgan, J. L., Sweetman, B. J., Potts, J. T., Jr., and Oates, J. A. N. Engl. J. Med. 293:1278-1283, 1975.
51. Bockman, R. S. Cancer Invest. 1:489-493, 1983.
52. Karmali, R. A. Cancer J. Clin. 33:322-332, 1983.
53. Cummings, K. B. and Robertson, R. P. J. Urol. 118:720-723, 1977.
54. Plescia, O. J. In: Prostaglandins and Cancer, First Internatl. Conf., (Eds., T. J. Powles, R. S. Bockman, K. V. Horr, and P. W. Ramwell), Alan R. Liss, Inc., New York, 1982, p. 619.

AFRRI TECHNICAL REPORT

Cleanup of Johnston Atoll missile launch facility

B. E. Vesper
M. Dooley
T. H. Mohaupt
E. T. Bramlitt

AFRRI TR88-1

DEFENSE NUCLEAR AGENCY
ARMED FORCES RADIOBIOLOGY RESEARCH INSTITUTE
BETHESDA, MARYLAND 20814-5145

REVIEWED AND APPROVED

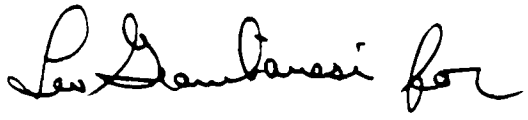

GEORGE N. CATRAVAS, Ph.D., D. Sc.
Chair of Science

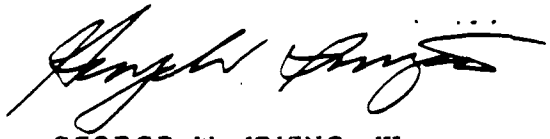

GEORGE W. IRVING, III
Col, USAF, BSC
Director

CONTENTS

BACKGROUND

Johnston Atoll is a small group of four islands about 800 miles southwest of Hawaii (Figure 1). The main island, Johnston Island (Figure 2), is about 2 miles long and 0.75 miles wide. The other three islands are smaller and are used mainly as wildlife refuge areas. The atoll has been under United States military control since the early 1930's and is currently administered by the Defense Nuclear Agency (DNA) of the Department of Defense. In 1962, during the testing of high-altitude nuclear detonations, a missile failed at lift-off. To prevent any nuclear yield, the test device was command-detonated, resulting in plutonium contamination of the launch site. Although no nuclear tests were conducted after 1962, the facility was operated under strict radiological controls until decommissioned in 1977.

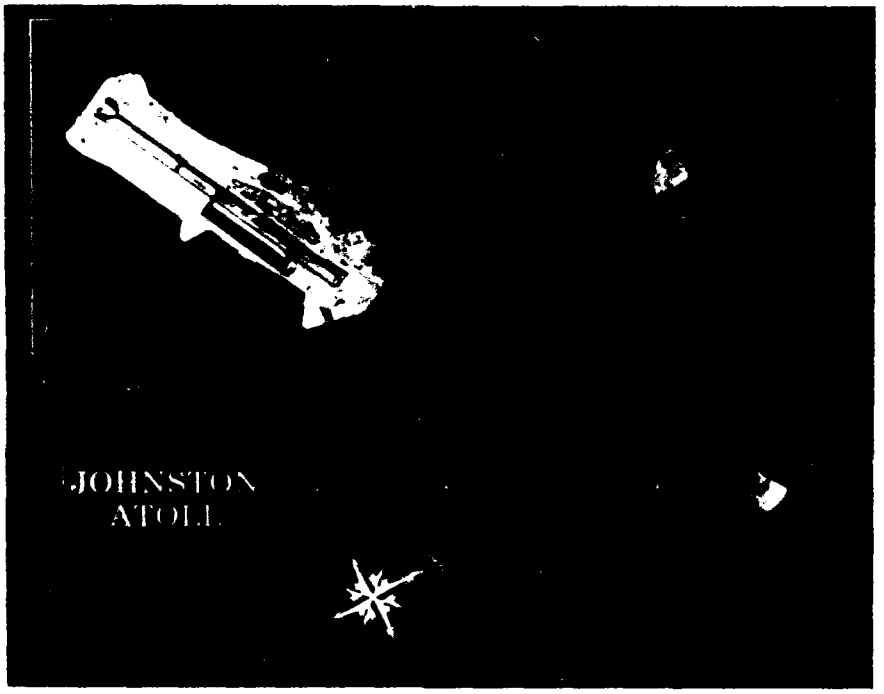

Figure 1. Islands of Johnston Atoll

When the launch facility was deactivated, almost all the missile components were decontaminated and removed from the site. However, the remaining structures could not be decontaminated economically. Included in these structures were the launch erector base, missile shelter building, two large steel revetments, fuel tank, liquid oxygen tank, and the launch pad itself (Figure 3). The launch pad was approximately 138 feet long by 25 feet wide and up to 1 foot thick in some sections. Partially covering the launch pad was the missile shelter building, which was a barnlike structure resting on steel wheels guided by typical railroad tracks. The building consisted of a steel frame covered by honeycomb panels of metal sheet and cardboard spacers. Before a missile was launched, the shelter was driven back about 100 yards; the missile was then raised to the vertical position and fired.

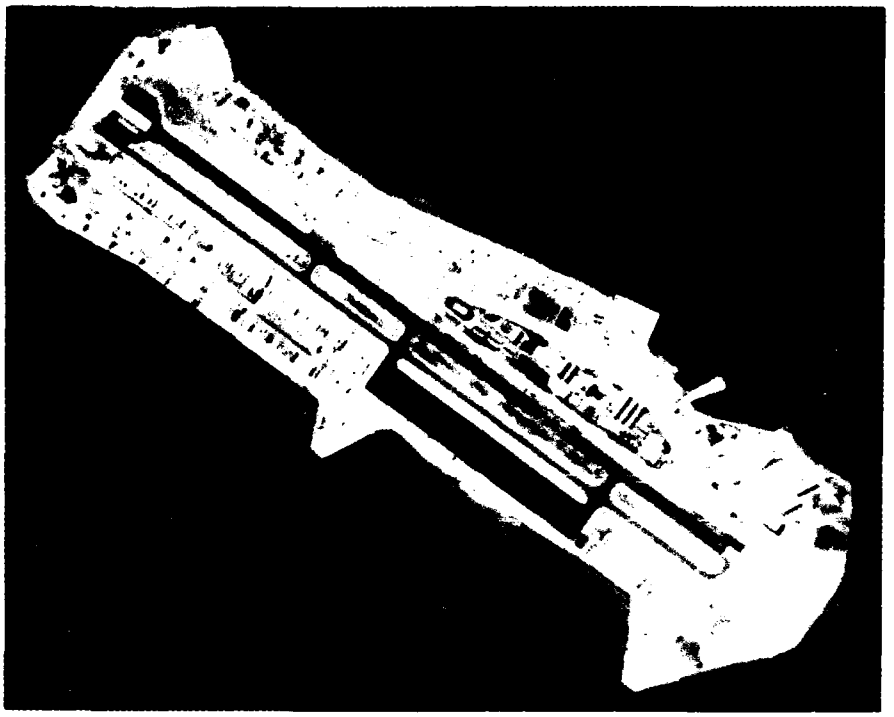

Figure 2. Johnston Island, main island of Johnston Atoll

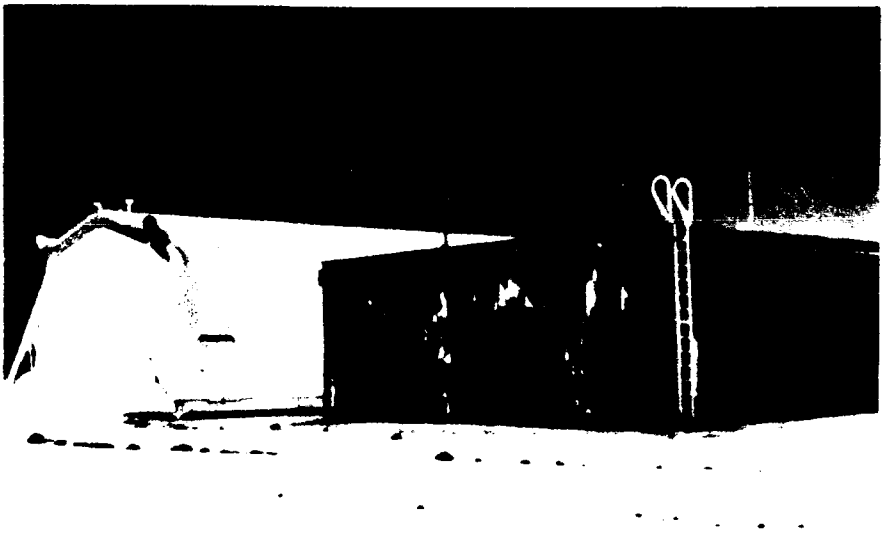

Figure 3. Missile shelter building (background) and steel blast revetments (foreground)

On either side of the moveable missile shelter were revetments constructed of steel piling and thick steel roof plate covered with asphaltic material. The interior and exterior walls were about 4 feet apart, and the space between was filled with aggregate coral. These revetments stored control and diagnostic missile equipment and protected vehicular trailers (which also stored missile equipment) from the blast and heat of the missile launches. Situated near the revetments about 5 feet below grade were the large fuel tank and liquid oxygen tank (Figure 4). The tanks were mounted on concrete pads surrounded by embankments constructed of loose gunite concrete. Also on the site were four 28,000-gallon water tanks (installed after the launch failure); several small concrete pads; and arrays of cable trenches, conduits, metal piping, and electrical cables.

Figure 4. Below-grade liquid oxygen tanks and 28,000-gallon water tanks

During the years the facility remained in use, missile launches and the harsh ocean atmosphere chipped and degraded the paint used to fix the contamination in place. In addition to routine maintenance of the facility, radiological safety procedures required frequent collection of the paint chips and repainting of the surfaces to ensure that the contamination remained fixed. When the site was decommissioned and the majority of missile components were removed, general maintenance at the site was discontinued, necessitating an increase in the radiological maintenance of the facility.

By 1980, there had been significant deterioration of the metal structures at the launch site. Concerns were raised that a strong typhoon might destroy the facility and redistribute the contamination to uncontrolled areas. To protect against further damage from severe weather conditions, the two large steel revetments were dismantled and placed inside the moveable missile shelter (Figure 5). At that time, a comprehensive radiologic survey was completed to determine the extent of contamination. Most of the contamination was fixed to the steel revetments, the doors of the moveable shelter building, and the launch pad. It consisted mainly of plutonium isotopes and an americium impurity (americium-241) typically present with plutonium. The americium-241 impurity is a daughter product of plutonium-241, which decays with a 13.2-year half-life. The primary radiations from these contaminants were alpha particles, characteristic X rays from the most abundant plutonium isotope (plutonium-239), and 60-keV gammas from the americium-241. Because the photon radiation was low and did not have much penetration ability, the major health hazard was from the intake of alpha-emitting plutonium and americium isotopes.

Figure 5. Remains of steel revetments stored in missile shelter building

PLANNING

With the completion of the survey, several options for decontamination were considered. Among these were entombing the entire launch facility in concrete, dismantling the facility and storing the debris locally on Johnston Atoll, and dismantling the facility and transporting the waste to a disposal site in the

continental United States. The final option was favored because it would reduce the need for further maintenance and radiologic controls at the site. Also, this option would enable the soil cleanup to proceed, allowing more efficient use of the very limited land space on Johnston Island. A disposal permit was requested and granted from the Department of Energy, and an environmental assessment was performed. It was concluded that packaging the debris and transporting it from Johnston Atoll to the continental United States storage site would have no significant impact on the environment.

A comprehensive operations plan was then developed, which exactly outlined how the cleanup operation would be accomplished and indicated the time allotted for each segment of the project. Responsibilities for logistical, radiation safety, financial, and transportation aspects of the project were designated in the operations plan. Overall management of the project was the responsibility of the DNA Health Physicist, who also served as the Radiation Safety Officer for the operation. Funding was obtained from the Department of Defense Environmental Restoration Fund, which is comparable to the Environmental Protection Agency's "super fund." Personnel to perform the dismantling, packaging, and transport were provided from several sources. DNA provided military health physicists to assist the Project Officer by serving as Assistant Radiation Safety Officer, and enlisted members of the U.S. Air Force Military Airlift Command provided radiation safety technician support. The Air Force personnel were trained as explosive ordnance disposal specialists, with radiation safety as a collateral duty. The actual disassembly of the facilities and the packaging of debris were performed by the Johnston Atoll operating contractor with assistance from a subcontractor, who removed the contaminated concrete surfaces. The Military Sealift Command, which is controlled by the Military Traffic Management Command, transported the debris from Johnston Atoll to the continental United States. Finally, a commercial trucking company provided the overland transportation to the storage site.

There was continuous coordination with the agencies mentioned above (Department of Energy, Military Sealift Command, Military Traffic Management Command, USAF, etc.) before and during the operation. In addition, coordination was effected with appropriate elements of the Environmental Protection Agency and state radiological safety offices. A public affairs plan also was developed to provide prompt and accurate response to questions from the public. This painstaking planning and coordination were necessary to ensure that all state and federal laws and regulations were followed in all phases of the operation.

REGULATIONS OF DEPARTMENT OF TRANSPORTATION AND NEVADA TEST SITE

Based on the measurements of the 1980 radiologic survey, it was presumed that most of the contaminated material would fall under the Department of Transportation (DoT) category of low specific activity (LSA) material. According to DoT, plutonium-contaminated material may qualify as LSA in one of two ways. First, LSA material may be nonradioactive material externally contaminated with an activity of less than 100 nCi/cm^2 when averaged over a square meter. Second, plutonium may be uniformly distributed throughout a volume of nonradioactive material if the average activity is less than 100 nCi/g. Because LSA materials are

considered inherently safe to transport, they are excepted from the DoT requirements of specification packaging, marking, and labeling if transported as an exclusive-use shipment in strong, tight containers so that there are no leakage of radioactive materials and no shifting of lading under normal conditions of transportation. A shipment is for exclusive use if the transport conveyance is used solely by a single consignor. The conveyance can be a freight container for highway transport, or a hold or defined deck area for ship transport. In addition, there must be no significant surface contamination on the packages and no loose radioactive material in the conveyance. Finally, the transport vehicle must bear the yellow-black-and-white RADIOACTIVE placard, and each package must be labeled "Radioactive - LSA." Any material that did not meet the LSA criterion was expected to be packaged in DoT Type A shipping containers (specified type 7A 55-gallon drums). The DoT criterion for use of a Type A container is that the activity in each package must be less than 2 mCi. If a material was so "hot" that it exceeded the criterion for the Type A container, then it would be packaged in drums and stored in a secure place on Johnston Island, pending ultimate disposal at a DOE waste isolation pilot plant. In addition to the DoT regulations, the contaminated material had to meet the Nevada Test Site (NTS) criterion for low level waste. That is, activity in each container had to be less than 100 nCi/g, where the mass includes all materials buried.

EXECUTION

CONCEPT OF OPERATION

The basic assumption of this operation was that all material on the site was contaminated, until measurements proved otherwise. Before the disassembly began, the structures and equipment left on the site were evaluated to determine if they could be salvaged. Several items (such as the fuel tank, liquid oxygen tank and water tanks, and copper cabling) were still serviceable, and their decontamination would be relatively easy. However, most of the structures were severely rusted and corroded, and it was considered more economical to dispose of them than to attempt their decontamination.

To ensure that the nonsalvageable contaminated materials met the DoT and storage-site requirements, the structures on the Launch Emplacement Site 1 (excluding the concrete pads) were first disassembled and cut into workable sizes (Figures 6 and 7). When possible, the debris was cut into pieces about 6 feet by 8 feet to conserve space in the freight containers. Because there were so many different types of debris (pipes, cabling, ladders, railroad ties, etc.), the sizes of the cut pieces varied greatly. Each piece was then cleaned and painted. The debris was painted to effectively fix any remaining contamination in place, meeting the DoT requirement that there be no loose contaminants. The loose Gunite concrete could be broken up into workable pieces and processed in the same manner as the structural debris. However, it was not practical to remove the massive concrete pads. Instead, only the contaminated surfaces were removed through a process called scabbling, in which the top layers were chipped away. That material was then stored in 55-gallon drums. The scabbling process, described below, resulted in rubble where contamination was uniformly distributed. Before

Figure 6. Missile shelter building before disassembly

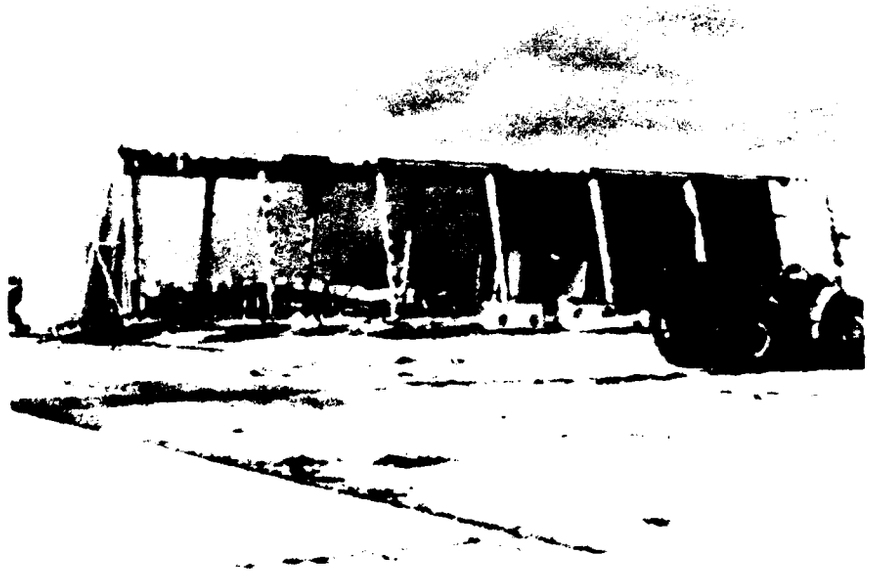

Figure 7. Missile shelter building with panels removed

packaging, all debris was monitored by counting the 60-keV photons from americium-241, using either an intrinsic germanium detector or a sodium iodide detector with a well-defined source-detector geometry.

Structural debris meeting the LSA criteria was loaded onto large (20 feet long by 8 feet wide by 9 feet high) dry-cargo freight containers (Figure 8), and the concrete rubble and any Type A material were loaded into 55-gallon drums. The freight containers were lined with plywood on each of the six surfaces to prevent puncturing of the walls, and were braced to prevent settling or rearrangement of the contents during shipment. These containers served as both package and transport vehicles for the bulk LSA material. One freight container was dedicated to the material packaged in the 55-gallon drums, and for these materials, the freight containers served only as the transport vehicle. Detailed records were kept of the material and the total amount of activity loaded into each container so as not to exceed the DoT or the Nevada Test Site criterion. The freight containers were shipped from Johnston Island to the Naval Construction Battalion Center in Port Hueneme, California, and then were transported by truck to the disposal site at the Nevada Test Site.

Figure 8. Debris being weighed before loaded into freight container at rear

FLOW PATTERN OF DEBRIS

The missile launch facility was located on the northern shore of Johnston Island, the main island of the atoll. Prevailing winds blew from east to west; residential and most work areas on the island were upwind from the launch site (Figure 9). The layout of the site was organized to establish an efficient flow pattern for the removal of the contaminated materials. The different processing stations were arranged so that they were crosswind of each other. The break area, storage shed, and laundry trailer were all upwind of the contaminated area; a road barrier and open water were downwind of the site.

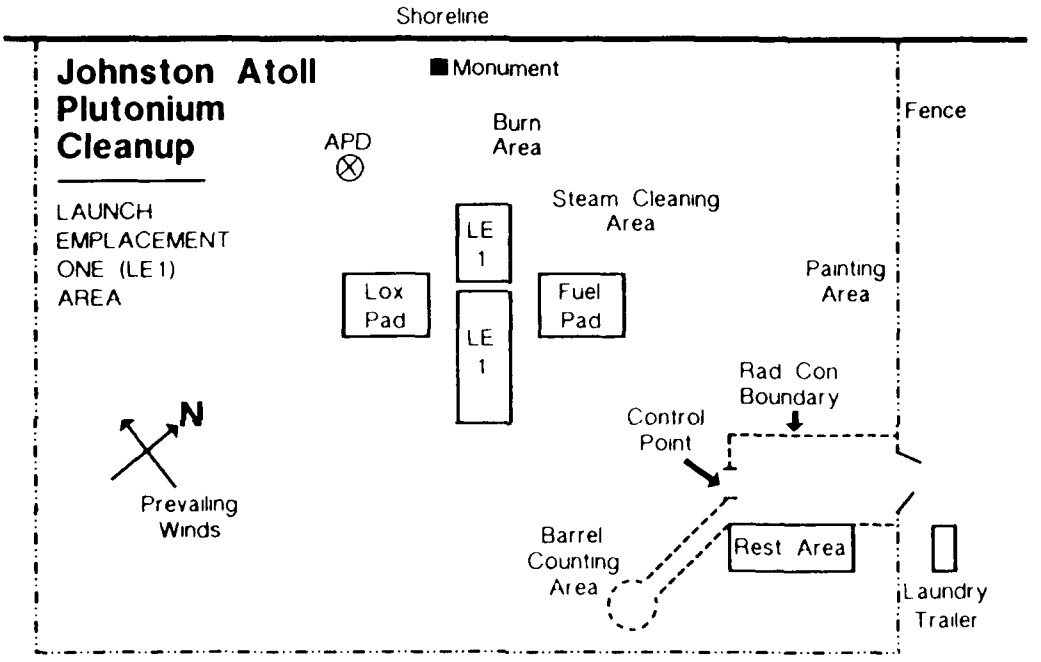

Figure 9. Layout of cleanup site

The first step in the removal process was to reduce the materials to workable sizes. The debris was cut into smaller pieces using acetylene torches, saws, and chipping hammers. After the materials were cut, they were either steam cleaned or rinsed with a high-pressure water hose to remove any loosely bound contaminant, paint, or dirt. The material was then loaded onto a clean pallet and moved to the painting area. At this station, any remaining contamination was fixed in place with a thick coating of black piling paint or white or yellow road-striping paint (which was outdated and not suitable for road use) (Figure 10). After all the exposed surfaces were painted, the materials were sent to the exit hot line for delivery by forklift to the counting site (Figure 11). Before leaving the contaminated area, the debris was smear-monitored to check for loose contamination.

Figure 10. Debris paint area to fix contamination before monitoring

Figure 11. Transporting painted debris from paint area to counting pad

The counting area was about 800 feet east of the launch site and was chosen for its relatively low background radiation. When the pallets reached the counting area, they were laid out in rows (Figure 12), and each piece of debris was numbered (Figure 13). To locate areas with high levels of contamination, a preliminary

Figure 12. Debris laid out in rows at counting area

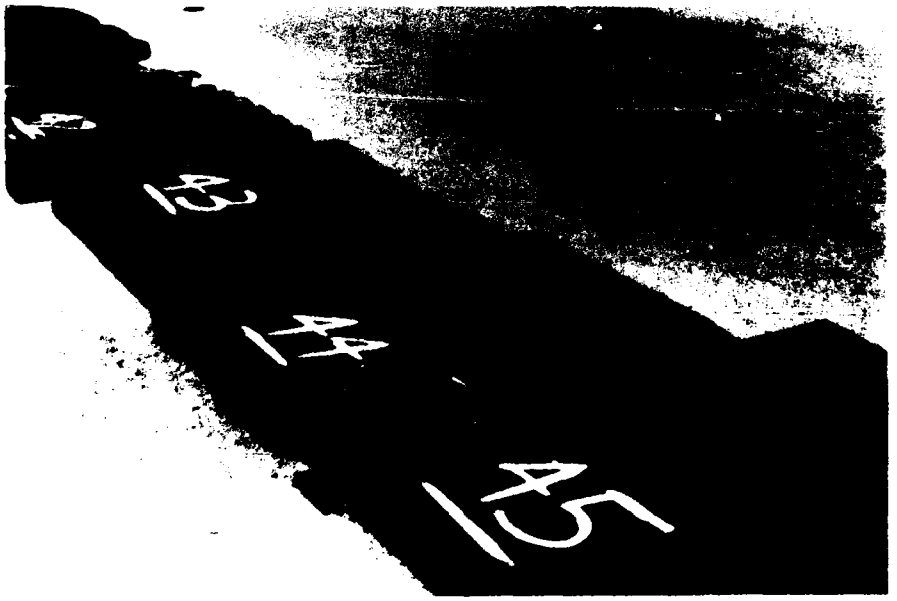

Figure 13. Numbers painted on each pallet of debris for identification

survey was performed over the surface of each piece with a modified FIDLER (field instrument for detection of low-energy radiation). The FIDLER used for screening had a 2-inch-diameter sodium iodide crystal connected to an analog ratemeter and earphones, and the window was set to detect the 60-keV photons from the americium-241. When "hot spots" were located, they were marked with spray paint and counted separately. The activity on each piece (and hot spot) was measured using the germanium detector (Figure 14) or the backup sodium iodide detector. The counting system is discussed in detail below.

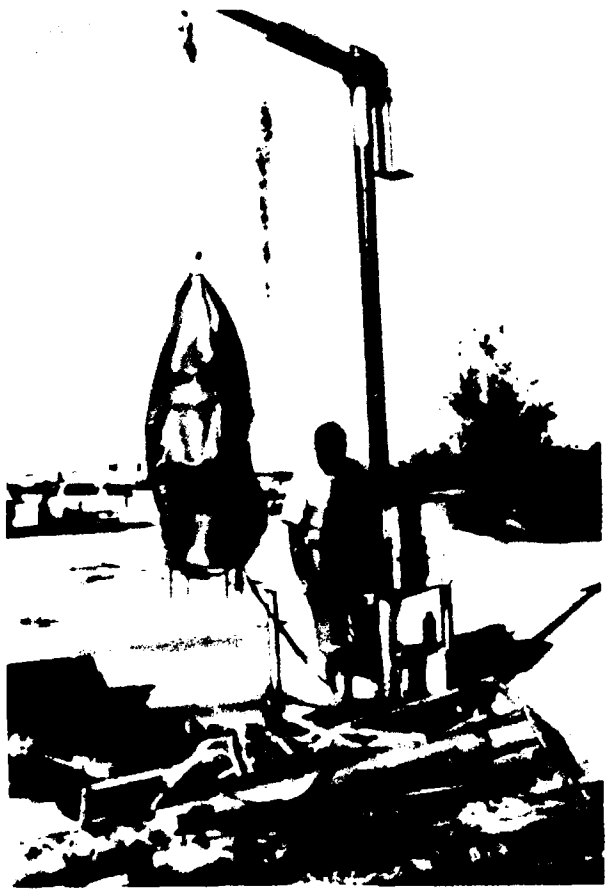

Figure 14. Monitoring pallet of debris with germanium detector system

After counting, the materials that met the LSA criterion were loaded into the freight containers, and the physical dimensions (weight, length, and width) and a brief description of the material were recorded in the packaging logbook.

DECONTAMINATION OF CONCRETE PADS

As mentioned above, the large concrete pads were decontaminated instead of removed from the site, because the launch pad and the pads beneath the fuel tank and liquid oxygen tank were far too massive. To significantly reduce the waste volume, it was decided to remove only the contaminated surfaces. This was accomplished through the scabbling process, in which the proximate concrete surface was hammered away. The scabbling device had five heads with carbide-tipped nipples that were used to finely chip the concrete surface to about a 7-mm depth. A wooden box enclosed the chipping head to prevent dispersal of contaminated concrete chips and dust. The box was continuously evacuated to a cyclone separator, which deposited the heavier particles into a 55-gallon drum through an HEPA (high-efficiency particulate air) vacuum system. While most of the concrete rubble was removed by the cyclone separator, a small amount (about 5%) remained in the HEPA filter system. The filters were later disposed of in the 55-gallon drums. A Vacublaster was used to decontaminate the cracks and expansion joints in the concrete pads. Before using the Vacublaster on the expansion joints, the joint filler material was removed and disposed of in a 55-gallon drum. The Vacublaster used a narrow nozzle to propel steel shot onto the concrete to wear away a few millimeters at a time. The concrete debris and used steel shot were then vacuumed up by the Vacublaster through the HEPA system. Most of the shot was then recycled by the Vacublaster for continued use. A quantitative assessment of the amount of contamination removed from the pad was obtained through the use of the intrinsic germanium counting system (discussed below in Radiation Measurements section). The pads were monitored after the scabbling and use of the Vacublaster, and these processes continued until the contamination was below the minimum detection limit of the counting system (about 10 nCi/cm^3). After the concrete pads were successfully decontaminated, they were covered with a layer of "clean" dirt to prevent recontamination.

MEASUREMENTS OF RADIATION

The quantitative measurements were performed using a high-resolution germanium detector coupled to a portable multichannel analyzer. As a backup, a FIDLER with a 13-cm sodium iodide crystal connected to a scaler was used with the multichannel analyzer. (Note that similar systems have been used in other cleanup operations.) The backup FIDLER was needed toward the end of the operation when the preamplifier failed on the germanium detector. Both detectors were used with an 11-inch-long cylindrical collimator so that the field of view was circular and limited to about 35 degrees. The detector in use was suspended from a rope attached to a mobile rig. This was done to reduce the interference from microphonic noise caused by the heavy equipment and aircraft on the nearby runway. To accommodate the wide range of sizes of the contaminated material, the detectors could be adjusted from 1 to 6 feet above the ground. Calibration of the detectors was checked once a day with an americium point source, and background readings were taken at least twice a day (before and after counting). The counting system measured the americium-241 activity per area, and this had to be converted to total transuranic alpha activity from all the plutonium and americium isotopes. The transuranic activity of the Johnston Island plutonium contamination was 8.7 $\pm$ 2.9 times the americium-241 activity.

The detector was placed above the center of a piece of debris so that the field of view covered the longest dimension. If this was not possible, either the piece was cut into smaller sections or more than one count was made. When a hot spot was indicated on the debris, the detector was placed above the hot spot so that the field of view encompassed one square meter with the hot spot in the middle. Each piece was counted for 2 minutes, and the material identification number, peak display, and net area counts were recorded on multichannel analyzer minicassette tapes. The taped data were later input and stored along with the packaging data in a Compaq Plus (Houston, TX) computer.

Assessment of the contamination present on the concrete pads was more complicated. The pads were first cleaned with the HEPA vacuum to remove loose contamination, and then a uniform grid survey was performed. This was accomplished by dividing the pads into square blocks, 6 feet by 6 feet, and sequentially numbering each block. Also, hot spots and hot lines (mainly found in the joints) were identified with the FIDLER and numbered separately. The germanium multichannel analyzer counting rig was rolled over the center of each box, and counting was performed as described above. To count the hot spots and hot lines, a steel plate about 1/4-inch thick was placed over the rest of the block so that only the area of interest was counted. Similarly, when the entire block was counted, steel was placed over the hot sections so that they were not included in the counting. The data from each block, hot spot, and hot line were stored in the computer. During the scabbling and Vacublaster operation, a careful talley was kept so that it was known in which drum each section of concrete pad was stored. The total weight in each drum then could be divided by the total activity to determine the activity per gram.

Several 55-gallon drums had been filled with radioactive waste from the many cleanup operations over the years at the site. Included in this waste were hot pieces of coral, americium smoke detectors, and other miscellaneous items. Although this material was already packaged, the amount of activity needed to be assessed. This was done by cutting the bottom 6 inches off a 55-gallon drum and filling it with the contaminated material. The detector was then placed over the drum, and the calculations were performed, considering the material in the drum as a disc source. The material was repackaged in 55-gallon drums, but the amount of transuranic activity contained in each was now known.

SCREENING FOR LSA

The amount of activity contained on the different types of debris was carefully measured so that compliance with the DoT regulations could be demonstrated. As discussed earlier, two criteria apply for plutonium-contaminated material to be considered LSA: (a) nonradioactive material that is externally contaminated, with an activity of less than 100 nCi/cm^2 averaged over a 1-square-meter area, and (b) contamination uniformly distributed throughout a volume of nonradioactive material with an average activity of less than 100 nCi/g. Note that the first criterion was applied to the painted structural debris, and the second to the concrete rubble. A screening level of 50% of the DoT standards was chosen to be conservative, that is, 50 nCi/cm^2 for the structural components and 50 nCi/g for the concrete debris. As expected, almost all material met this conservative

screening level. Only one 55-gallon drum had to be shipped as a Type A container, and no waste exceeded the criteria for a Type A container (less than 2 mCi per package).

PACKAGING AND SHIPPING

All the bulk LSA debris was loaded directly into the reinforced freight containers, and one container was dedicated for the 55-gallon drums. The debris counting data, which had been stored in the computer, were sorted by container number, enabling printout of the contents and weight of each container, as well as the total activity and mass of plutonium contained in each. This was a convenient method of ensuring that each freight container met the Nevada Test Site criterion for low-level waste (this screening level was also set at 50 nCi/g). Before a filled container was moved to the holding area, the door was welded shut and the outside of the container was smear-monitored to check for contamination.

All of the freight containers were placarded, and all but the container with the 55-gallon drums were labeled as radioactive LSA. However, each drum containing LSA material in this freight container was labeled "Radioactive - LSA." A commercial freighter under contract by the Military Sealift Command was used to transport the containers to the Naval Construction Battalion Center. A Radiation Safety Officer accompanied the shipment to monitor the containers in the event of container damage. Radiation measurements of the ship container storage areas were made before loading the containers aboard ship and after the containers were off-loaded. Radiation surveys were also conducted at the Naval Contruction Battalion Center port handling facility after the containers were moved to the waste site. The final leg of the journey was made by a trucking company, which was fully certified to transport radioactive materials.

DISCUSSION

The cleanup described above was an extensive operation requiring resources from many government and civilian organizations. Throughout the project, several logistical and technical challenges were met, and some lessons were learned that may be of interest to others beginning similar operations.

RADIATION SAFETY

The major radiological danger throughout the operation was the possibility of inhaling alpha-emitting actinide particles. For this reason, strict radiological control procedures were maintained. Full anticontamination clothing and respirators (Figure 15) and full-body monitoring with alpha detectors at the hot line contributed to a successful program. The airborne contamination hazard normally associated with winds was mitigated because of the heaviness of the plutonium contaminant. Air monitors were run continuously at 30, 50, and 100 meters downwind of the site. These read as high as 50 fCi/m^3 averaged over a 24-hour period. As expected, they gave high readings when there was activity that involved mixing up the debris (such as torching, cutting, and scabbling) and low readings (tens of fCi/cm^3) when there was not much activity. The air monitors upwind of the site typically read 10-50 fCi/cm^3.

Figure 15. Removing respirators at contamination hot line: Note use of full anticontamination clothing

All personnel were monitored with LiF dosimetry to document the external exposure received during the project. A 24-hour urine specimen for each person was taken for radioanalysis before working at the site and after conclusion of the job. The thermal luminescent dosimeters and the urine samples were processed by the Air Force at the Occupational Environmental Health Laboratory. The results indicated that no external or internal doses were received as a result of the operation.

The laundry trailer was used to return uncontaminated and contaminated anticontamination suits to use. After laundering, each piece was monitored with alpha detectors to determine if it was radiologically clean. The washing machine was then smear-monitored before another load was started, and the water from the washer was piped back into the controlled area.

HEAT PREVENTION PROGRAM

Most of the heavy labor was done in full anticontamination suits, including full-face respirators, which caused serious concern for heat-related injuries. Therefore, a heat prevention program was implemented and followed conscientiously. A bottsball thermometer was used to indicate the heat conditions. All personnel wearing the protective clothing were briefed on the nature of heat illness, means of notifying personnel when the temperature is critical, proper response to be taken for various temperature conditions, and appropriate first aid for a heat-related casualty. Intake of water and the work-rest cycles were based on the bottsball temperature (Figure 16). These measures proved to be effective, as there were no heat-related injuries during the operation.

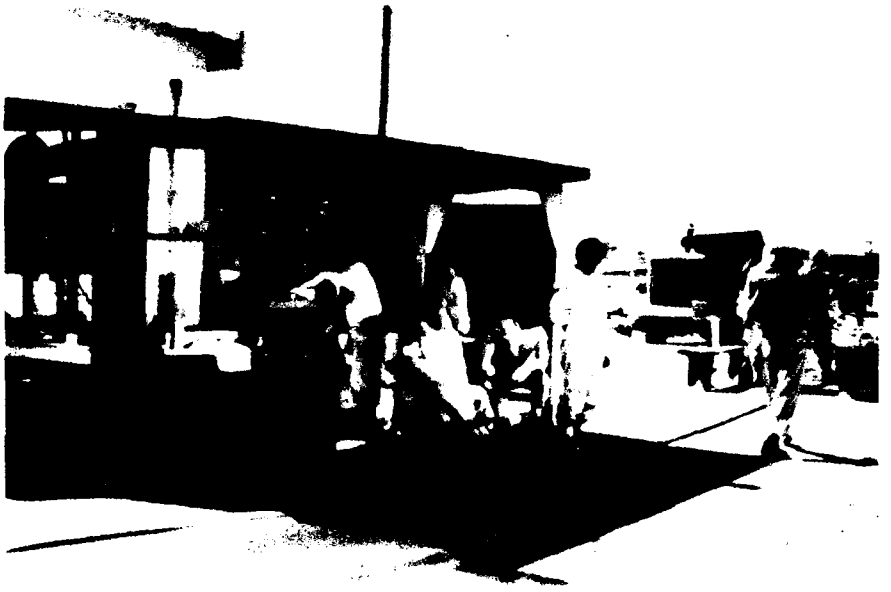

Figure 16. Workers resting at rest area outside contamination hot line before and after working inside site

DECONTAMINATION OF EQUIPMENT

Several pieces of equipment were salvaged from the site, including fuel tanks, liquid oxygen tanks, water tanks, and some copper cabling. The equipment was decontaminated by steam cleaning the outer surface and then surveying and smear-monitoring it to ensure that all contamination was removed. If the contamination had not been removed, the procedure was repeated. Equipment used in the operation (such as forklifts), which had to be removed from the controlled area, were treated similarly. They were surveyed, smear-monitored, and released after negative results. If contamination was indicated, the equipment was steam-cleaned and checked again.

PACKAGING AND COUNTING

A unique aspect of this operation was the use of freight containers as both package and transport vehicle. This dual use of the containers was considered the most efficient method of transporting the large pieces of steel debris, which made up most of the contaminated material. An added advantage of these freight containers was that because of their low cost, they were disposed of with their contents at the waste-disposal site.

Novel techniques were also used to measure the activity of all the debris packaged and transported from Johnston Atoll. This was done through several modifications of a typical counting system. Debris with essentially uniform surface contamination, volume contaminated debris, and debris considered as a disc source were all effectively monitored to determine the total transuranic activity.

COMPUTER

A Compaq Plus computer was used with Symphony software (Lotus, Cambridge, MA) to store, reduce, and analyze the data collected. After an initial period of familiarization with the computer and software, the computer became an invaluable tool and time-saving device. Data for each shipping container were readily available, and total amounts of volume and activity could be easily retrieved from the data base. In fact, the computer was used to produce the manifests for the shipping documents.